AD-A174 209 MULTICHANNEL NEPHELOMETER(U) BOEING AEROSPACE CO 1/2
SEATTLE WA S BECK ET AL OCT 86 CRDEC-CR-87007
DAAK11-83-C-0089

UNCLASSIFIED F/G 7/4 NL

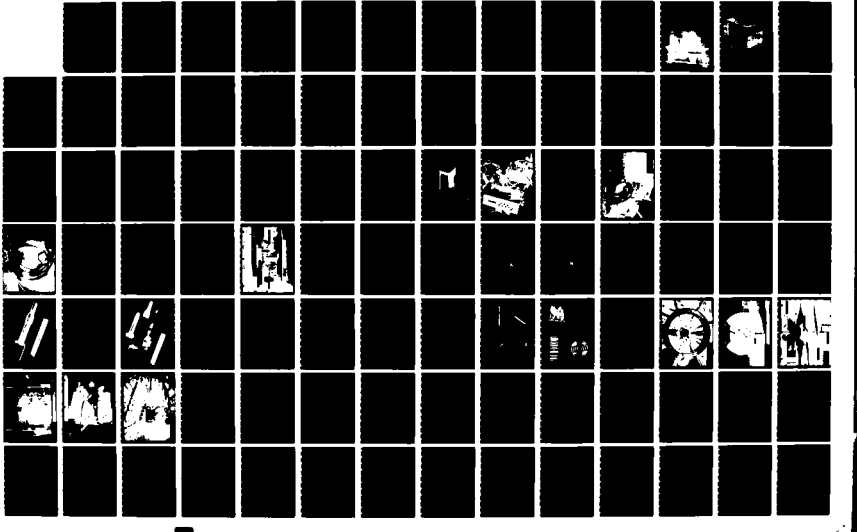

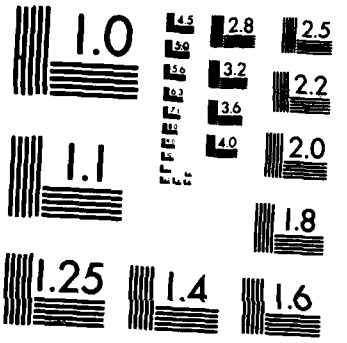

CROCOPY RESOLUTION TEST CHART
NATIONAL BUREAU OF STANDARDS-1963-A

CHEMICAL
RESEARCH,
DEVELOPMENT &
ENGINEERING
CENTER

CRDEC-CR-87007

MULTICHANNEL NEPHELOMETER FINAL REPORT

by Sterling Beck
Tim Majoch
David Capps

BOEING AEROSPACE COMPANY
Seattle, WA 98124-2499

October 1986

U.S. ARMY
ARMAMENT
MUNITIONS
CHEMICAL COMMAND

Aberdeen Proving Ground, Maryland 21010-5423

Disclaimer

The findings in this report are not to be construed as an official Department of the Army position unless so designated by other authorizing documents.

Distribution Statement

Approved for public release; distribution is unlimited.

UNCLASSIFIED

SECURITY CLASSIFICATION OF THIS PAGE

REPORT DOCUMENTATION PAGE

1a REPORT SECURITY CLASSIFICATION UNCLASSIFIED	1b RESTRICTIVE MARKINGS
2a SECURITY CLASSIFICATION AUTHORITY	3 DISTRIBUTION / AVAILABILITY OF REPORT Approved for public release; distribution is unlimited.
2b DECLASSIFICATION / DOWNGRADING SCHEDULE	
4 PERFORMING ORGANIZATION REPORT NUMBER(S) CRDEC-CR-87007	5 MONITORING ORGANIZATION REPORT NUMBER(S)
6a NAME OF PERFORMING ORGANIZATION Boeing Aerospace Company 6b OFFICE SYMBOL (*If applicable*)	7a NAME OF MONITORING ORGANIZATION
6c ADDRESS (*City, State, and ZIP Code*) Seattle, WA 98124-2499	7b ADDRESS (*City, State, and ZIP Code*)
8a NAME OF FUNDING / SPONSORING ORGANIZATION CRDEC 8b OFFICE SYMBOL (*If applicable*) SMCCR-RSP-B	9 PROCUREMENT INSTRUMENT IDENTIFICATION NUMBER DAAK11-83-C-0089
8c ADDRESS (*City, State, and ZIP Code*) Aberdeen Proving Ground, Maryland 21010-5423	10 SOURCE OF FUNDING NUMBERS PROGRAM ELEMENT NO / PROJECT NO / TASK NO / WORK UNIT ACCESSION NO

11 TITLE (*Include Security Classification*)
Multichannel Nephelometer Final Report

12 PERSONAL AUTHOR(S)
Beck, Sterling; Majoch, Tim; Capps, David

13a TYPE OF REPORT	13b TIME COVERED	14 DATE OF REPORT (*Year, Month, Day*)	15 PAGE COUNT
Contractor	FROM 83 09 TO 86 06	1986 October	96

16 SUPPLEMENTARY NOTATION
COR: Dr. J. Bottiger, SMCCR-RSP-B, (301) 671-2395

17 COSATI CODES			18 SUBJECT TERMS (*Continue on reverse if necessary and identify by block number*)	
FIELD	GROUP	SUB-GROUP		
15	02		Nephelometer	Mueller Matrix
			Light Scattering	Scattering Matrix
			Nonspherical Particles	Particle Functions

19 ABSTRACT (*Continue on reverse if necessary and identify by block number*)
A Multichannel Nephelometer has been designed and built. The instrument records the far-field light scattering pattern for individual aerosol particles in the size range 0.3-10.0 micrometers. The scattering pattern is sampled over a full 4π steradian solid angle. Incorporated in the Nephelometer is an aerosol handling system which can sample from a source with particle densities as high as ~~10^6 cm^{-3}~~, dilute this, and present one particle at a time to the light scattering chamber. ~~This~~ report documents the Nephelometer design, including the aerosol handling system, light scattering chamber, electronics and software.

20 DISTRIBUTION / AVAILABILITY OF ABSTRACT	21 ABSTRACT SECURITY CLASSIFICATION
☒ UNCLASSIFIED/UNLIMITED ☐ SAME AS RPT ☐ DTIC USERS	UNCLASSIFIED
22a NAME OF RESPONSIBLE INDIVIDUAL TIMOTHY E. HAMPTON	22b TELEPHONE (*Include Area Code*) (301) 671-2914 / 22c OFFICE SYMBOL SMCCR-SPS-T

DD FORM 1473, 84 MAR 83 APR edition may be used until exhausted
All other editions are obsolete.

SECURITY CLASSIFICATION OF THIS PAGE

UNCLASSIFIED

PREFACE

The work described in this report was performed under Contract No. DAAK11-83-C-0089. This work was started in September 1983 and completed in June 1986.

The use of trade names or manufacturers' names in this report does not constitute endorsement of any commercial products. This report may not be cited for purposes of advertisement.

This report has been cleared for public release.

CONTENTS

FIGURES

FIGURES Continued

TABLES

MULTICHANNEL NEPHELOMETER
FINAL REPORT

1. SYSTEM OVERVIEW AND EXECUTIVE SUMMARY

The Boeing Aerospace Company has developed and built a multichannel nephelometer designed to measure and record the far-field visible light-scattering pattern generated by the interaction of individual particles of an aerosol with a laser beam. The nephelometer will allow the light scattering patterns of complex-shaped aerosol particles (including their polarization characteristics) to be catalogued in a large data base. Efforts will then be made, based upon this data, to determine the relationship between each particle type and its characteristic scatter. Future identification of aerosols would hopefully be based on scatter measurements alone. This instrument will also be useful in comparing actual light-scattering measurements to theoretical scattering models that are being developed.

The multichannel nephelometer unit includes an aerosol system, scattering chamber, and data acquisition system. Figure 1 shows the main multichannel nephelometer unit, which is mounted on a three foot by six foot optical table with casters and retractable support pads. The overall unit height is eight feet. Aerosol diluters, which draw the sample from a source, are mounted on rollout slides for ease of maintenance in their overhead location. The rack holding these diluters can be dismounted, which will allow the system to clear the top of doorways. The laser is mounted under the table, allowing the entire system to maintain mechanical and optical alignment once initial setup is completed. The main unit is thus basically self-contained, requiring only power, aerosol source, and data output connections. Depending on their configuration, it is possible that additional small aerosol sources could be mounted directly to the diluters to perform other operations such as calibration.

The front-end electronics are attached directly to the photomultiplier tube detectors on the scattering chamber. The remainder of the data acquisition system, which is shown in Figure 2, consists of a computer, monitor, keyboard, A/D converter, printer, and power supplies mounted on a computer cart. The data acquisition system is tied by a 25 foot long cable bundle to an interface box on the main unit which ties in with the front-end electronics.

Figure 1 illustrates the relationship between system-level requirements and allocated system requirements. The system goals shown in the center block determine the design requirements of the three systems. In addition, each system has individual design objectives shown in the outer blocks. Other system-level requirements, shown in the ovals, result in design compromises between only two systems. The design process consists of optimizing this interactive network of requirements. These systems are described in detail in the Sections that follow and are briefly summarized below.

1.1 Aerosol Sampling System.

Section 2 of this report provides details on the aerosol sampling system, which is designed to sample aerosols of number densities up to 10^6 particles/cc, dilute as required (with minimal size biasing) to produce a flowing stream of single aerosol particles, and entrain that flow in a laminar clean air sheath directed through the laser beam. The particles traverse the laser beam, one at a time, at a nominal rate of 10 particles/sec, and are expected to rotate less than 3.6° during their transit through the laser beam.

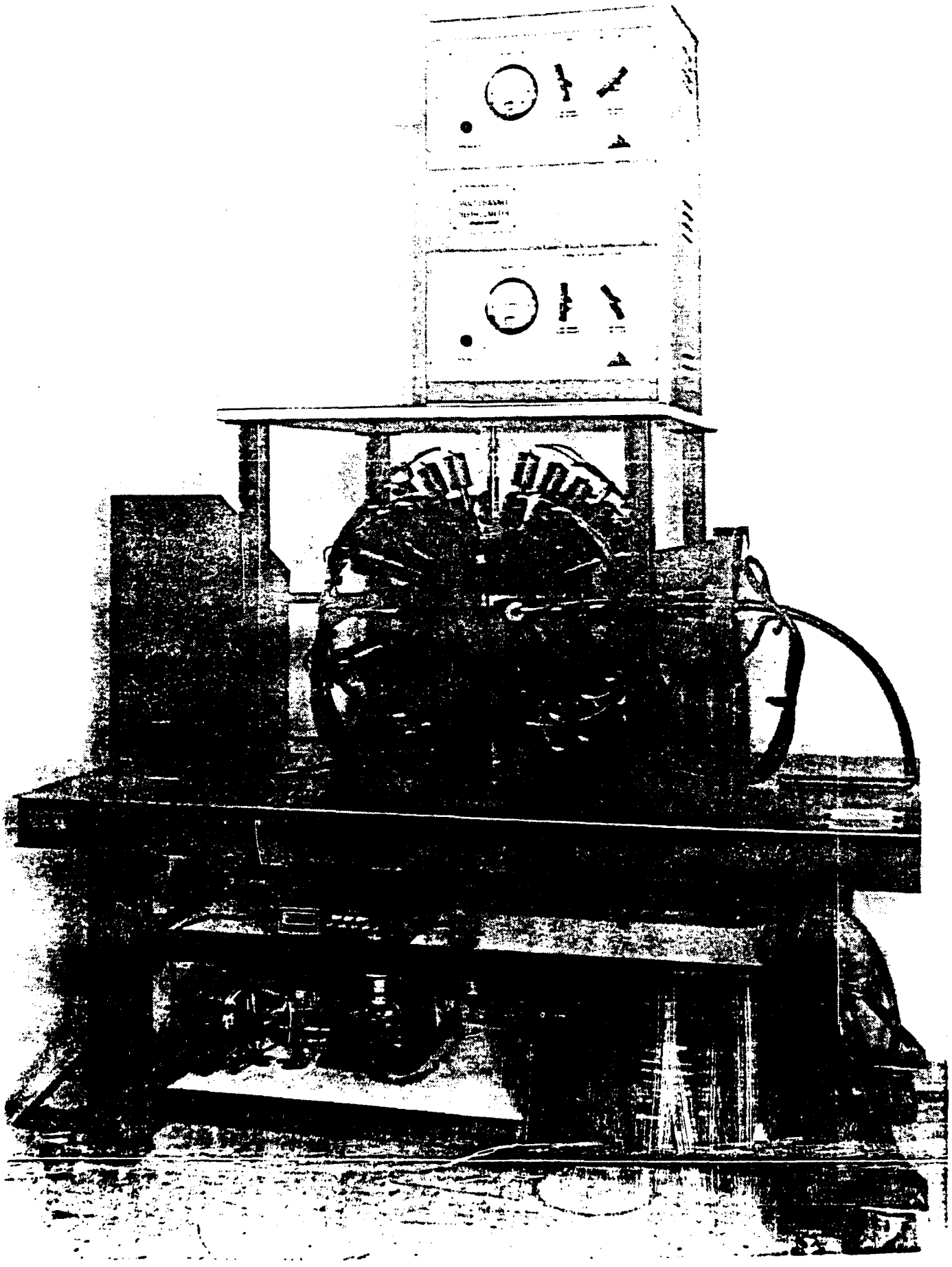

Figure 1. Multichannel Nephelometer Main Unit

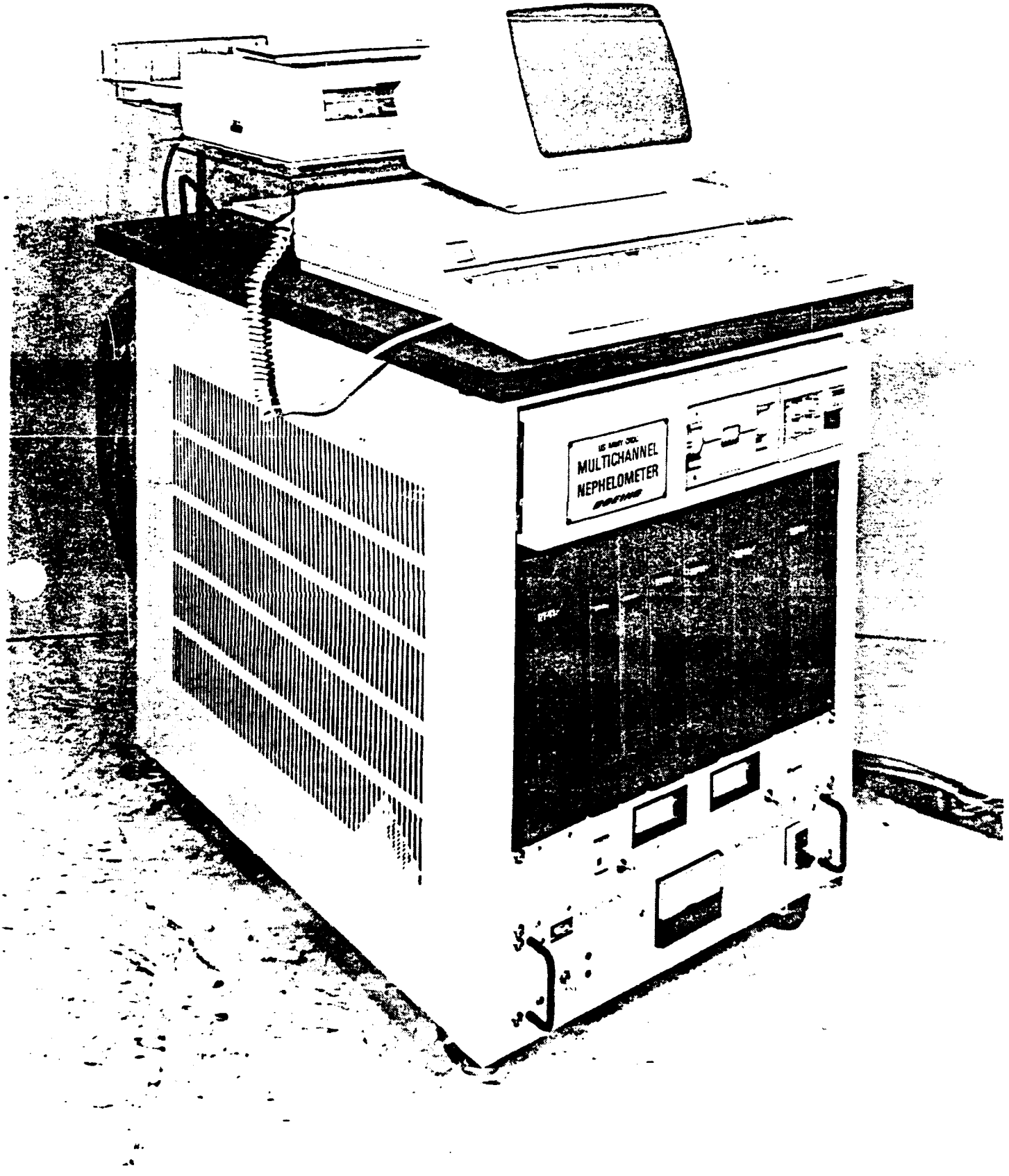

Figure 2. Multichannel Nephelometer Computer Unit

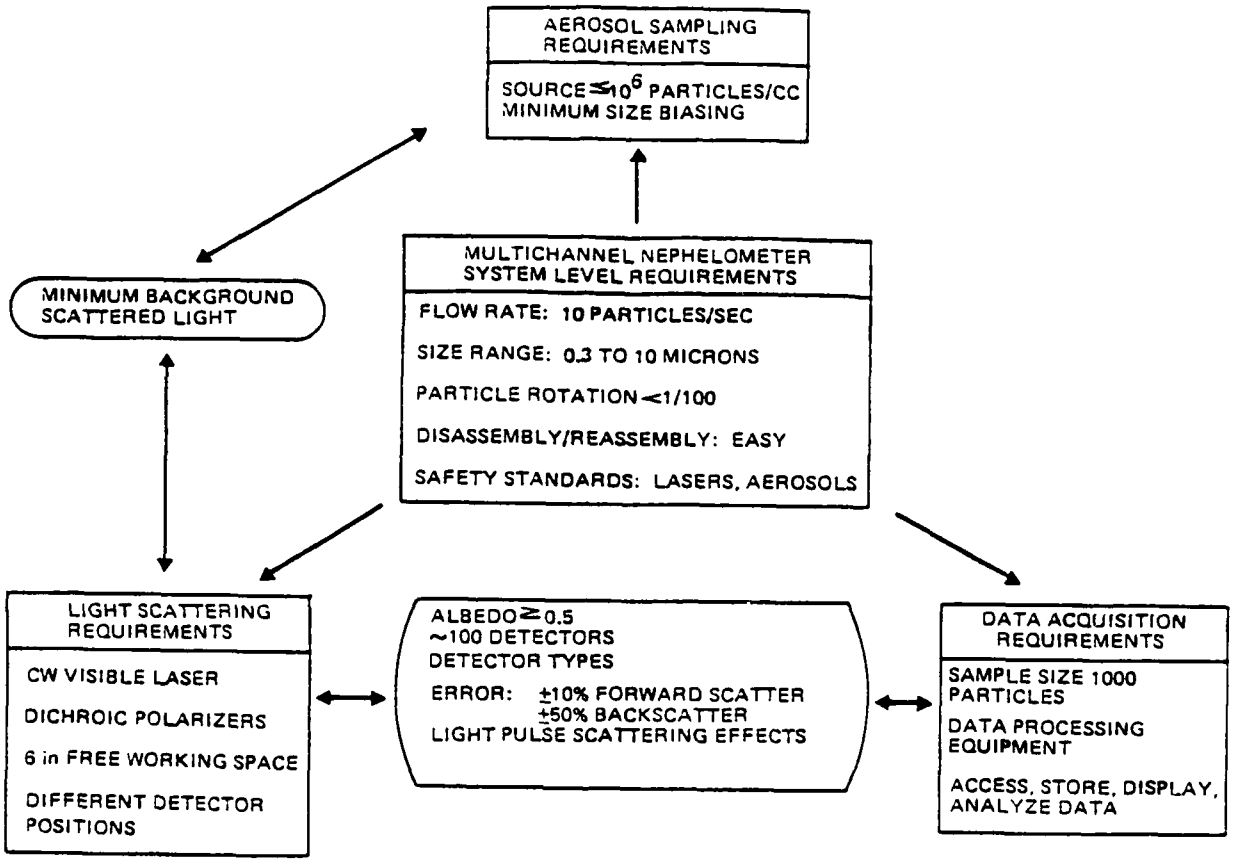

Figure 3. Multichannel Nephelometer Design Requirements

Dilution is accomplished by two ATEC 303-LF diluters, which achieve the desired aerosol concentration by successively drawing off samples of the aerosol through capillary tubes and mixing them with clean air. The diluters are stacked vertically to minimize the bias of larger particle sizes and allow cascading.

Localization and confinement of the diluted stream through the laser beam sampling volume is provided by sheath air to the sample flow and forms a and purge air flows working in conjunction. The sheath air is added to the sample flow in a specially designed block and forms a laminar flow jet surrounding the diluted aerosol sample which serves to localize the particles and minimize contamination to the light-scattering chamber and optics. A purge air flow is added directly to the light-scattering chamber and is regulated so as to reinforce the integrity of the sheath air jet across the gap where the scattering event occurs.

All the aerosol particles are trapped on filters prior to exhausting the air. The entire sampling train is constructed to allow easy disassembly for routine cleaning and inspection.

1.2 Light Scattering System.

Section 3 describes the light-scattering system, which includes a visible argon-ion laser, a 10.4-in-diameter scattering chamber, and 108 photodetectors. The 1.5-mm-diameter CW laser beam is shielded by an optically sealed entrainment system that complies with TB MED279, "Control of Hazards to Health From Laser Radiation" and provides class I laser (eye safe) system operation. A 14-in access space is provided in front of the scattering chamber for additional beam optics.

The scattered light resulting from the intersection of the 0.3- to 10-micron particles with the laser beam is received by individual and arrayed photodetectors surrounding the intersection point. The detectors are arranged in an unsymmetric fashion along great circles of the spherical chamber and lie in three planes spaced by 45°. Detection begins at about 9° from forward scatter and extends to within 11° of the backscatter.

The arrayed detectors, situated from 8.5° to 21.5° off the forward scatter direction where additional resolution is required, use Hamamatsu R1770 photomultiplier tubes selected for their response, geometry, and spacing attributes. As reflected light was not considered a problem for the array units in the near-forward direction, a simple optical design was developed, consisting of a rotatable polarizer and an aperture plate in front of eight rectangular photomultiplier tubes. Each detector element subtends 1.64°.

The individual detectors use Hamamatsu R647 photomultiplier tubes, selected because of their cylindrical geometry and response characteristics. They are mounted in black plastic molded assemblies which contain a removable sheet-type dichroic linear polarizer preceded by a lens and pinhole system that strictly limits their field of view, thus minimizing the "noise" factor from reflections within the chamber. Their unsymmetric spacing also prevents specular reflections off optics in thenear-forward scattering directions from reaching detectors in the near-backscatter direction. Each individual detector subtends 6°.The response levels from the detectors allow intensity measurement accuracies of the scattered light to $\pm 15\%$ in the 0° to 90° region and $\pm 50\%$ in the 90° to 110° and 140° to 180° regions. These accuracies are based on the "worst case" of a 0.3-micron particle with albedo not less than 0.5.

The scattering chamber itself consists of two near-hemispheric shells bolted to a mounted plate housing the sampling system. Its walls are anodized black to decrease

surface reflections. The chamber is designed for easy access and disassembly. Numerous O-rings seal the system both mechanically and optically.

1.3 Data Acquisition System.

Section 4 gives details on the data acquisition system, which reads the detector responses to each scattering event, digitizes that information, and stores the results on computer memory for subsequent analysis. The front-end electronics package filters the signal from the photomultiplier tubes using a bandwidth selected (as determined by the pulse width of the scattered light) to reduce the system's sensitivity to molecular scattering and signal noise. Further signal processing on detected scattering waveforms is performed to allow dynamic rejection of data from particles moving slower and faster than the "design" velocity. The signal is then amplified, logarithmically compressed into a standard voltage range, stored by a track/hold amplifier, and digitized for input to the computer. The computer stores the intensity measurements of 119 of these signal channels at a nominal rate of 10 particles/sec. Data sufficient to characterize six aerosols (six Mueller matrixes) can be held on a mass storage disk. The data to characterize each aerosol may be transferred to three floppy diskettes for long-term storage. In addition to the basic data acquisition circuitry and main computer, the data processing equipment includes a graphics terminal, a graphics printer, and the auxiliary floppy diskette drive used for long-term storage.

1.4 System Integration and Testing.

Final system integration, testing and delivery were completed in October 1985. Total operation of the aerosol system was achieved and confirmed. Difficulties in generating appropriate test aerosols plus the complexities of the data acquisition system complicated the final system checkout which was subsequently completed after the system was delivered to the Edgewood Arsenal in Aberdeen Proving Grounds, Maryland.

While the data acquisition system appears to be working correctly, full checkout of the system has not yet been possible because of noise in the laser. One critical aspect of system noise which had been overlooked in development, was the laser beam ripple (0.2%) of beam intensity) component of the molecular scatter from the air in the chamber. This signal is strong enough to wash out most of the signals from all but the largest particles. An effort is currently underway by the Chemical Research and Development Center (CRDC) to obtain and integrate a laser beam modulator into the system to reduce the laser beam noise levels by one to two orders of magnitude. Completion of that task is expected to allow final checkout of the data acquisition.

1.5 Report Coverage.

This report covers the basic multichannel nephelometer system configuration and development. Detailed information on system configuration, part drawings, operation and maintenance, software, and laser safety are covered in other documents referenced in Section 6.0.

2. AEROSOL SAMPLING SYSTEM

The first main task of the multichannel nephelometer is to obtain a sample of the test aerosol, condition the sample to the operational capabilities of the system, present it to the laser beam for scattering and measurement, and then dispose the sample in a safe manner. This task is accomplished by the aerosol sampling system. The overall aerosol sampling system, shown schematically in Figure 4, was designed to provide the

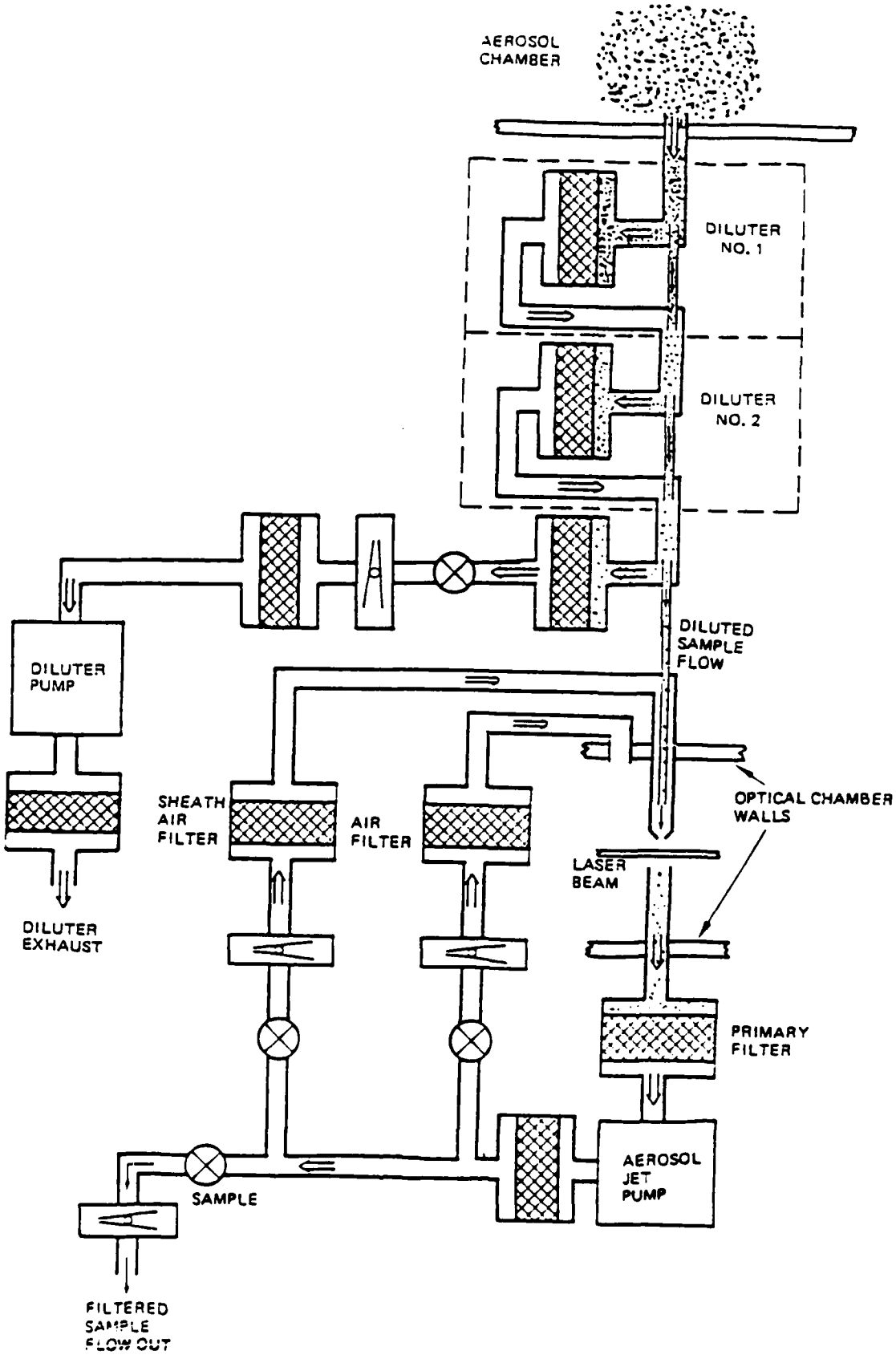

Figure 4. Aerosol System Schematic

features listed in Table 1 and the main components of this system are listed in Table 2. It consists of two basic subunits: the dilution system and the sampling system. These are discussed separately below.

2.1 Dilution System

The nephelometer is designed for nominal sampling rate of 10 particles/second, but must also be capable of drawing from test aerosols with concentrations of up to 10^6 particles/cm^3. To meet this requirement, it is necessary to incorporate a variable dilution capability into the nephelometer. This is accomplished by the dilution system. The dilution system is based on the ATEC diluter system shown schematically in Figure 5. This system has high flexibility, allowing dilution and source changes by using a path select knob. Additional dilution capabilities are available by exchanging the dilution capillaries among the eight that have been supplied with the system. A ninth, smaller capillary is available from ATEC should it be required. With the full range of flow rates and capillary sizes, each of these diluters is capable of nominal dilution ratios of up to 1000:1. Two diluters are used in tandem to produce sufficient dilution for sampling concentrations of up to 10^6 particles/cm^3.

The diluters are standard units with special features: stainless steel fittings and valves, and tapered capillary edges. The stainless steel fittings are more resistant than the standard brass and are less likely to corrode or interact chemically. The capillary tubes are normally cut with a diamond saw. This leaves a square-ended capillary end that would divert a small portion of the airflow and could create some avoidable bias. Using an alternate abrading technique, these tubes were cut off in such a manner as to leave a tapered edge, thus minimizing edge effects from the capillary tube. A similar set of capillaries is used at the dilution/sampling system interface to provide the sampling probe for the aerosol jet.

At each of the diluters as well as downstream at the sample probe, the capillary probe draws off a small sample from the center of the influent flow. Thus, each probe samples only the center of the influent flow. For optimum dilution when two diluters are cascaded and upstream of the sample probe, the aerosol must be well distributed in the output of each of the diluters. At the same time, the need for minimum particle bias is best accomplished by minimizing the perturbations to smooth, laminar flow. Since the capillary of each diluter releases its output in the center of the effluent flow, the dilution effectiveness could be greatly reduced at the next sampling probe if mixing is insufficient. There are several techniques which have been indentified which are intended to increase the effectiveness of the diluters while minimizing the system bias. One is a series of interface nozzles and the second is a flow baffle near the capillary output. Each is described below. Any technique to increase the distribution of the aerosol in the effluent must introduce disturbances to the flow and will thereby increase the sample bias. Since some mixing will always occur, for many conditions no additional mixing will be required and minimum bias can be achieved. The stronger measures outlined below are provided for those situations when the dilution must be maximized at the expense of sample bias. Figure 6 shows the cross-sections of four interface nozzles designed to more uniformly distribute the aerosol in the airflow by reducing the cross

section of the diluter output to cause mixing. The first three are designed to maintain nonturbulent flow throughout, whereas the fourth intentionally introduces some turbulence. Greater uniformity is expected to be achieved with the interface nozzles with smaller bores, but at the cost of greater particle bias. Providing a selection of interface nozzles allows for optimization of mixing characteristics to meet different requirements and conditions. Figure 7 shows a typical interface nozzle installation

Table 1. Aerosol Sampling System Requirements

- Draw the sample from a suspended aerosol chamber
- Minimize particle bias for particles in the 0.3 to 10.0 micron size range
- Trap all aerosol particles on filters prior to exhausting the air
- Deliver a serial particle train to the optical system providing

  Nominal 10 particles/sec
  Chamber sampling densities of up to 10^6 particles/cm^3
  Low rotation during observation
  Low contamination of the optical chamber
  Low particle velocity (10 m/sec or less) through aerosol jet
  Small (1 mm) sample cross section

- Provide operational flexibility
- Allow for easy disassembly to clean and inspect
- Be capable of simply modifying several key parameters to allow optimization and flexibility

Table 2. Selected Aerosol System Purchased Components

Item	Figure 2.1 Location	Vendor	Model No.	Comments
Diluters	No. 1 & No. 2	ATEC	303-LF	Stainless steel valves and fittings Full set of sample capillaries w/tapered ends
Sample Capillaries	S	ATEC	SPECIAL	Tapered capillary ends
Diluter pump		GAST	0531-1028-347X	12.7 liters/min, 3450 RPM
Aerosol pump		KNF Neuberger	N75 MVP	5.5 liters/min, 3200 RPM
			N79 MVP	9.2 liters/min, 3200 RPM
Mass flow controllers:		Sierra	4-993151-49-942-1-1	Total system with electronics
Sample	1		54	0-100 SCCM* (1.67 cm^3/sec)
Sheath	2		57	0-1000 SCCM (16.67 cm^3/sec)
Purge	3		58	0-2000 SCCM (33.33 cm^3/sec)
Diluter	4		59	0-5000 SCCM (83.33 cm^3/sec)
Particle filters:		Balston	DFU-9933-05-BQ	99.9991% retention @ 0.1 micron Alternate sizes and ratings available. Box of 10 (4 spares).
Primary	A			
Secondary	B			
Recycle	C			

SCCM = standard cubic centimeters per minute

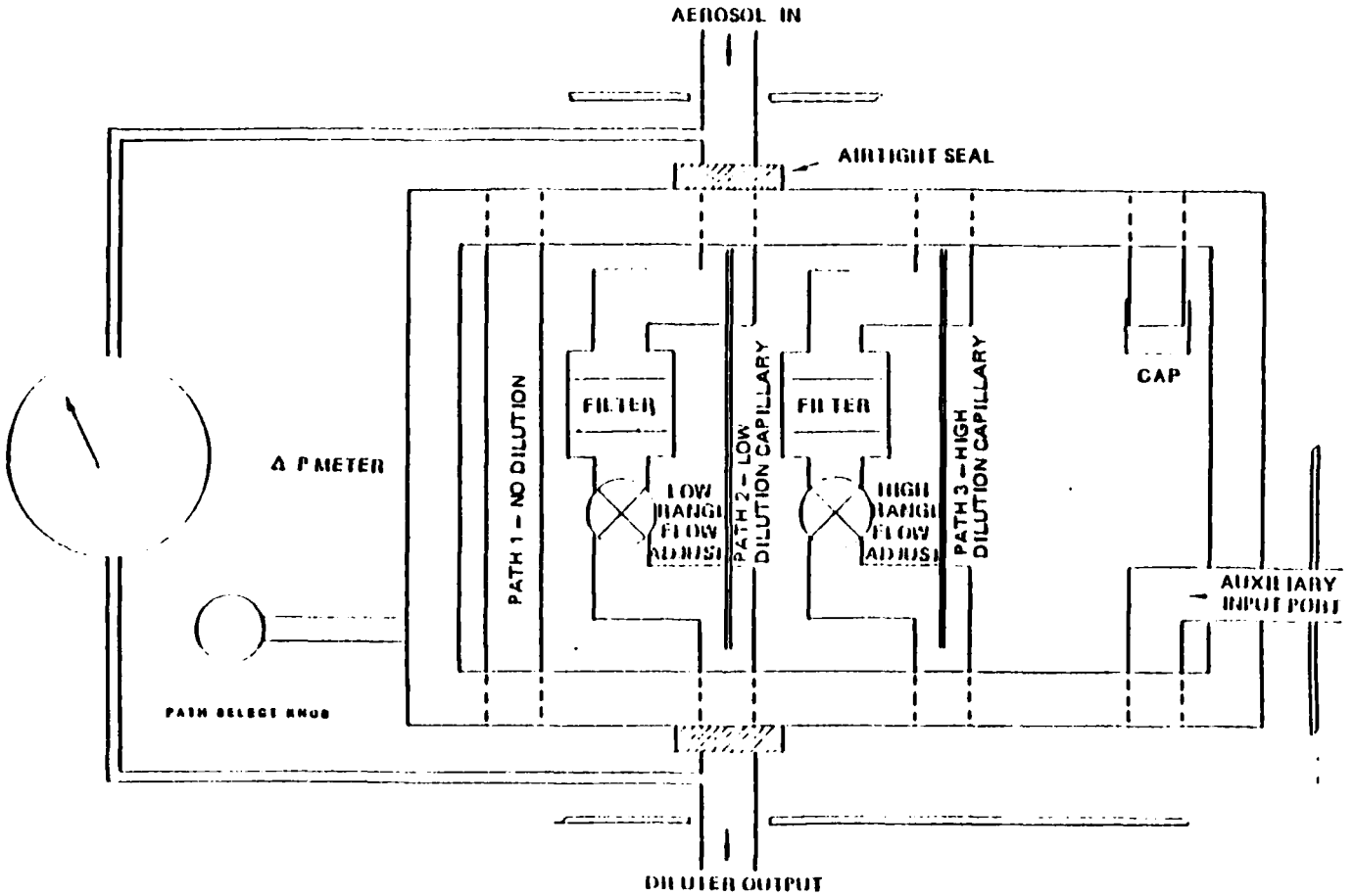

Figure 5. ATEC Diluter System Schematic

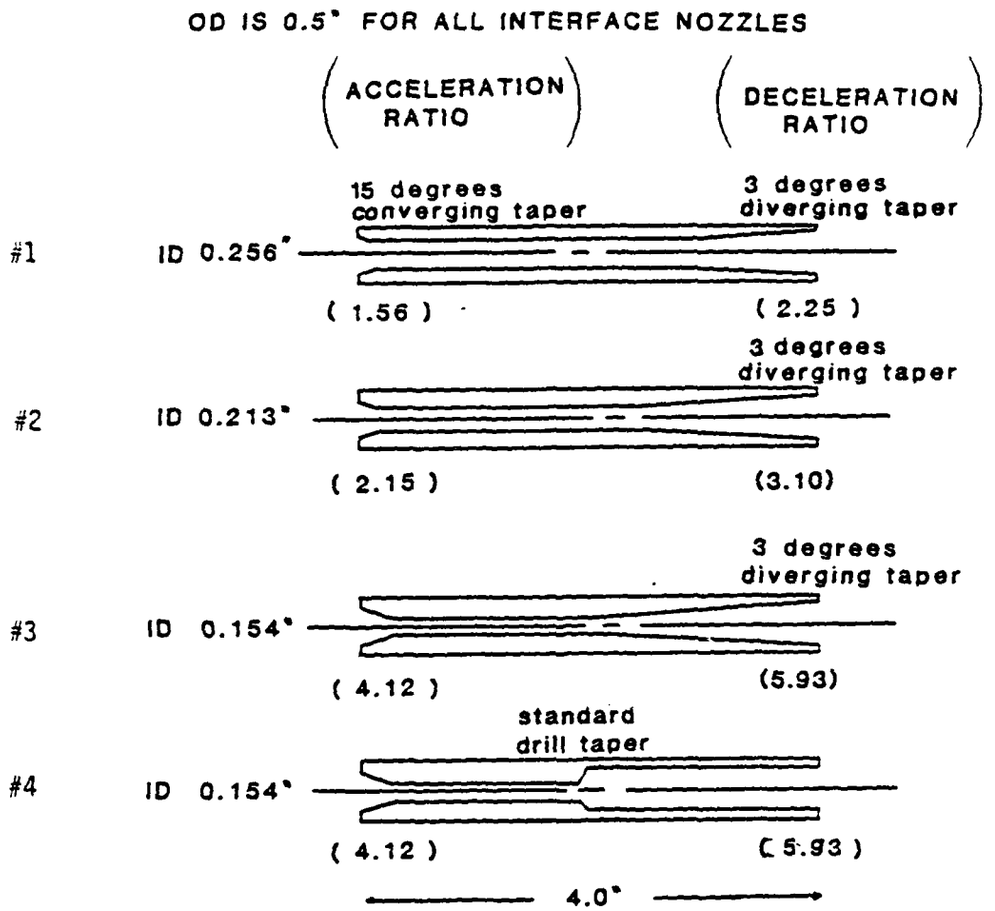

Figure 6. Interface Nozzle Design Profile

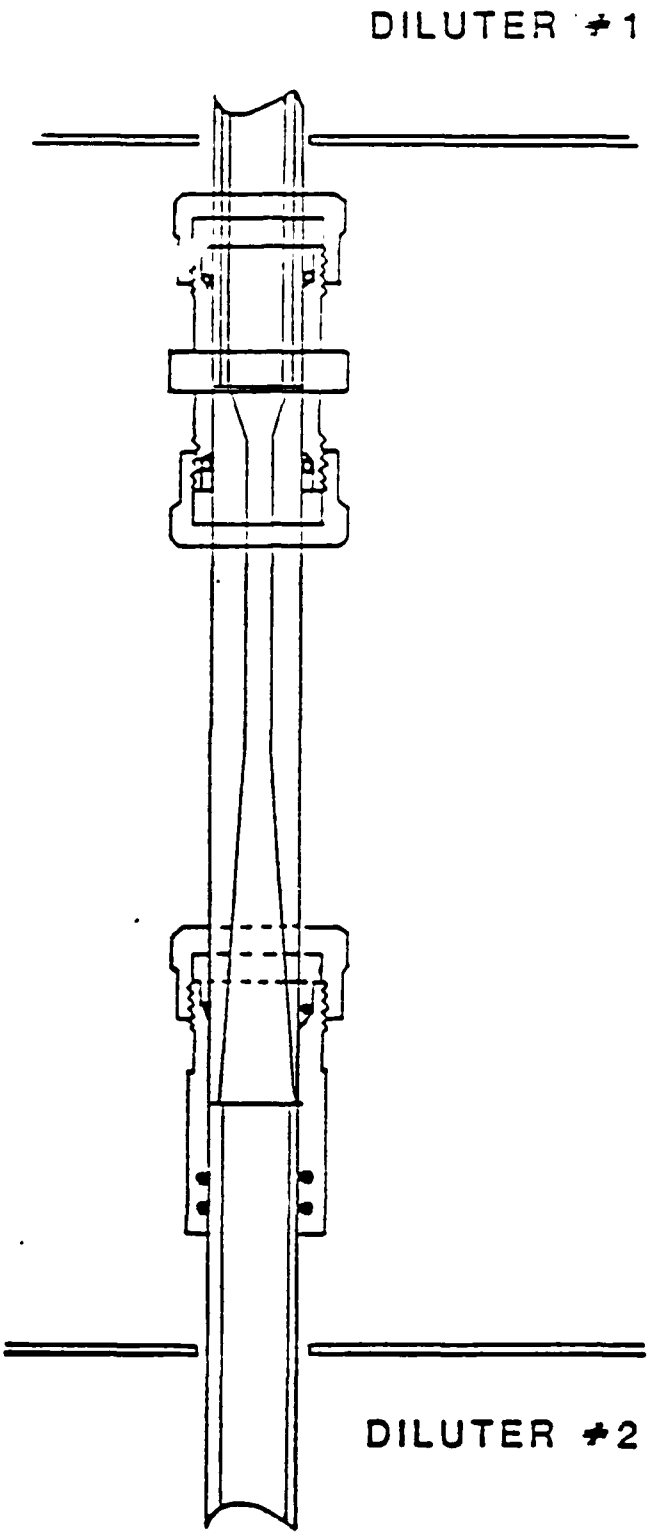

Figure 7. Typical Interface Nozzle Installation

between the two diluters using specially modified Swagelok fittings. Installation of a second interface nozzle to the output of the second diluter is similar.

The second concept, installation of a flow baffle near the capillary output, is illustrated in Figure 8. This technique would be accomplished by installing a convient baffle on the lower end of the capillary prior to installation in the diluter. The variables here include the size of the baffle and its proximity to the end of the capillary tube. A wide range of mixing efficiencies should be acheivable. Again, the primary tradeoff appears to be sample bias.

While the interface nozzles have been incorporated into the system and utilized for system development, no attempt has been made to measure or characterize their effectiveness or their influence on sample bias. Nor has the flow baffle system been tried. For all of the development efforts the #1 nozzle was found to be quite sufficient for the test aerosol sources which were utilized. As a further consideration to minimize bias, the diluters can be set up to operate under isokinetic conditions at each diluter capillary inlet. Based on tubing geometries there are 10 idealized isokinetic inlet dilution ratios available for each diluter (including the 1:1 setting with no capillary and the additional ninth capillary) and 55 unique combination ratios using the tandem diluters. Preliminary calculations indicate that the available idealized dilutions, in addition to the 1:1, are 35:1 through 810,000:1, with a maximum factor of 1.83 between any two possible ratios. The idealized ratios for the 8 supplied capillaries are presented in the Multichannel Nephelometer Instruction Manual.[1]

Non-isokinetic flow at the capillary outlet can also help induce flow mixing of the aerosols ample with a minimum impact on particle bias. This can be achieved without permanent modification to the diluter by reducing the inside diameter of the diluter output tube by inserting a smaller tube into the outlet of the diluter tube. Figure 9 shows such a double-wall tube in the exit nozzle of diluter No. 1.

To prevent unnecessary modification of the input sample, only the essential diluter components have been located upstream of the sampling system probe. All of the air flow control systems are located downstream. After passing the sampling probe, the air is first filtered to prevent contaminaton of the flow controller and pump. The flow controller is located upstream of the pump in the dilution system to ensure total flow control. The pump used in the dilution system is a rotary vane pump which is capable of high flow with very little ripple in the flow. However, there is also substantial seal leakage in the diaphragm pump so the pump so the pump must be located downstream of the flow controller. Additional fillers are located on both the input and exhaust of the pump to mute pulsatious in the dilution system and to reduce noise levels in the exhaust. The filtered dlution system air is exhausted into the room air.

2.2 Sampling System

The sampling system performs a crucial function in the multichannel nephelometer. Its task is to take a sample of the property diluted source aerosol and entrain the particles into a narrow, serial stream through the laser beam. Although this system is

[1] Multichannel Nephelometer Instruction Manual, Contract DAAK11-83-C-0089, prepared for the Army Chemical Research and Development Center, Boeing Aerospace Company, Seattle, WA. May 1986.

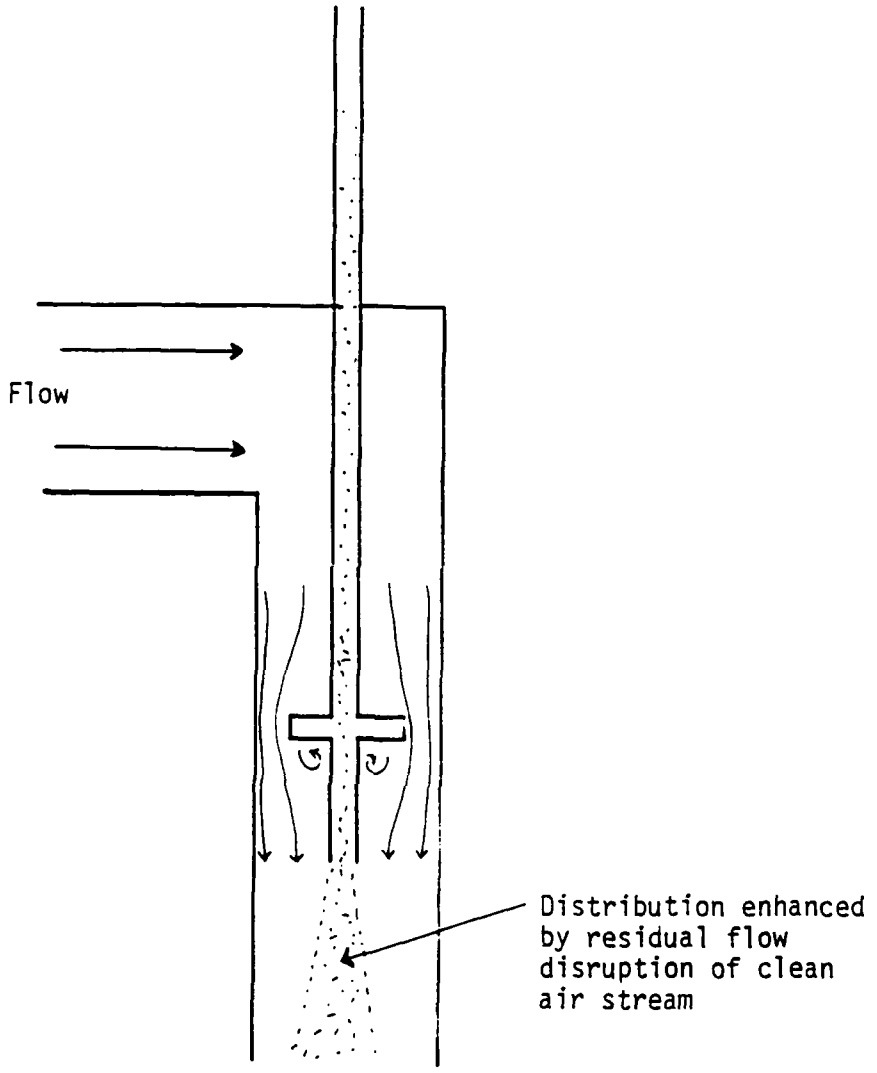

Figure 8. Concept for Increasing Aerosol Distribution in Diluter Effluent by Adding a Flow Baffle Near the Capillary Output

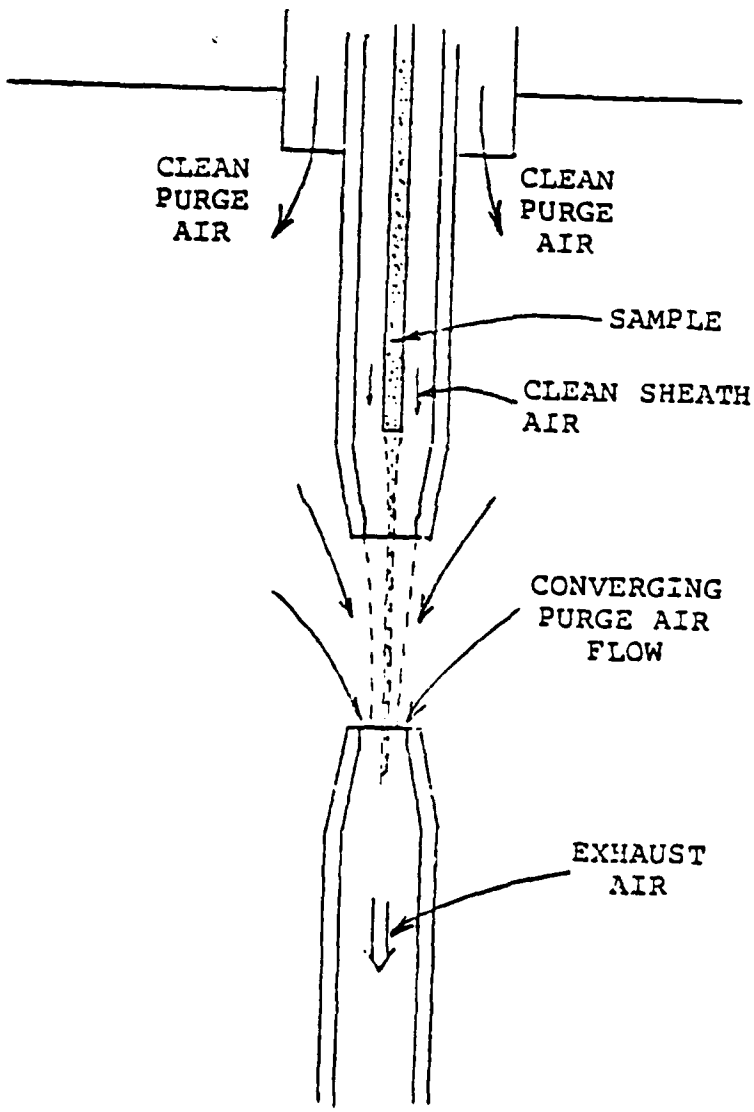

Figure 9. Basic Coaxial Jet Concept

based on proven coaxial jet techniques, it has extended the state of the art by operating at much lower velocities and across wider gaps than had been previously accomplished.

This system has been designed to provide maximum operational flexibility and capability within reasonable system constraints. Some of its more salient features are discussed below.

2.3 Operating Concepts

The basic coaxial jet concepts on which the sampling system is based are illustrated in Figure 9. The sample to be measured is surrounded by a coaxial jet of clean filtered air as it travels between two nozzles. This technique, which is widely used in optical particle counters is most often accomplished using only sheath air although some commercial systems have been based on purge concepts. The nephelometer design was based on the combined use of both sheath and purge air to allow maximum jet stabilization and to maximize the nozzle separation potential of the system. In this system the sample is delivered to the center of sheath flow in the input nozzle through a capillary tube. As the flow exists the nozzle the sample is carried in the laminar flow at the center of the jet formed by the clean sheath air. Although the integrity of the sheath jet diminishes (from the outside in) as the jet passes through the chamber, the jet will enter the exit nozzle before the sample portion is disrupted and no particles will escape to the chamber if the gap is not too large. The purge air, which is delivered to the main chamber cavity, creates a symmetrical converging flow whose influence is strongest at the exit nozzle. It serves in this system to stabilize the sheath flow and significantly increases the distance the jet can travel before the sample flow is disrupted.

Figure 10 is a simplified schematic of the aerosol system and allows easy visualization of the system operating concepts. The dilution system is an independent system whose only interface with the sampling system is the input of the sample capillary tube. In the samping system three flow controllers control the circulation of the air which is driven by the aerosol pumps. Most of the air in the system is filtered and recycled in a closed loop. Generally the largest flow is purge air which generally exceeds sheath air flow by an order of magnitude. A small portion of the filtered flow is exhausted to the room air by the sample flow controller. This creates a partial vacuum within the closed sampling system which serves to draw in a replacement volume of air through the sample capillary. This allows control of the sample flow with minimum interference of the sample stream prior to measurement. All of the flow controllers are based on mass flow measurement principles so that velocity and pressure variations within the system can be ignored by the control system. A more detailed schematic of the aerosol system was given in Figure 4.

2.4 Nozzle/Chamber Interface

One of the critical aspects of the sampling system design was the mechanical interface with the scattering chamber. The size of the scattering chamber was determined by detector system constraints. It is composed of two near hemispheres mounted to a 1" thick mounting plate. This entire chamber must be sealed air tight for proper operation of the sampling system. Further, because the system is so complex, frequent disassembly of the sphere is undesireable. Detectors are mounted throughout the sphere, some coming within 14° of the vertical nozzle axis. This means that vignetting of the light scatter pattern by the aerosol nozzles is also a concern. Established coaxial jet systems normally use small gaps (less than 1 cm) and the size of the achievable stable gap was unknown. It was therefore decided to design the system

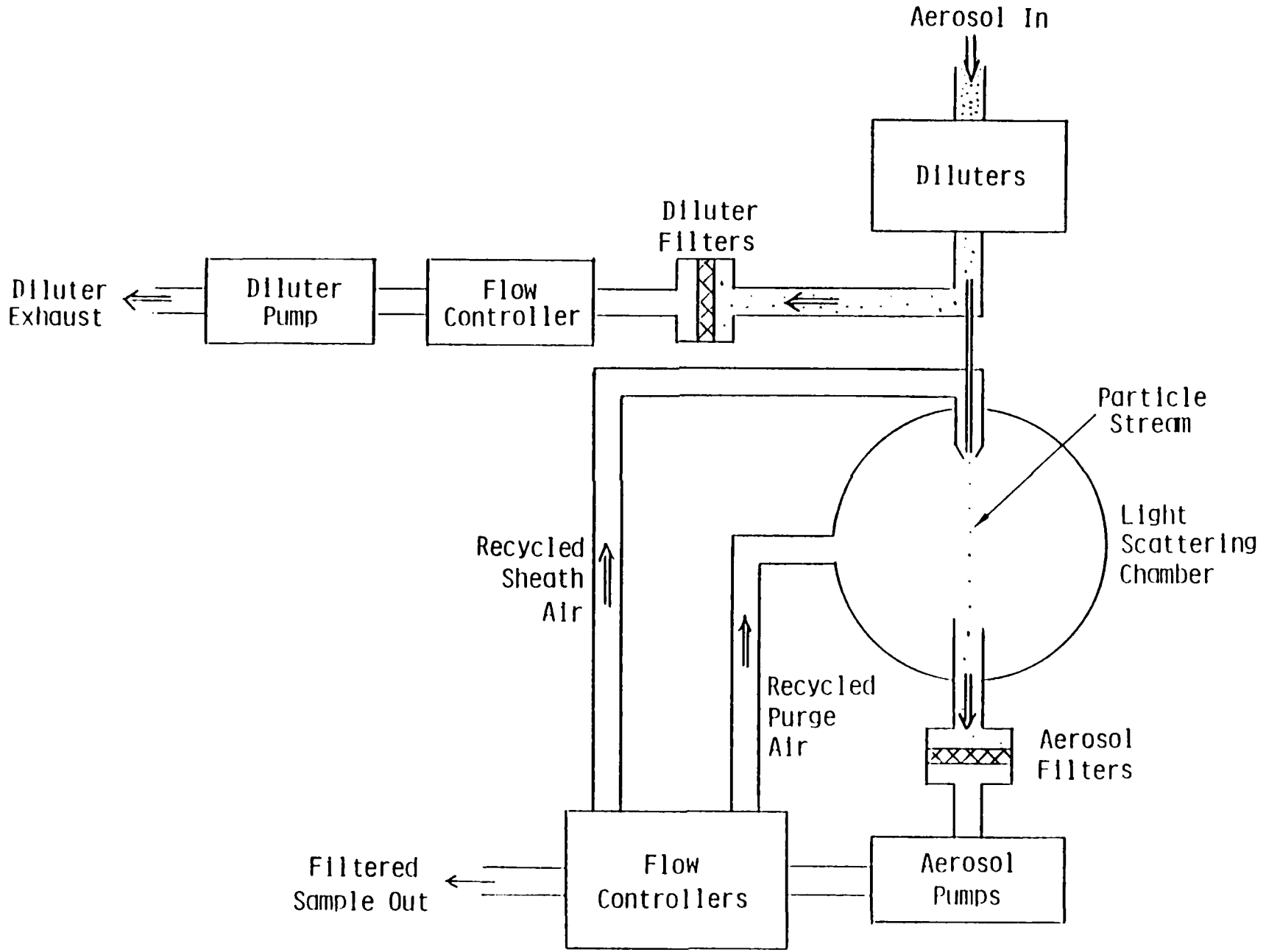

Figure 10. Simplified Aerosol System Schematic

for a minimum nozzle gap of 0.6" with each nozzle capable of 1.5" of adjustment. This would allow nozzle gaps ranging from 0.6" to 3.6" with the additional capability of setting the nozzles to some intermediate setting and shifting the jet vertifcally with respect to the chamber center. This feature might affect the particle presentation in the jet flow and could prove useful, for example, in the control of particle rotation during measurement. The minimum nozzle spacing of 0.6" was set to keep the nozzles out of the brightly illuminated region immediately surrounding the laser beam. Another critical concern was the interface of the shealth air and input nozzle with the sample capillary dilution system flow. Flow through a capillary tube can have a strong effect on the particles in the flow so a short capillary tube is desireable. The size of the chamber and the adjustment range tended to push towards a long capillary. One final consideration was maintaining alignment. The aerosol sample and laser beam must meet in the center of the chamber within the composite viewing volume of all of the detectors or the nephelometer output would be unreliable.

These goals were accomplished using the design concepts shown in Figure 11. The final system was slightly modified from what is shown in this drawing, but the concept is the same. This drawing is essentially a cross-section through the center plane of the sphere mounting plate to reveal how these systems interact. The most critical aspect of this design is the capillary block which fits into a slot cut into the edge of the main support plate.

The aerosol sampling system shown in Figure 11 is essentially integrated into the 1" thick main support plate to which the sensor hemispheres are mounted. A sliding fitting ties the output of the interface nozzle at the output of the second diluter into the capillary block. The sampling capillary shown is a modified version of the diluter capillaries. A set of eight sample capillaries have been provided to allow optimization for different aerosol conditions. The capillary block allows exhaust of the diluter air, input of sheath air, and motion of the input nozzle while keeping the sample capillary length to a minimum. It fits into a milled cutout in the edge of the 1" plate, which allows the capillary block to be brought in closer than the sphere radius without breaking the integrity of the chamber seal. The capillary block also incorporates a vertical fine-adjustment screw and four beveled surfaces that interface with screws in the plate to allow alignment of the capillary block with the output of the diluters. Intrusion into the chamber system is minimized since the nozzles can be adjusted, the sample capillary can be removed, replaced or adjusted, and the entire nozzle system can be removed from the chamber for cleaning without opening the sphere. The exit nozzle flow requirements are noncritical so standard fittings are used and the plumbing does not intrude into the sphere radius. Braces are included inside the sphere for stabilization and alignment of the exit nozzle. The sphere sealing O-ring indicated in Figure 11 is for reference only. The actual sealing rings are continuous and allow continuous seals on both sides of the main support plate. The actual sphere has an inside radius of 4.50 inches and an outside radius of 5.20 inches. It was sized large enough to prevent interference between detectors and yet small enough to avoid further complications in the aerosol system.

The remainder of the sampling system is located on two lower shelves and is tied into the chamber section by lengths of black polyethylene tubing. The black polyethylene was chosen to keep stray light from entering the chamber through any of the sampling system interfaces.

The following discussion centers on the trades involved in the selection of the aerosol sampling system components that control the flow of air through the two flow systems: the diluter flow system and the aerosol jet flow system. The purchased components that control the flow through these two flow systems are in the pumps, mass

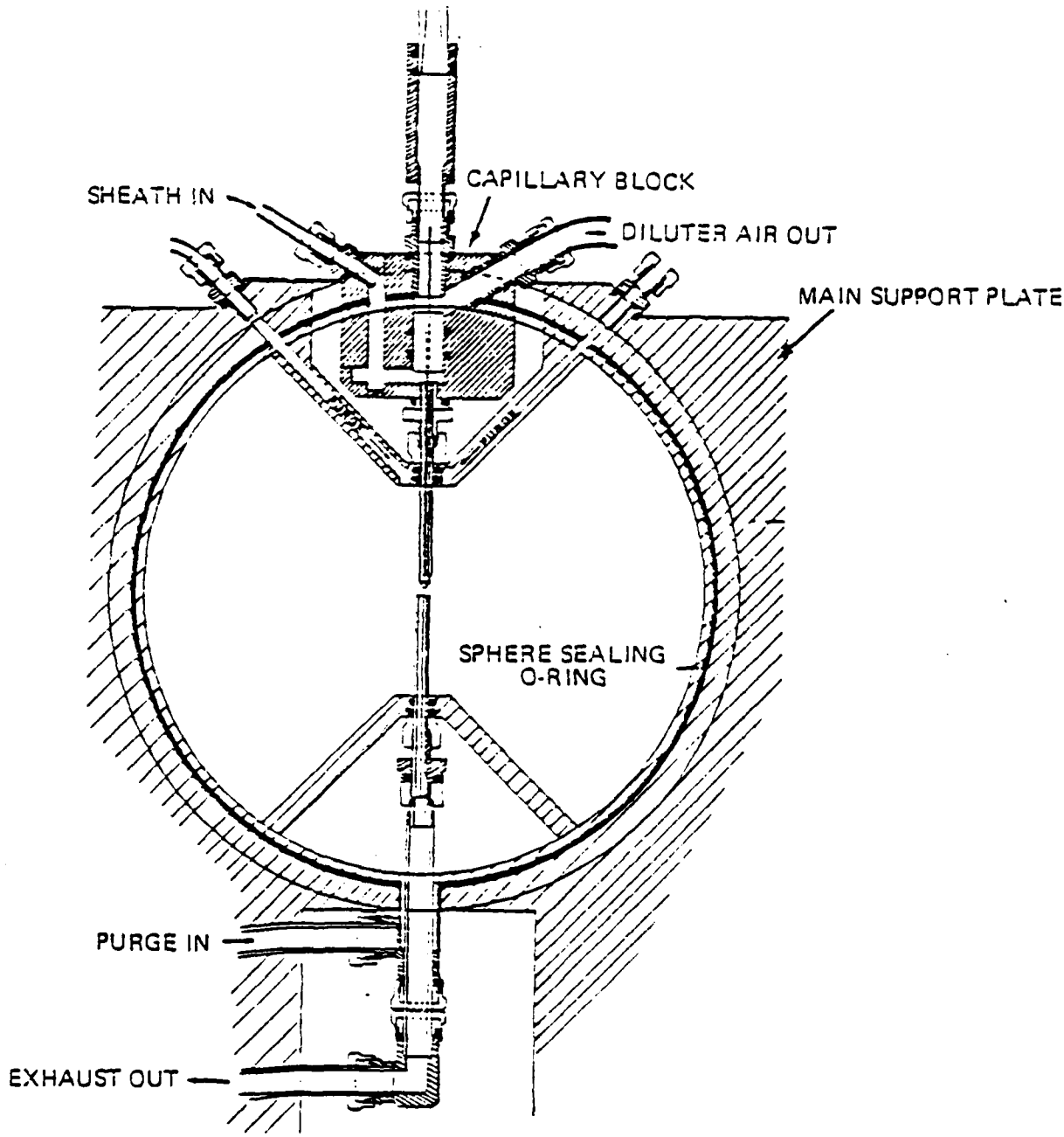

Figure 11. Aerosol Sampling System/Scattering Chamber
Mechanical Interface Concept

flow controllers, and filters. These components must provide even, controlled airflow through the diluters and the aerosol jet systems. They must also filter the air for system output and provide the sheath air and purge air. Table 2 listed the main aerosol sampling system components.

2.5 Air Pumps

The operation principles and, in particular, the control system for sample input makes system sealing a critical feature. Only bellows and diaphragm pumps provide positive sealing for air systems. Since they are operationally equivalent, diaphragm pumps were selected for their lower cost. The main concerns for selecting the pumps used in the system were flow capacity and pulsations. Diaphragm pumps by their very nature generate strong pulsations, one pulse per revolution of the motor. Pump capacity is determined by the pumping volume (per pump cycle) and the number of cycles per unit time.

Pulsations are a concern since pressure variations at the nozzles will create instabilities in the flow and disrupt the aerosol jet. Thus, muting the pump pulsations is a major concern. The first consideration is minimizing the pump pulsations. This can be accomplished by minimizing the total capacity while selecting a pump with a high cycle rate. This leads to selecting a pump with smaller, more rapid pulses that are more readily damped out by other system components to give a smooth flow at the critical points in the system. This lead to the original selection of the two KNF Neuberger diaphragm pumps listed in Table 2, one for the aerosol system and one for the dilution system. During subsequent system development it was found that the pump capacities were insufficient for the required flows. The minimum pulsation advantages for the aerosol system were retained by using both of the diaphragm pumps in the aerosol system and a new low pulsation rotary vane pump was obtained for the dilution system.

The pump operation proved to have a major impact on system operation and will be discussed further under system development.The other techniques which were planned to help suppress the pump pulsations included extra filters, an arrangement called a Quincke tube, plus the effects of the controller restrictions and the tubing volume. These too will be discussed in the Section on system development.

2.6 Flow Control

The airflow through the system is controlled using mass flow controllers which incorporate mass flow meters and accurate flow control valves. Mass flow meters use a heating element and careful heat flow measurement in a calibrated portion of the flow to determine the actual air mass flowing though the meter. These meters are more accurate and consistent than the more common rotometer-type airflow meters which depend on momentum transfer from the air and are therefore subject to errors from temperature and pressure variations within the system. In addition, the output of these flow meters is electrical, which is compared to an electrical set point used to automatically control the airflow. These meters are not subject to friction or other mechanical effects and can be used to monitor flows as low as 0.1 cc/min (0.0017 cc/sec) with a repeatability of +20%. This means that even very low sample flows can be accurately measured.

Flow controllers were selected over flow meters with manual valves for operational reasons. A manual system requires careful adjustment of each valve with the system running until the desired flow values can be obtained. Each fixed-control orifice must also be manually adjusted to compensate for variations as conditions in the system

Table 3. Balston DFU-9933-05 Series Filter Element Characteristics

Grade	Maximum Pore Size[a] (microns)	Gas Filtration Efficiency (%)[b] 10-psi ΔP	Gas Filtration Efficiency (%)[b] 2-psi ΔP	Flow Rate (liters/min)[d] @ 10 in H_2O Pressure Drop	Flow Rate (liters/min)[d] @ 2 psi (55.34 in H_2O) Pressure Drop
DQ	25	93	98	6	85
CQ	8	98	99.8	6	85
BQ	8	99.999	99.9991	4	25
AQ	0.9	99.9999+[c]	99.9999+[c]	2	13
AAQ	0.3	99.9999+[c]	99.9999+[c]	1	6

NOTES:

a. Measured as 98% minimum retention for specified particle size with liquid filtration.

b. These retention efficiencies are measured using 0.1 micron particles and have been independently confirmed by Benjamin Y.H. Liu and Kenneth L. Rubow of the Particle Technology Laboratory at the University of Minnesota.The 0.1-micron particle was used because minimum particle retention efficiency (and this was also experimentally confirmed) was at 0.1 micron.These efficiencies were measured using a high flow to generate a 10-psi pressure drop across the filter and a lower flow rate to produce a 2-psi pressure drop across the filter. The given retention is the worst case measured.

c. Actual particle gas filtration efficiency for these grades is beyond the sensitivity of the measuring instruments. Because of their small pore size and the resulting modification of flow, these filter grades are recommended only as finishing filters for one of the coarser grades.

d. These measurements reflect the relatively low pressure drop across the small disposable filters and show that in all cases it is less than 2 psi. Using BQ filters it will more generally be at or less than 10 in H_2O.

change, such as when changing from a filtered input to the test aerosol. This process is complicated even further since the three flow controls in the aerosol flow system all feed off the same air plenum resulting in significant interaction between them. Thus, the adjustment process would have to be iterated several times to obtain satisfactory settings. This would involve significant effort each time some input or control condition changed, and could be particularly serious if the system was drawing its sample from a limited-volume aerosol chamber. Thus, a manual system requires constant monitoring and readjustment of system settings, and is quite cumbersome.

On the other hand, flow controllers continually monitor the metered mass flow electrically and automatically adjust the valves as necessary to maintain the desired conditions. Interactive effects and system variations are quickly and automatically compensated for, making system operation simple and straight forward. This allows the system to be started up using filtered air and stabilize without introducing contamination onto any of the critical surfaces in the sensor sphere. The system can then be shifted to either a monodisperse particle generator for calibration verification or the test aerosol for the actual measurements. The automatic controllers will adapt to the pressure and other system parameter variations to ensure that the desired flows and flow ratios are maintained.

The Sierra Sierra-Trak^{TM} flow controller system was chosen for its combination of features. This system has a fast response and can operate with input to output pressure differentials of less than 5 psi. The control valves are normally closed when the system is shut down and therefore do not require the use of auxiliary shutoff valves. Other advantages include a straight, easy-to-clean measuring capillary and a high-quality five-channel microprocessor controlled control system.

2.7 Filters

The filters called out in Figure 4 fulfill three requirements. Those shown at locations marked "A" are the primary filters. These filters trap most of the aerosol particles before they enter the pump to prevent contamination of the aerosol flow systems. These filters also help to dampen the pump pulses on the suction side of the system. The secondary filters shown at locations marked "B" and "C" provide backup filtraton to ensure total trapping of the aerosol particles before the air is exhausted to the laboratory. They also muffle the pump prior to exhaust, dampen the pump pulses on the pressure side of the system, and trap any particles released from the control system or mass controllers. After careful evaluation, depth-type coalescing filters from Balston Filter Products were chosen.

A depth-type filter uses a combination of predominately Brownian motion effects for particles 0.1 micron and smaller and predominately inertia effects for particles 0.1 micron and larger to trap particles using Van der Waals forces on a relatively deep, open pore microfber mesh. This results in a very efficient filter with low pressure drop and relatively slow loading, with a consequently long filter element life. Depth filters also have a distinct advantage when the test aerosol contains a significant quantity of liquid. Membrane filters tend to load and reduce throughout while increasing the probability for re-entrainment, while depth filters act as coalescers, drawing the liquid away from the filter and preventing loading and re-entrainment. These filters are rated for gas operation using 0.1 micron aerosols (they are least efficient at 0.1 micron because of the crossover between the two trapping mechanisms). A summary of the available Balston DFU-9933-05-BQ disposable filter grades and their charactistics is given in Table 6. As indicated, these filters can be estremely efficient. Should absolute retention be required, the AAO grade filter with a pore size of 0.3 micron can be used at the

secondary filter locations: however; for normal operation it is felt that the use of BQ grade filters at all locations will prove more than adequate.

When the system was operated using dense input aerosols the small primary filters loaded up fairly quickly and required frequent replacement. Larger DQ grade (93-98% trapping effiency) prefilters were added to both systems just ahead of the original filters. The primary filters are now two stage filters. Loading and replacement is now much less frequent and general filtration efficiency is improved.

2.8 Scattering Chamber Table

The aerosol system, laser, and optics closely associated with the scattering chamber require careful alignment to maintain proper operation. This is best accomplished by mounting all three systems on a comman table. Because the multichannel nephelometer is a laboratory device, major consideration has been given to operational access and flexibility. For operational access, the system must allow reasonably easy system adjustments and setup modifications yet avoid external connections and hookups that make movement about the apparatus more difficult. To maintain flexibility, the system should include ready space and mounting provisions for experimental laser optics, additional space for associated equipment, and simple relocatability for experimental reconfiguration.

A three foot wide by six foot long four inch thick laminated honeycomb tabletop was selected as the basic table surface, allowing sufficient space for the fixed chamber apparatus plus space for laser optics. The tabletop has mounting holes on one inch centers, permitting ready mounting for the fixed equipment and flexible mounting for the laser optics. This tabletop has sufficient stability and damping capability to ensure proper alignment of the critical systems. This is a shelf above the tabletop to support the aerosol diluters and two shelves below to support the laser, detector signal interface box, aerosol control systems, and laser power supply.

The combined aerosol, laser, chamber, and table system weighs approximately 1000 lbs. If it were permanently fixed in place, the nephelometer would not have the flexibility desired in a laboratory device that must be used in different experimental setups. Therefore, provisions were included for a retractable caster and leveling system on the table. The weight distribution of the assembled system was also considered from a stability and safety aspect. The three heaviest items are the tabletop, laser power supply, and laser head which, since they are mounted fairly low, contribute to a relatively low center of gravity. An estimated weight analysis indicates that the center of gravity of the entire system is within the tabletop at about one third of the total height. The legs were designed to stay within the size outline of the tablestop yet with a relatively wide stance for maximum stability.

The height of the assembled system was constrained principally by the aerosol sampling system design above the scattering chamber. Straight, minimum-length aerosol flow paths were traded against physical constraints on the chamber size, detector locations and interfaces, diluters, and interface techniques. Below the scattering chamber the thickness of the tabletop, height of the laser head and power suppply, and caster clearance were the factors which determined final system height. The tabletop is at a comfortable working height of 32 to 33 inches above the floor, and the top of the diluter cabinet is about 96 inches (about 8.0 feet) high. When the assembled system must be moved through doorways, the 33 inch high diluter cabinet can be removed and replaced relatively easily.

2.9 Svstem Development

Development of the aereosol system proceeded in two stages. Prior to assembly of the main nephelometer unit, the aerosol system components were assembled on a bench to ensure the system was functional prior to integration with the rest of the system. The second stage was completed after the system had been integrated into the nephelometer in its final configuration. We will discuss each of these separately below.

As soon as all of the necessary parts were available, the aerosol system was assembled on a bench to verify its operaton. Clear plexiglass covers were used to simulate the scattering chamber and allow visualizaton of the aerosol jet for system development. A dense sugar aerosol from a T51 tri-jet aerosol generator was used to visualize the aerosol portion of the nozzle jet flow. Of particular concern were factors such as airborne pulsations, component interactions and verification of system configuration. The techniques planned for pulse suppression included Quincke tubes, extra filters, controller restrictions and tubing volume. To accomplish full checkout, the system was assembled with the approximate tubing lengths and hook-ups that were expected to be used in the final system.

The Quincke tube is a simple arrangement where the flow is divided evenly between two lines of different length and then recombined. The goal is to split the flow and then recombine it out of phase to obtain pulse reduction. The output of a diaphragm pump is limited to half of each cycle so pulse cancellation is not possible. However, if the contributions from the long branch of the Quincke tube can be delayed for one half cycle, the pulsations can be interspersed and rendered easier to mute, much like the difference between a half wave and a full wave rectifier in electronics. While the variable flow velocity in the tubes has an effect on the effective pulse length, this contribution proved to be quite small when compared to the sonic velocity in the tubes and was ignored. With a cycle rate of 3200 rpm (Table 2) and a nominal sound velocity of 1100 feet/sec a sound pulse should travel just over 20 feet between equal points in a cycle. The longer branches in the Quincke tubes were therefore set a little over 10 feet longer than the short branch to give an approximate offset of one half cycle.

The filters help mute pulses through two mechanisms. The filter media itself acts as a flow restriction which evens out the flow while the filter chamber acts as a small chamber which complements this muting effect. A filter is associated with each Quincke tube to provide a muting effect to compliment the equalization effects of the Quincke tube. The constrictions present in the flow controllers also help to smooth out the pump pulsations. Additional filters are located at the output of both the purge and sheath controllers to complement their effect. Finally, different tubing sizes were used for the various tubing runs between the sphere and aerosol systems. This helped prevent incorrect hookup and also increased the overall system volume to help to further smooth out the pulsations.

When the system was first assembled it was possible to obtain a semi-stable jet, but neither pump was capable of producing the maximum desired flow rates through the system. It was decided to combine both diaphragm pumps into the aerosol system and obtain a rotary vane pump for the less critical open loop diluter system. During subsequent development it became apparent that both airborne pulsations and structural vibrations have a marked effect on jet stability. The use of two smaller diaphragm pumps in place of a single larger one proved to be a serendipitous arrangement which helped make achievement of a stable jet traversing a wide nozzle gap possible. Figure 12 shows the aerosol pumps and flow controllers in the development set-up. Figure 13 shows the main support plate and scattering chamber elements with a dense sugar

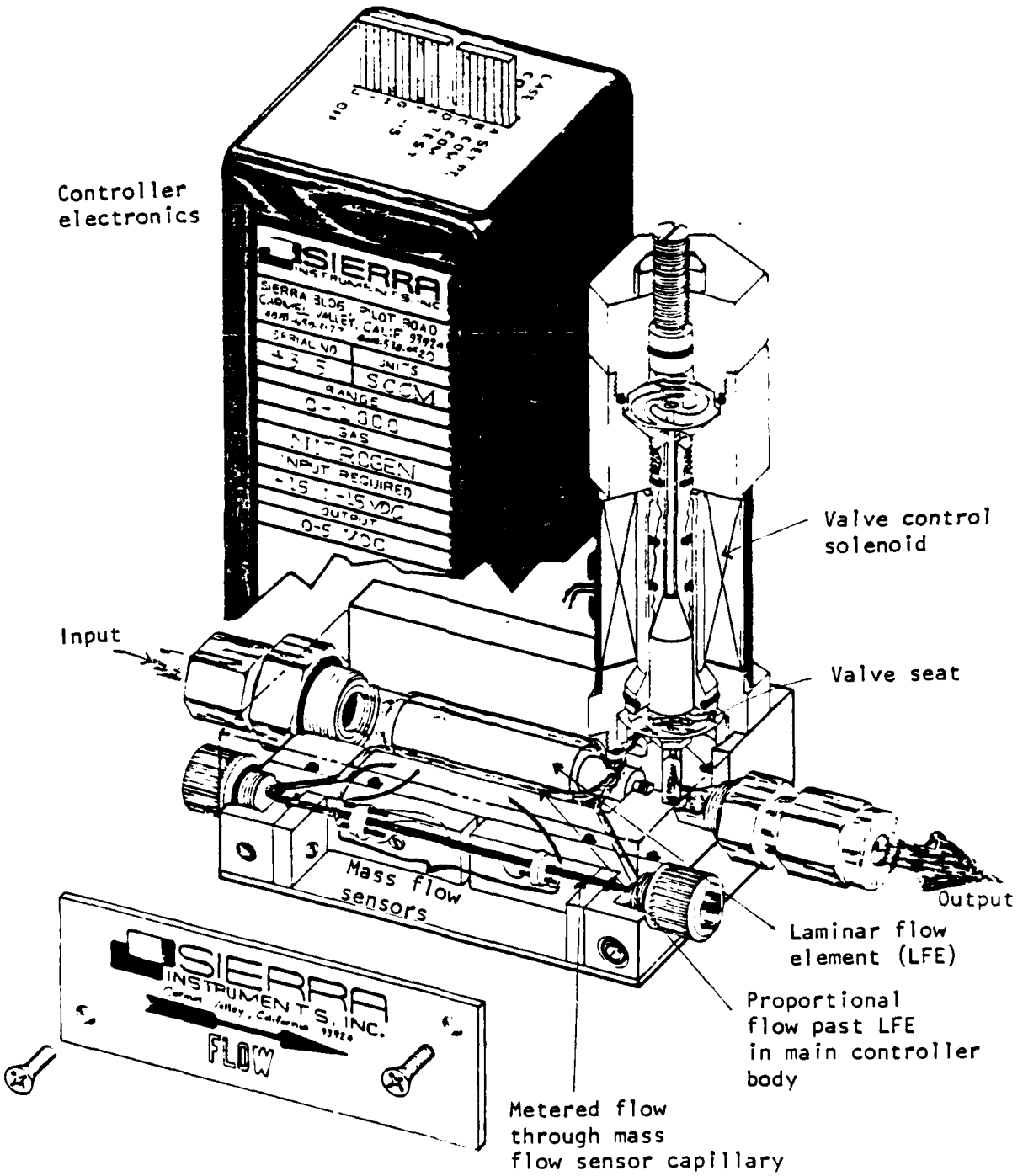

Figure 12. Sierra Side-Trak Flow Controller

Figure 13. Aerosol Pumps and Flow Controllers in Table Top Developmental Set-up

aerosol crossing the gap inside the plexiglass chamber. The final sampling system configuration is diagramed in Figure 14 and features the two unequal diaphragm pumps operating in series with the larger pump issuing into the smaller one. Quincke tube and aerosol filter combinations are used before, between, and after the pumps and serve to mute the strong pump pulsations and reduce feedback between the pumps. This configuration produced the desired steady flow rates with very low accompanying pulsation levels at the chamber inputs. Several other pump configurations were tried unsuccesfully. One such configuration was the pumps-in-parallel arrangement shown in Figure 15 that was basically equivalent to a single, larger pump (with the better, higher pulse rate feature available only in the smaller pumps). We were not able to make careful measurements to confirm our hypothesis, but after careful evaluation of the different configurations and their results, we believe the system operates basically as follows.

The aerosol sampling system consists of a closed-loop system with pumps, filters and controls; a large sample chamber; and a controlled drain to draw new sample into the loop. At the low flow rates we are dealing with, the control systems (i.e., the sheath and purge flows in the chamber) are effective but not extremely powerful. Without a disrupting influence they are capable of maintaining a stable aerosol stream across very large gaps. However, if the jet is sufficiently disrupted, the control systems are overcome, the jet breaks down, and aerosol is distributed throughout the chamber. One confirmed disruptive influence is vibration, either from structure or through the air stream. The pump pulsation effects, a steady airborne vibration, appear to be very significant and, even when greatly reduced, are capable of disrupting the aerosol jet.

The large volume viewing chamber with its relatively small ports has a very strong damping effect on pulses due to the inertia of the air within the chamber. This effect is similar to that of a choke coil in an electric circuit and its influence on the jet increases as the nozzle spacing is increased. This characteristic can be either an asset or a liability, depending on the relationship with the rest of the system. In a closed-loop system where there is a region of pressurized air and a region of partial vacuum, there are of necessity two null points where the system transitions between the regions of pressure and vacuum. One is near the pumps and the other is opposite the pumps in the loop. It is the null opposite the pumps with which we will be concerned. Depending on the exact location of these null points in the closed circuit, the chamber can be made to be driven predominantly by vacuum, pressure, or a mixture of both.

Because of the inertia of the air in the chamber, the relationship between the null point and the chamber has a crucial effect on the stability of the jet. If the null point is in or beyond the chamber, the jet is driven by pressure and the chamber air mass acts to resist the residual pulsations in the input airflow. This increases the influence of the pulsations on the input flow patterns, disrupts the laminar flow, and prevents the formation of a stable jet (c.f. the pumps-in parallel configuration in Figure 15. However, when the system is reconfigured in such a manner that the null point is located before the chamber as in the final pumps-in-series configuration shown in Figure 14, the chamber is then driven by vacuum and the chamber air becomes an asset. Vacuum pulsations at the exit nozzle are not critical and do not serve to scatter or disrupt the jet. The already muffled vacuum pulsations at the exit nozzle are totally muted by the chamber volume and the vacuum energy delivered to the chamber inputs ports is steady. This pulseless flow creates and maintains a steady, stable jet. It therefore becomes imperative to configure the system to operate with the chamber in this vacuum-driven mode. Using two smaller pumps in series makes this much easier to accomplish.

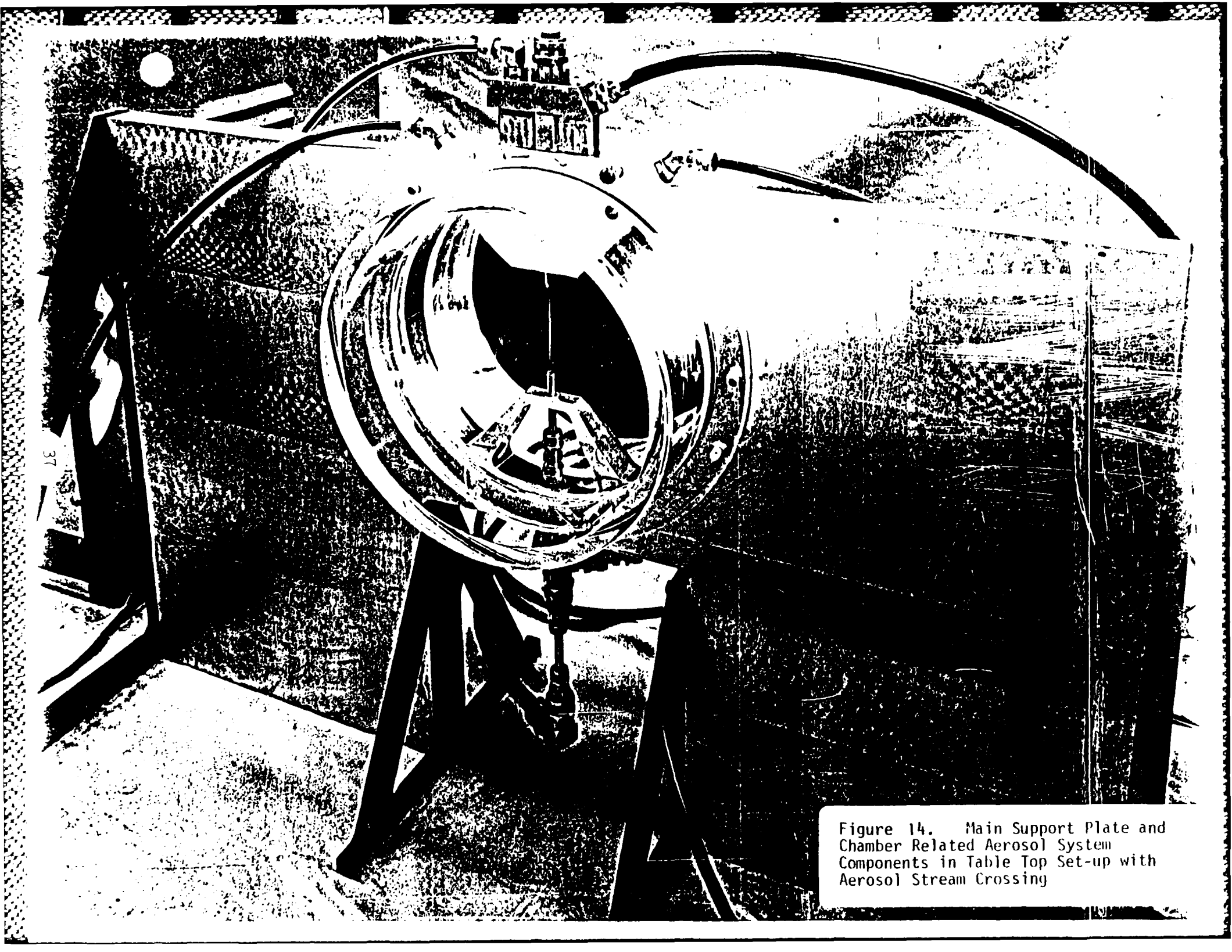

Figure 14. Main Support Plate and Chamber Related Aerosol System Components in Table Top Set-up with Aerosol Stream Crossing

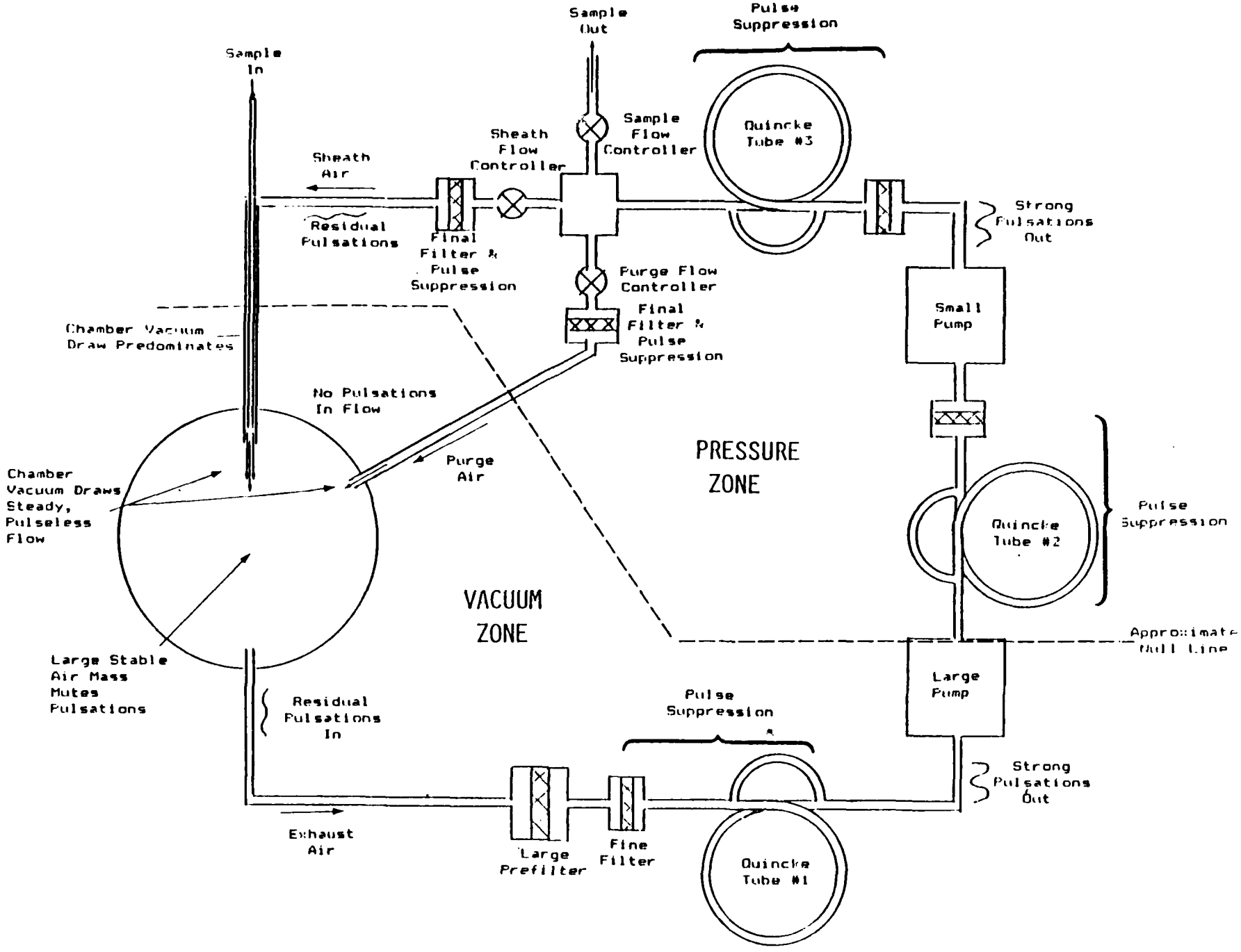

Figure 15. Final Pumps-in-Series Aerosol System Configuration (Stable Jet)

One inherent characteristic of diaphragm pumps is that they push harder than they pull. These pumps push approximately 40-50% harder than they pull. As a result the null opposite the pumps is offset farther from the pump outputs and closer to the input, increasing the portion of the aerosol circuit that operates in the pressure-driven regime. The system as designed puts most of the flow resistance load between the pump outputs and the chamber, which helps to shift the chamber towards the vacuum-driven region. To be effective, the chamber must be totally in the vacuum-driven region. The system loading is insufficient to accomplish this with a single pump or pumps in parallel. Putting the pumps in series, with the strongest first, shifts the null points and reduces the peak pulsation levels sufficiently that when combined with the system loads, the chamber is brought totally into the vacuum-driven region of the circuit, creating a stable, reliable jet. Figure 16 shows a close-up of a stable aerosol jet crossing a gap exceeding 6 cm with an estimated velocity of less than 10 meters per second using the final pumps-in-series configuration of the developmental set-up. The dense sugar aerosol is made visible by backlighting from a microscope illuminator located behind the main mounting plate.

Final development of the aerosol system was completed after the system was mounted into the main nephelometer unit. When the system was initially installed, all three of the pumps were securely mounted to the bottom shelf of the nephelometer table. With the pumps mounted securely to the bottom shelf, the pump vibrations were strongly coupled into the optical table support structure and transferred to the light scatter chamber and aerosol nozzles. These strong vibrations were sufficient to create disturbances in the aerosol jet, and necessitated changes in the way the pumps were mounted. The pumps were subsequently suspended from the bottom side of the laser shelf using a combination of plastic strap clamps and 0-rings or polyurethane belts to decouple their vibration from the table. Since the vibration of the diaphragm pumps is primarily in the vertical pump plane, they were rotated 90 degrees prior to being mounted. The rotary vane pump was mounted to a similarly suspended plywood shelf. The hose connections between the pumps and the firmly mounted parts of the system were also replaced with soft tubing as a further vibration isolation precautionary measure. Subsequent tests of the aerosol jet stability showed that these measures have successfully isolated enough of the vibration. The remaining vibrations, which appear to arise primarily from air pulsations in the tubes being coupled back into the table, are not sufficient to disrupt a properly configured jet. The final mounted configuration is shown in Figure 17.

The decision to use diaphragm pumps instead of vane-type impeller pumps was verified as crucial in terms of allowing precise measurement and control of flows within closed-loop aerosol sampling system. The rotary van pump used in the diluter system was originally located upstream of the diluter flow controller where the diluter pump would have operated. When the diluter system was operated in this configuration it was impossible to get the desired diluter operation and it became apparent that the diluter flow was too high. It was then decided to determine how much leakage there was in this pump. The flow controller, still located downstream, was closed to block the pump exhaust. Evaluation of the diluter system set-up and meter readings indicated that the pump was still drawing in more than 6 liters per minute. This flow was apparently being exhausted around the pump's seals. While pump leakage poses no problem in the open-loop diluter system, this kind of leakage would have been unacceptable in the closed-loop aerosol sampling system (where all flows combined are less than the measured leak rate of the rotary vane pump). The diluter pump was subsequently relocated downstream of the diluter flow where pump seal leakage has no impact on the diluter system.

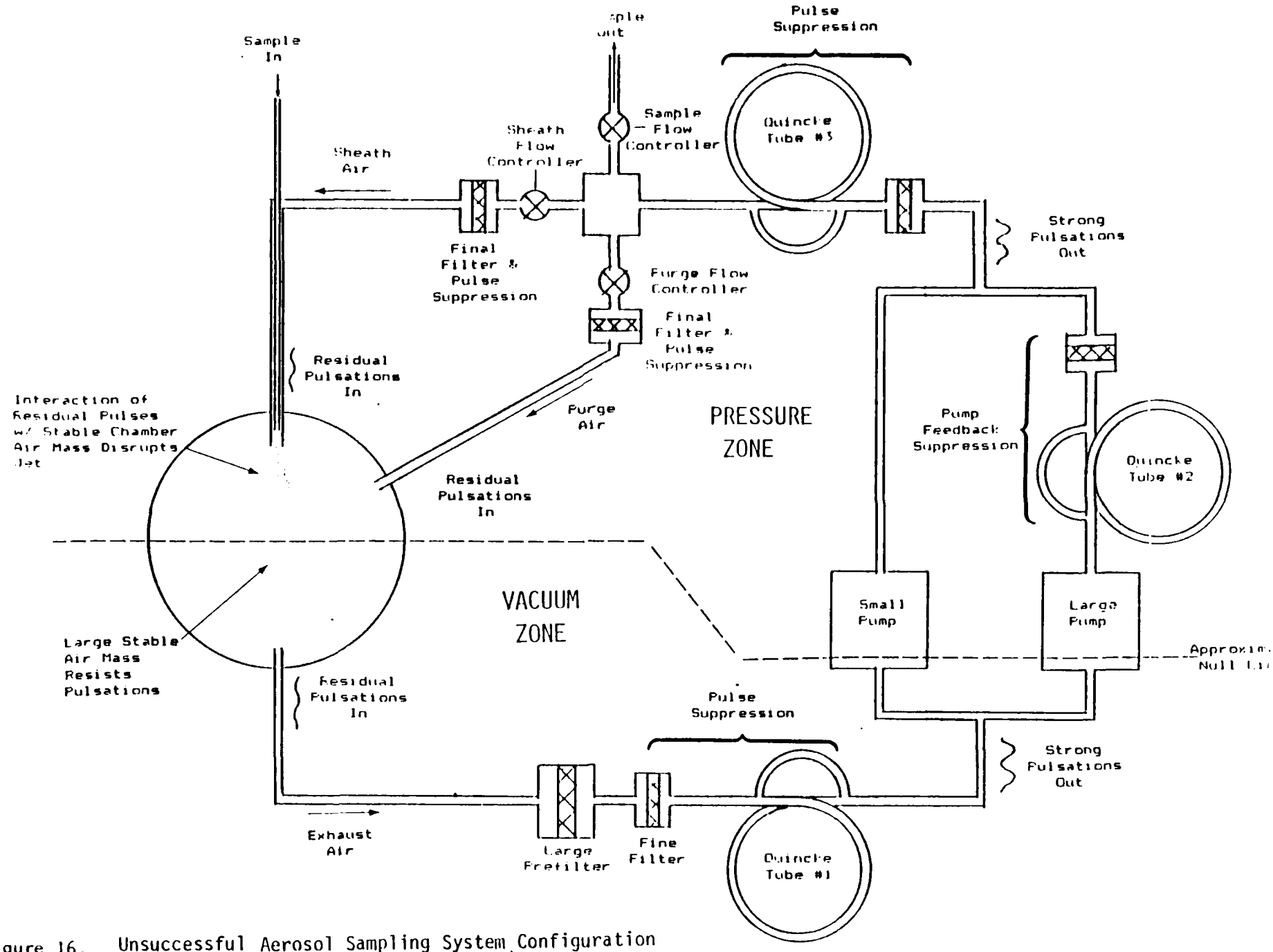

Figure 16. Unsuccessful Aerosol Sampling System Configuration Pumps-in-Parallel (Disrupted Jet)

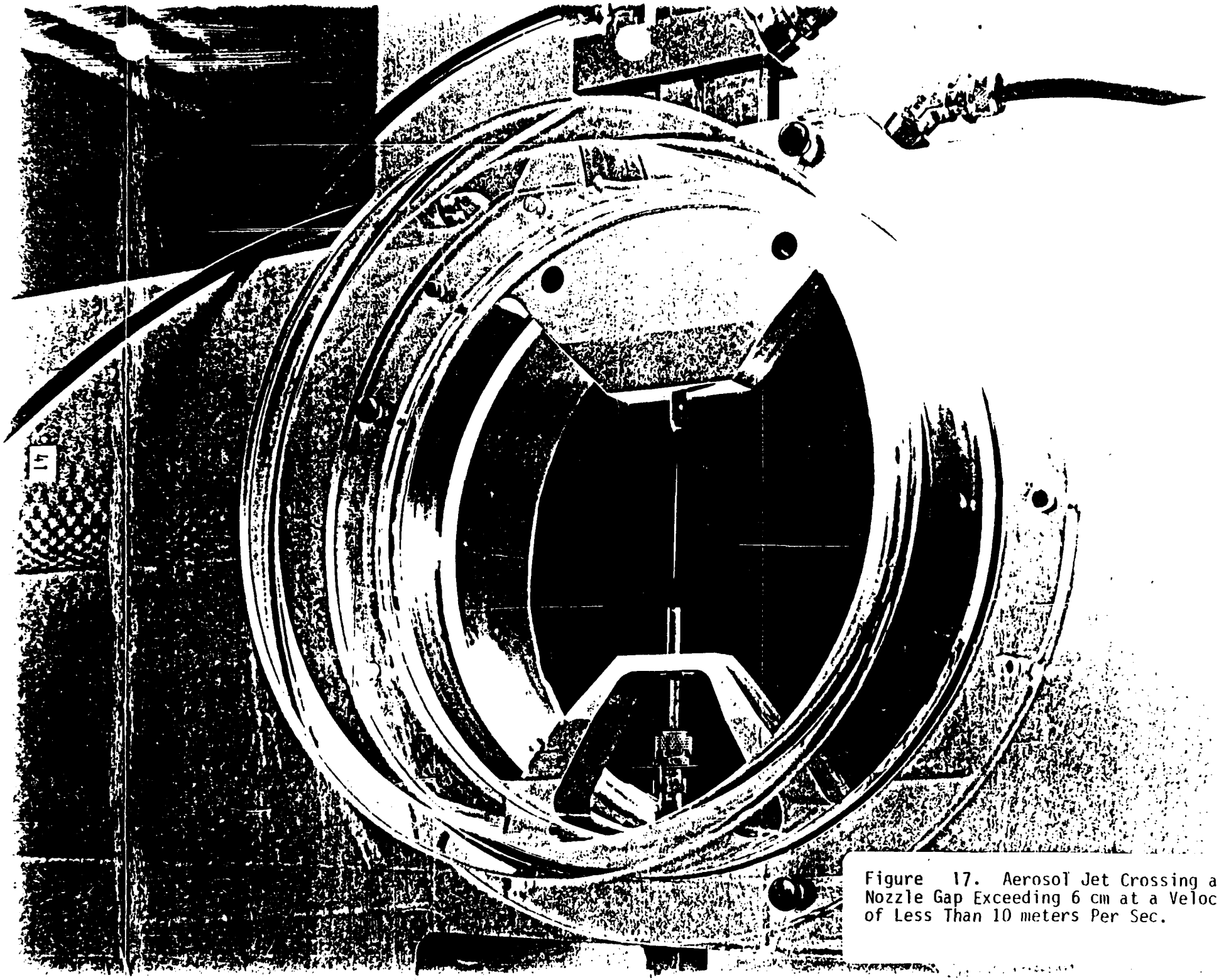

Figure 17. Aerosol Jet Crossing a Nozzle Gap Exceeding 6 cm at a Velocity of Less Than 10 meters Per Sec.

A series of tests was performed on the assembled sampling system to determine the range of diluter, sample, sheath, and purge air flows which produce the most stable aerosol jet. These tests were performed using the transparent plexiglass covers on the light-scattering chamber and a dense aerosol to facilitate observation of the jet. We were able to generate a clean, nondiffusing, stable jet with a cross-section of less than 0.2 mm across a 3.6-inch gap (the maximum possible in this system). The velocity of this jet was calculated to be 3 to 4 meters per second. It was found that if 1) flows were fast enough to avoid deflection by residual air currents in the chamber, 2) the aerosol portion of the jet was not too big around and 3) the jet velocity was low enough to avoid turbulance, then the jet remained stable.

The aerosol jet stability is a function of aerodynamic parameters related particularly to aerosol sample diameter and velocity within the jet. The effects of diluter, sample, sheath, and purge air flows are important in that they influence these jet aerodynamic factors. At velocities below one meter per second, the jet is very laminar but starts to deviate from a straight line flow because of minor flow currents within the scattering chamber. Above about four meters per second, the sample portion of the jet begins to encounter turbulence that diffuses aerosol particles into the chamber. The outermost portions of the jet (clean sheath air) start to diffuse shortly after leaving the upper nozzle but are unimportant so long as only the clean air portion of the flow is disturbed. Thinner jets (which have a lower Reynold's number) remain stable for greater distances. The aerosol flow can be thought of as a smaller, coaxial jet and as its diameter is decreased the location of turbulent disruption moves toward the exit nozzle. Jet turbulence in the aerosol must be avoided to prevent contamination of the optics and inside surfaces of the light scattering chamber. These tests were performed with the nozzles at maximum spacing to allow observation of jet breakdown within the operational limitations of the system. As the nozzles are moved closer, the operational limits increase since the stability requirements are reduced.

The purge and sheath air flows directly influence jet diameter and velocity and both are needed to stabilize the jet. One of the tests that was run on the system was to investigate jet operation with only sheath or only purge air flow. While total particle entrainment across a much smaller gap was possible with either system, the jet characteristics were significantly degraded. A stable, well controlled, aerosol jet across a fairly large gap was possible only when both the purge and sheath systems were operating. When these flows are properly adjusted, a high-quality jet can be generated across the full 3.5 inch gap.

After the final aerosol jet development had been completed and the scattering chamber hemispheres had been assembled with their detector assembles, the aerosol system was tested using the true chamber configuration. Operation of the aerosol system in the true scattering chamber configuration proved the importance of sealing in the operation of the aerosol jet. All of the exterior seals on the detector units have good compression seals to prevent leakage. The weak point in the detector assemblies are the seals around the lenses or windows where retention of snap rings provides only limited compression. The sealing in the individual detectors is backed up by additional seals under compression in the removable photomultiplier unit and present no problem. However, the dry seals in the four array units have no backup and the leakage was too high for proper aerosol system operation. The aerosol sample must be drawn into the chamber through a 6" long capillary from the diluter system where the pressure is slightly below ambient. As a result, the pressure differential required to draw in the aerosol sample is significant, and if any chamber leaks are present they will supply the required input flow with less resistance and no aerosol sample will be drawn into the chamber. The dry 0-ring seals in the array detector assemblies were tested and found to

have significant leaks. These seals were coated with apiezon grease to create a good low pressure seal. This restored proper operation of the aerosol jet.

2.10 Charge Neutralization

While excess electrical charges on aerosols may not present major problems in chamber tests, they can become significant in aerosol sampling systems, such as the multichannel nephelometer, where aerosols must be transported through restricted channels. These electrical charges can be quite high. For example, 3.75 micron aerosol droplets from a vibrating orifice aerosol generator have been measured with average charge loadings of as many as 7300 electrical charges/particle. These charges cause increased particle deposition and can have a significant impact on the aerosol throughput of the system. This problem is generally averted by deionizing the aerosol prior to passing it through the sampling system. Typically, a radioactive source such as Kr-85 or Po-210 is used to ionize the gas carrying the aerosol. The charged particles than draw the appropriate ions to neutralize their charge. Depending on the strength of the radiation source and the aerosol flow rate, the aerosol electrostatic charge can be effectively eliminated. This process allows the aerosol to be deionized without significant impact on the nature or composition of the aerosol.

The multichannel nephelometer has no provisions for ensuring deionization of the aerosol, and the extent of the potential problem is highly dependent on the charges resident on the source aerosol. For the purposes of this program, a neutral input aerosol was assumed. However, since source aerosol charging could affect operation of the multichannel nephelometer it should be considered when using this system.

3.0 LIGHT SCATTERING SYSTEM

This Section describes the light-scattering chamber with its associated laser system and detector assemblies. It is in the light scattering chamber that the central function, measuring the light scattering pattern of non-spherical aerosol particles, is performed. This system includes the laser system, light scattering chamber, individual detector assemblies, and array detector assemblies. Each of these will be discussed separately below. Relevant system requirements are listed in Table 4, along with the features of the designed system that satisfy that requirement.

3.1 Laser System

The laser system includes the laser and its power supply, laser optics, and laser safety enclosures and switches. The basic layout of the laser system on the main nephelometer table is shown in Figure 19. The laser head is mounted on a shelf just under the main table surface. It has an umbilical which ties it to the laser power supply which is located on the bottom shelf of the main nephelometer unit. For safety, the entire path of the laser beam is enclosed since the unmodified laser beam is potentially hazardous for eyesight or skin exposure. Two beam steering mirrors direct the laser beam up through the table and into the chamber. The upper beam steering mirror is adjustable to allow accurate alignment of the beam with the center of the light scattering chamber. Additional optics can be added to the beam path under the upper beam cover either before or after the upper beam steering mirror. After passing through the light scattering chamber, the beam is dissipated in the laser beam dump. Several safety switches are provided in the system to minimize the possibility of accidental exposure to the laser beam.

Table 4. System Requirements for Light Scattering Chamber

Requirement	Design System Features
Particles range in size from 0.3 to 10 micrometers with albedo greater than 0.5	Spherical water and carbon particles in the specified range were used to calculate expected scattered intensity and select the appropriate system geometry.
Continuous wave visible laser	3 watt CW argon ion laser operating at 488 nm mrad (Coherent INNOVA model 90-3)
Six inches of free space in front of window for laser optics	14 inches of free space left
Chamber shall disassemble easily	Chamber consists of two near hemispheres joined by standard, O-ring sealed flange. Each detector unit is removable without disassembling the sphere.
Approximately 100 detectors	108 photomultiplier tubes
Forward coverage to within about 5°, backward to within 10° to 15°	Forward coverage begins at 9° and extends to 15° from backward.
Detector types shall be evaluated with respect to photomultiplier tubes	Detectors are photomultiplier tubes.
Each detection element shall be supplied with a rotatable and removable sheet type dichronic polarizer	Each detector unit has such an element immediately before the photomultiplier tube.
Chamber shall be designed to minimize measurement error due to reflected light	Each individual detector unit has a lens and pinhole system to minimize detector FOV.
Reflection coefficient of chamber wall must be estimated	Entire chamber is black anodized, high illumination areas on forward sphere are also painted with ultra-flat black paint.
Reflective intensities should be accurate to within $\pm 10\%$ except in region 150° to 180° where $\pm 50\%$ is permissible	For 0.3-micrometer-sized particles, $\pm 15\%$ accuracy can be achieved in 0° to 90° region, $\pm 50\%$ in 90° to 110° and 140° to 180° regions; $\pm 50\%$ accuracy cannot be achieved in 110° to 140° region.

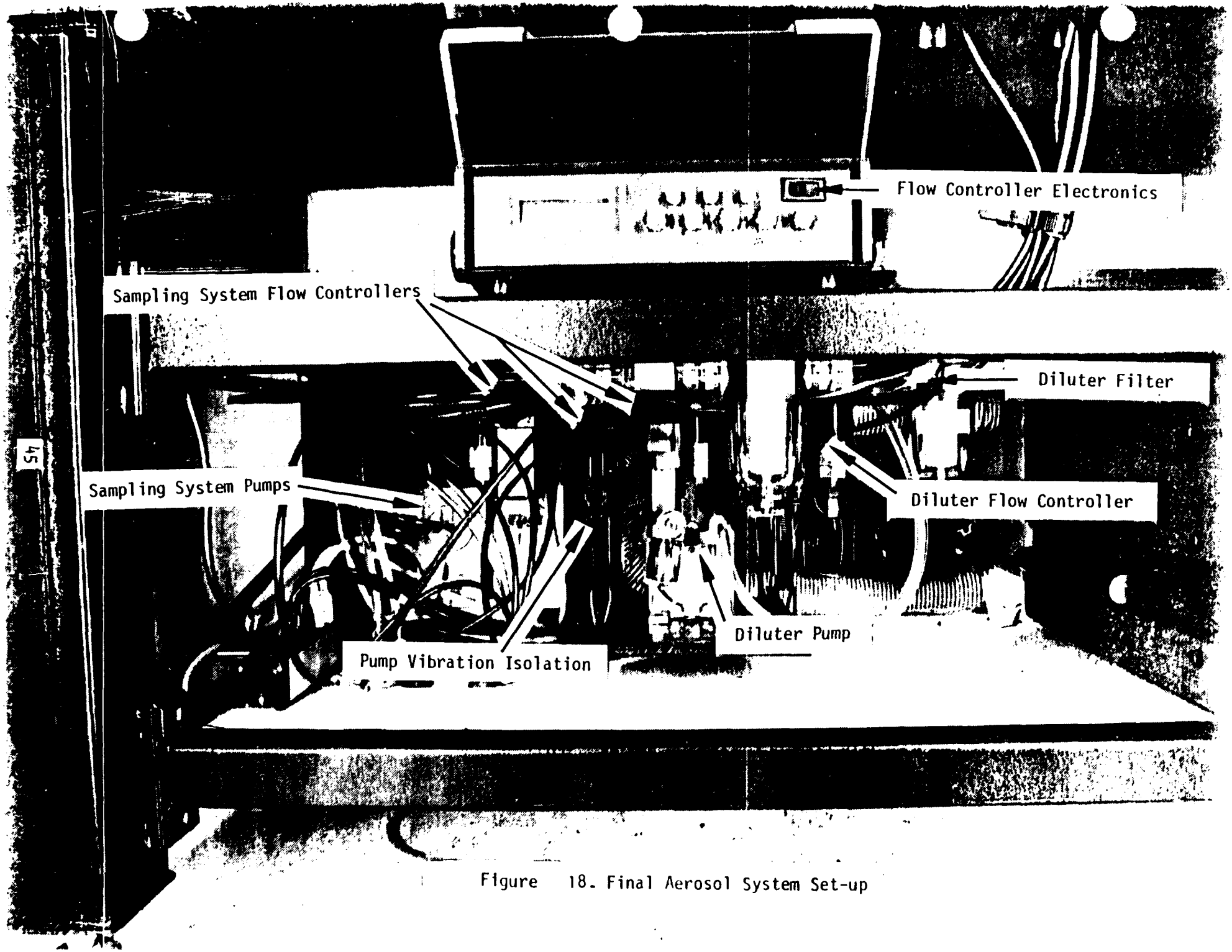

Figure 18. Final Aerosol System Set-up

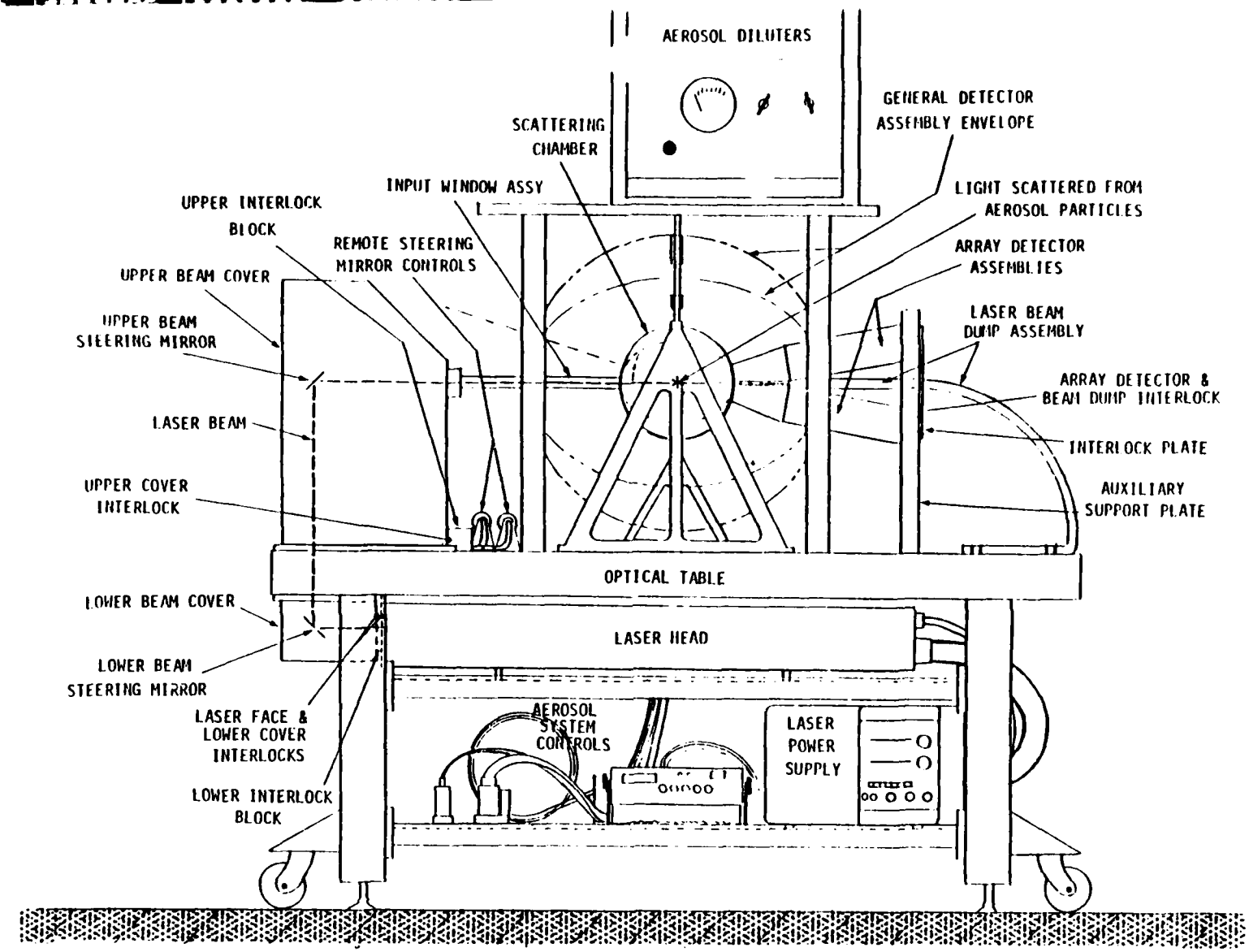

Figure 19. Multichannel Nephelometer Laser System Layout

3.2 Light Scattering Chamber

The purpose of the light scattering chamber is to support the detector assemblies in a known configuration about the intersection of the laser beam and the aerosol stream while it also seals out extraneous light and provides a sealed environment for the aerosol sampling system. The primary reference axis for a particle's light scattering is the axis of the incident illuminating beam. With nonpolarized illumination, the light scattering pattern of a spherical particle is symmetrical about this axis while a nonspherical particle will have variations which depend on its structure. The layout of the detectors in the scattering chamber was designed to use this symmetry to allow the detection and measurement of the scattered light well enough to permit characterization of the overall light scattering pattern. There are 108 detectors in the system.

The detectors are located in four planes spaced at equal angles about the laser beam axis. Figure 20 shows the orientation of these planes looking along the laser beam axis from the direction of the laser. There are two different detector arrangements for these planes. The vertical and horizontal planes use the "A" plane configuration with 20 individual detectors in each plane shown in Figure 21 . Each of the individual detectors has a 6° field-of-view (FOV) and is spaced at a minimum interval of 12° from its neighbors. In all planes the detectors in the forward scatter direction (i.e., on the right side of the circle in Figure 21) are offset 6° from the opposing detectors in the backscatter direction to keep them from looking directly at the opposing detectors to minimize the effects of scatter off their lens and planer optical surfaces. Further, the detector pattern in the upper (A) forward quadrant of the plane, along with its opposing pattern in the lower (A*) back quadrant, is offset from the detector pattern in the lower front and upper rear quadrants by 4°. Since there are two orthogonal "A" planes, this allows the matching quadrants in the two planes to provide some symmetry information while the 4° offset provides data at an intermediate angle in an effort to provide a more complete set of data.

The detector FOV layout for the "B" planes is shown in Figure 20. The FOV arrangement in these planes is totally symmetric about the laser beam axis. Like the "A" planes the opposing detectors are offset by 6° to minimize reflective crosstalk but there is no 4° offset within the plane. However, the entire pattern in the "B" planes is offset 4° from either of the patterns in the "A" planes. Thus, between the two sets of planes, some data is obtained at nominal 4° intervals at least two points about the laser beam axis. Since the "B" planes are totally symmetrical they also provide symmetry information in four orthogonal directions about the laser beam axis. The "B" planes also contain four detector arrays in the near forward direction. Each array detector assembly has eight adjacent detectors, each subtending a 1.64° square centered about 15° from the forward direction. These detectors are closely packed to allow sufficient resolution for the high spacial frequency variations which are normally present in the very near forward scatter directions. Table 5 provides a summary of the composite orientation angle coverage provided by this detector arrangement. All of the angles are measured from the forward laser beam axis.

The actual chamber is composed of two near-hemispheres mounted to a central one inch thick plate. This plate is centered on the vertical aerosol jet axis and is perpendicular to the axis of the laser beam. It provides mechanical support and alignment for the scattering chamber and also supports the aerosol system nozzles and components which are directly associated with the light scattering chamber. All of the detector assemblies are mounted to the chamber hemispheres. The backscatter hemisphere is shown in Figure 23. It includes 42 individual detector ports, two auxiliary

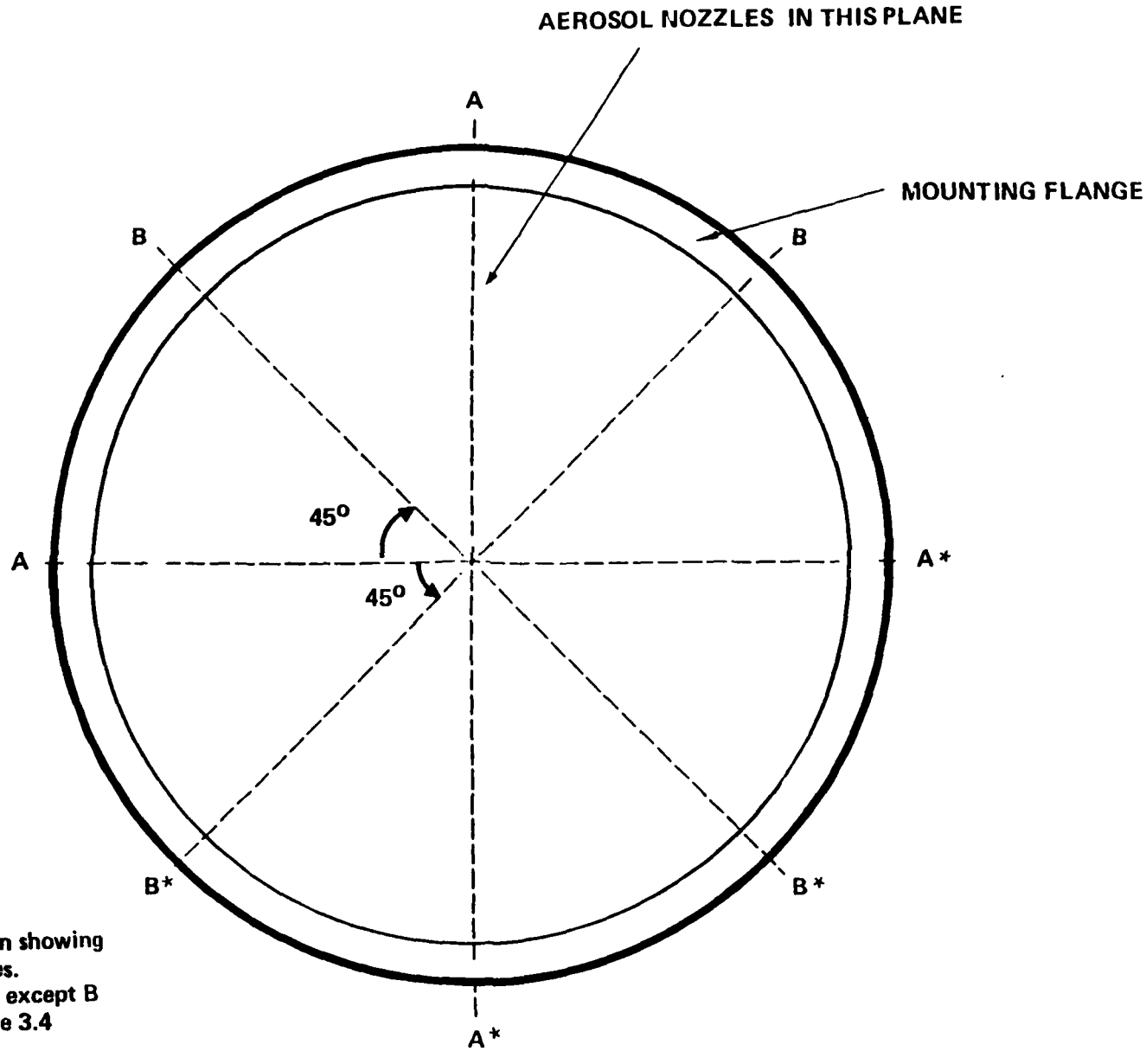

See Figure 3.3 for section showing detector FOV in A planes.
B planes are similar to A except B has array units, see figure 3.4

Figure 20. Light Scattering Chamber Detector Planes (Looking forward in the same direction as laser beam)

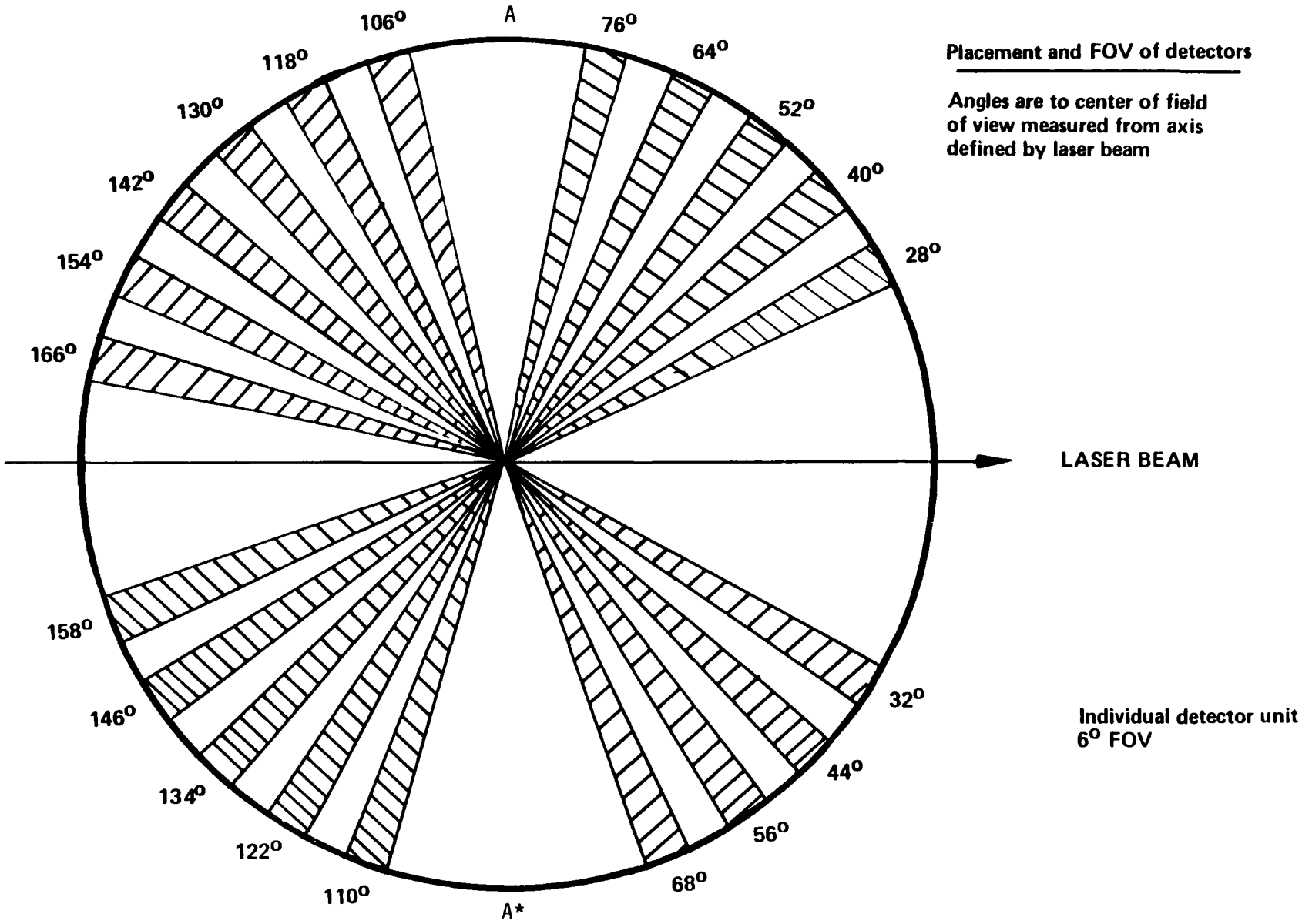

Figure 21. "A" Plane Detector FOV Layout

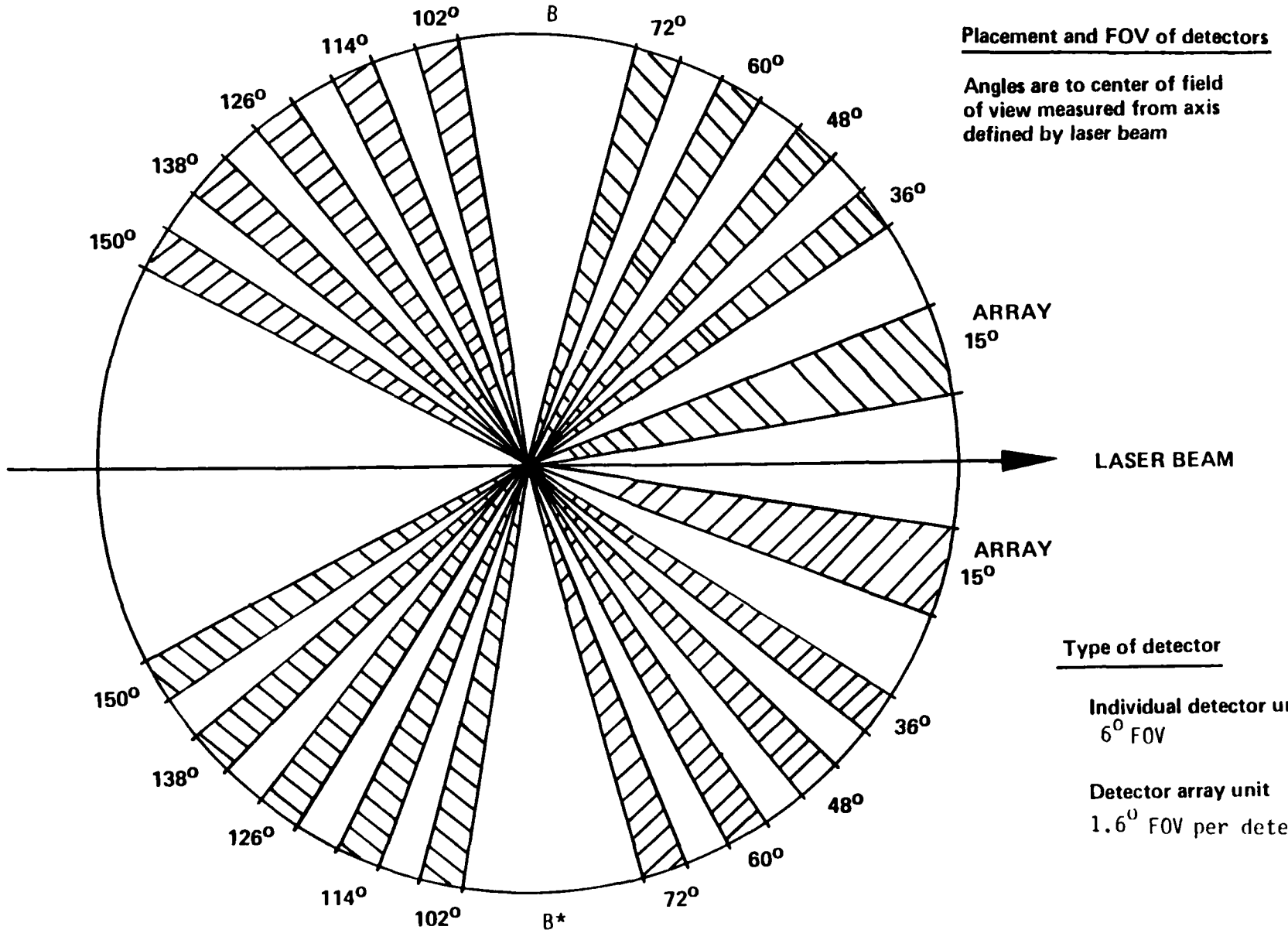

Figure 22. "B" Plane Detector FOV Layout

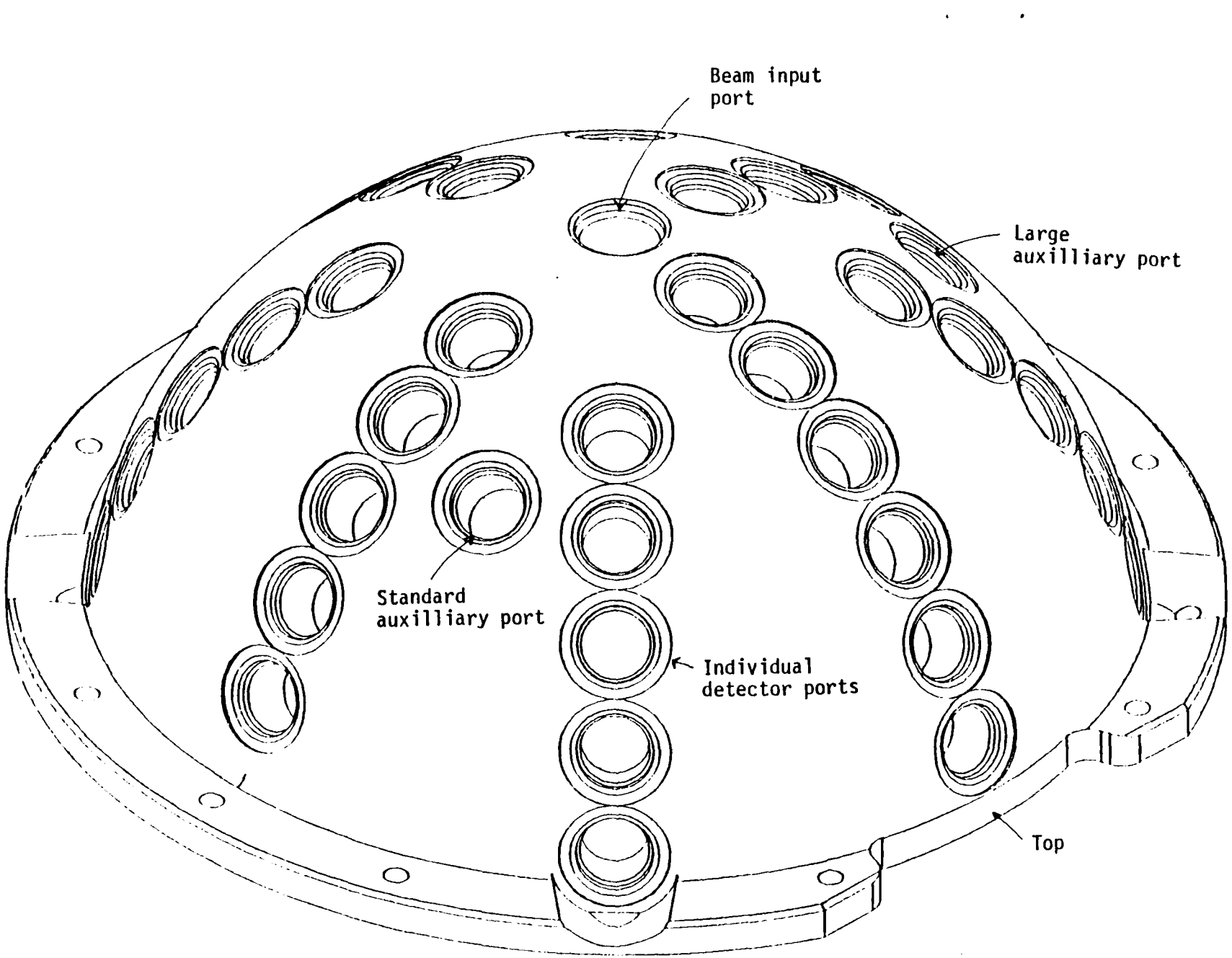

Figure 23. Isometric Drawing of Backscatter Hemisphere

Table 5. Light Scattering Chamber Detector FOV Coverage

		DETECTOR CENTER ANGLE	NUMBER OF DETECTORS IN SPECIFIED PLANE SECTOR A	A*	B
		9.27°			4
		10.91°			4
ARRAY		12.55°			4
ASSEMBLIES:		14.18°			4
15° CENTER ANGLE		15.82°			4
TOTAL COVERAGE		17.45°			4
8.45° to 21.55°		19.09°			4
		20.73°			4
		28°	2		
		32°		2	
		36°			4
		40°	2		
		44°		2	
		48°			4
		52°	2		
		56°		2	
INDIVIDUAL		60°			4
DETECTORS:		64°	2		
		68°		2	
EACH WITH		72°			4
6° FOV		76°	2		
	26° GAP				
		102°			4
		106°	2		
		110°		2	
		114°			4
		118°	2		
		122°		2	
		126°			4
		130°	2		
		134°		2	
		138°			4
		142°	2		
		146°		2	
		150°			4
		154°	2		
		158°		2	
		162°	NO COVERAGE		
		166°	2		

ports, and an axial beam input port. Each of these ports incorporates a standard straight thread boss which provides a positive O-ring seal once the mating assembly is installed. The auxiliary ports are provided to allow additional instrumentation or viewing of the inside the chamber. The standard port is identical to the detector ports and allows the use of a standard or modified individual detector assembly. The large port accepts a special insert with a one inch window for viewing or an adapter for an individual detector assembly. Solid plugs are also provided for both ports. The forward scatter hemisphere is shown in Figure 24. It includes 34 individual detector ports, 4 array detector ports, and a beam dump port. Each of these hemispheres is mounted to the main support plate and has O-ring seals to provide a positive seal at the hemisphere/plate interface.

The scattering chamber must also incorporate provisions for input and dumping of the laser beam. As with all the other systems these functions must be performed while maintaining the sealing integrity of the chamber. Ideally, all light would be limited to the actual beam. Light outside of the beam contributes to both molecular scatter and random scatter in the chamber and has a significant effect on the data acquisition system noise levels. Because of the beam energy, scattered light from the input window is quite substantial. The two inch diameter input window is set at a distance of 20 inch from the sphere center. This allows substitution of a 20 inch or longer focal length lens for focusing the beam should the need arise. The interior of the tube which ties the window mount to the chamber uses a series of baffles and velvet to trap most of the scattered light coming from the input window. As a result of these measures the molecular scatter is minimized and most of the scattered light accompanying the beam enters the beam dump at the far side of the chamber and is removed from the system.

The beam dump is required to absorb the laser energy while minimizing the amount of back-scattered light which can re-enter the chamber. It is essentially a very long tube gently curved, then sharply bent on the far end and sealed to maintain the integrity of the chamber. The entire section of the tube which is visible from the chamber is polished to enhance its specular reflectivity. This, combined with the relatively gentle curve in the upper beam dump is designed to keep these reflections at near grazing incidence to further enhance reflectivity and reduce diffuse back-scatter. As a further measure the beam dump is fabricated from brass and copper to enhance the absorption of the 488 nm wavelength light from the laser. Past experience has shown that laser light of the intensity present in this system will destroy any absorbing coatings such as paint used in a beam dump. The absorptive capability is therefore gradually increased as the distance from the chamber increases. As noted before, the long straight section is polished and back-scatter is low. It is primarily intended to pipe the light toward the end of the beam dump. The area where the main beam hits is polished and the curvature is designed to ensure that the second reflection of the beam is not visible from the chamber. The remainder of the curved tube is unpolished. The oxidized copper coating is more absorbant and also helps to further spread the light energy. The end of the beam dump is coated with a flat black paint. By the time the beam reaches this point its intensity is sufficiently low to preclude degradation of the paint. Back-scatter from the beam dump appears to be acceptably low.

3.3 Individual Detector Assembly

The 76 individual detector units are each composed of two major units installed in a two-piece molded plastic housing. One piece contains the lens and an aperture to limit the detector FOV and remains more or less permanently affixed to the spherical chamber wall to provide an airtight seal. The second piece contains the polarizer, photomultiplier tube (PMT), and front-end electronics. It can be rotated within the first unit to change polarization, or removed for other changes. Figure 25 shows an assembled individual

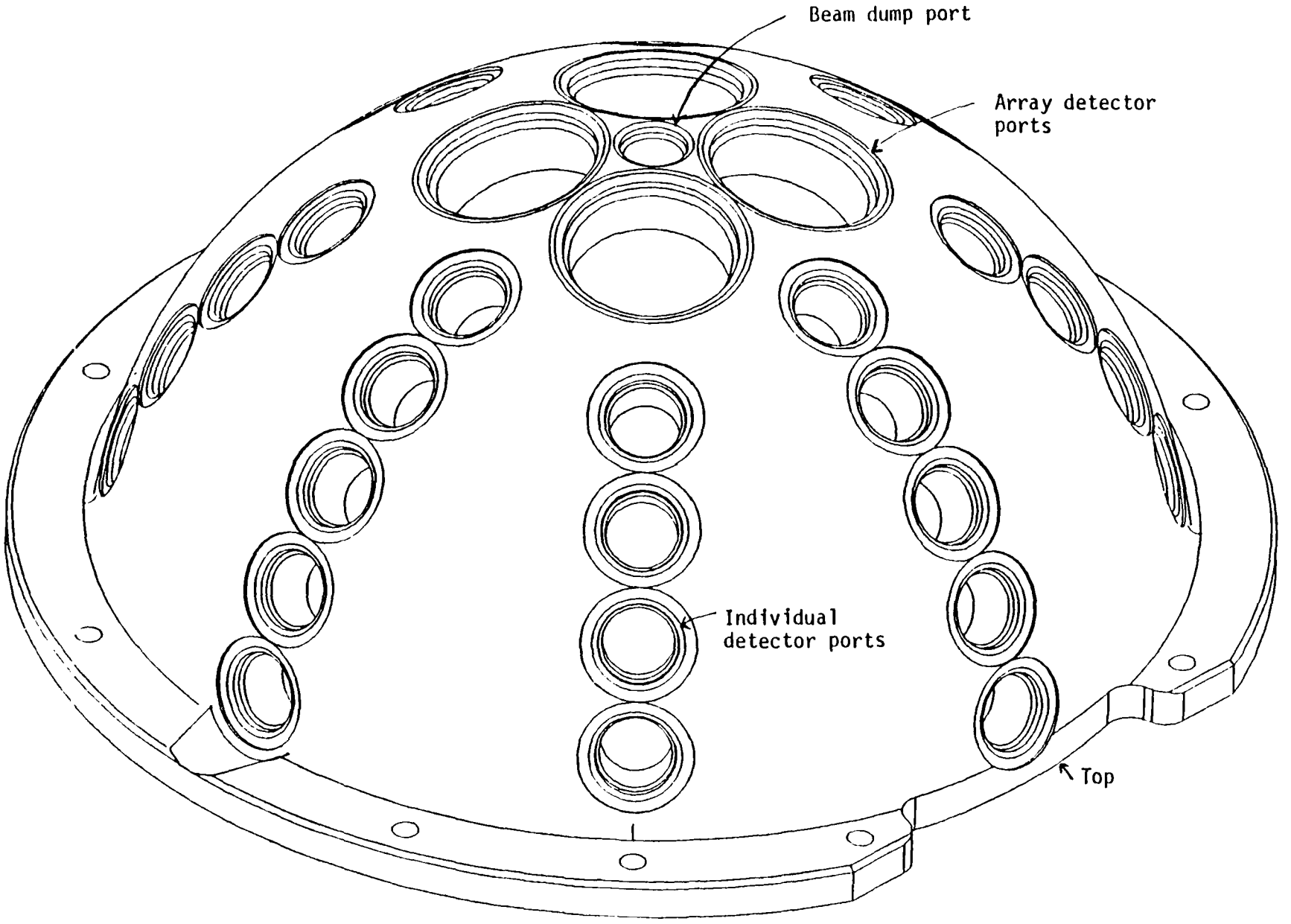

Figure 24. Isometric Drawing of Forward Scatter Hemisphere

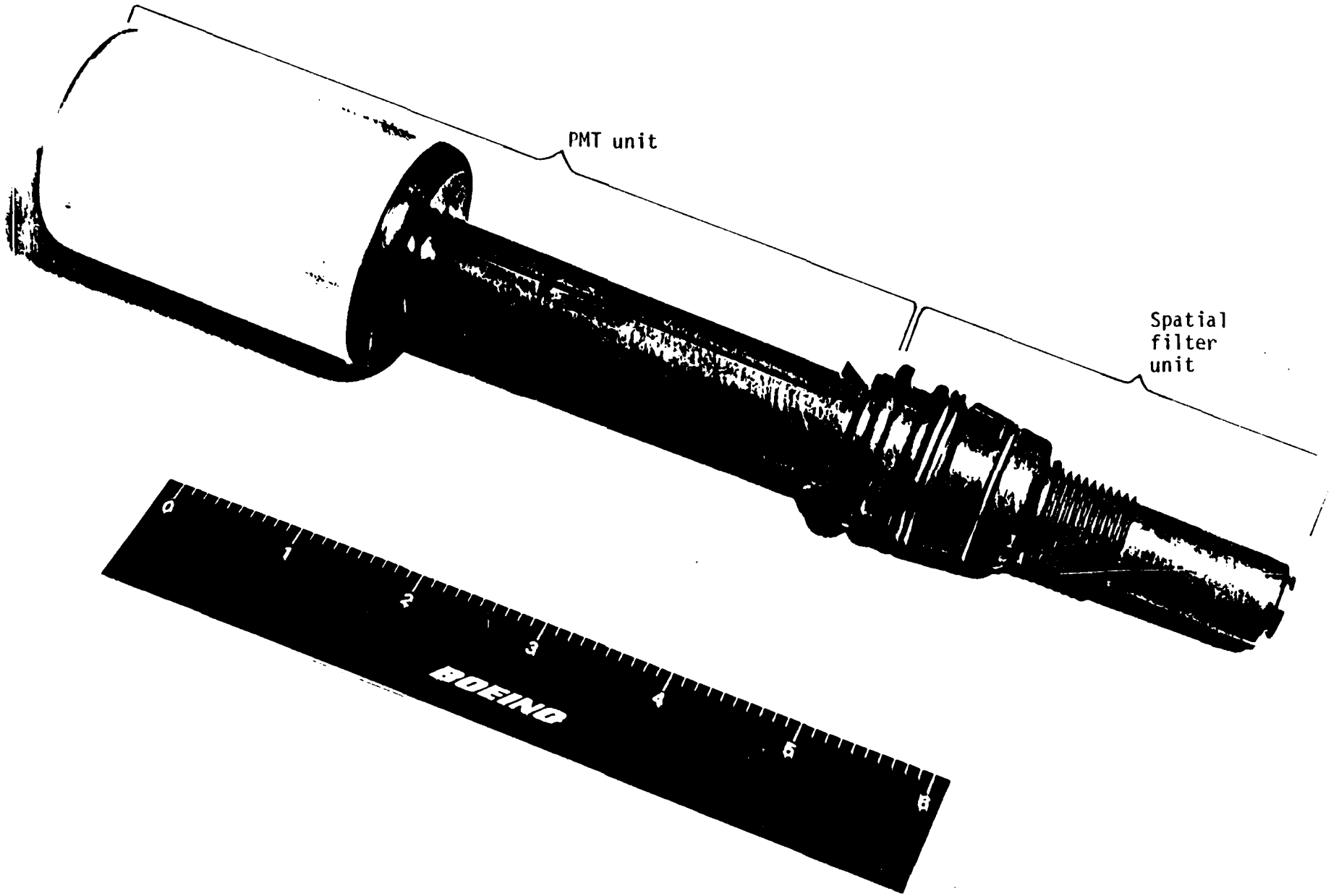

Figure 25. Assembled Individual Detector Unit

detector unit. The individual assemblies are designed to collect light scattered from a particle into a 6° (full apex angle) cone. This acceptance angle was chosen in a tradeoff between sensitivity and the number of detectors desired. The complete unit -- optics, mechanical mounts, photomultiplier and electronics -- was constrained to subtend less than 12° (at the particle) so that the individual detectors could be mounted on 12° spaced centers.

A major concern with the individual detector units, particularly those in the backscatter hemisphere, is that specularly reflected, forward-scattered light can be comparable to the backscattered light directly from the particle. Of equal importance is the detector's FOV at the center of the scattering chamber. During the period that the intensity measurements are being made it is important that all of the energy incident on the lens also be imaged on the face of the PMT. Failure to do this could produce variations in the measured intensity levels which were system artifacts instead of true scattering pattern variations. Thus, the field of view must be large enough to allow for particle location variations within the laser beam and also to allow for tolerance errors in the alignment of each of the individual detector special filter units in the light scattering chamber sphere. Unfortunately these two requirements work against each other and a compromise had to be made. The effects of reflected forward scatter are serious and can significantly degrade the data. However, it is directly related to the geometry of the system, and through careful system characterization the relationship between the intensity measured at the opposing forward detectors and the reflected light present at the backscatter detector could potentially be established. This would allow most of the effects of this problem to be removed through subsequent processing of the data. Though not a minor problem it is potentially workable. On the other hand, errors caused by too small of a field of view at the center could be unresolvable. These errors arise from the relationship between the instantaneous location of the particle and the pointing errors in each of the detectors. If the field of view is too small only part or none of the incident intensity at some of the detectors would be measured and the resultant data set would be rendered unusable. Because these factors vary with each particle and exact position data is unknown, it is not possible to back these errors out of the data. This problem is best resolved by making the FOV of all the detectors large enough that the central volume common to the FOVs of all of the detectors includes the full aerosol/laser beam interaction volume. As a result it was decided to meet the latter criteria while still limiting the field of view, in deference to the scattered light problem.

It should be noted that during this evaluation it was realized that the scattered light problem was less severe than might normally be expected. Because of their specular nature, the optical reflections off the opposing optical surfaces was expected to be very high. When the effects of the lens curvature are accounted for, however, the amount of light incident on the opposing detectors per unit of area viewed is on the same order as scatter from the other surfaces in the chamber. This problem then becomes less one of avoiding the opposing optics and more a problem of simply minimizing the total detector FOV at the opposite chamber wall.

A series of measurements was made and several different apertures were identified to bracket the calculated ranges. The final selection of aperture size was accomplished by testing the worst case units and selecting the smallest aperture which allowed full view of the light from a specially constructed calibration aperture plate. The alternate apertures were supplied with the unit to allow modification should the need arise.

The individual detector assembly was configured in two main units to allow easy adjustment of the individual detector polarizer orientation. Past aerosol research has shown that the light polarization of the scattered light carries valuable information and

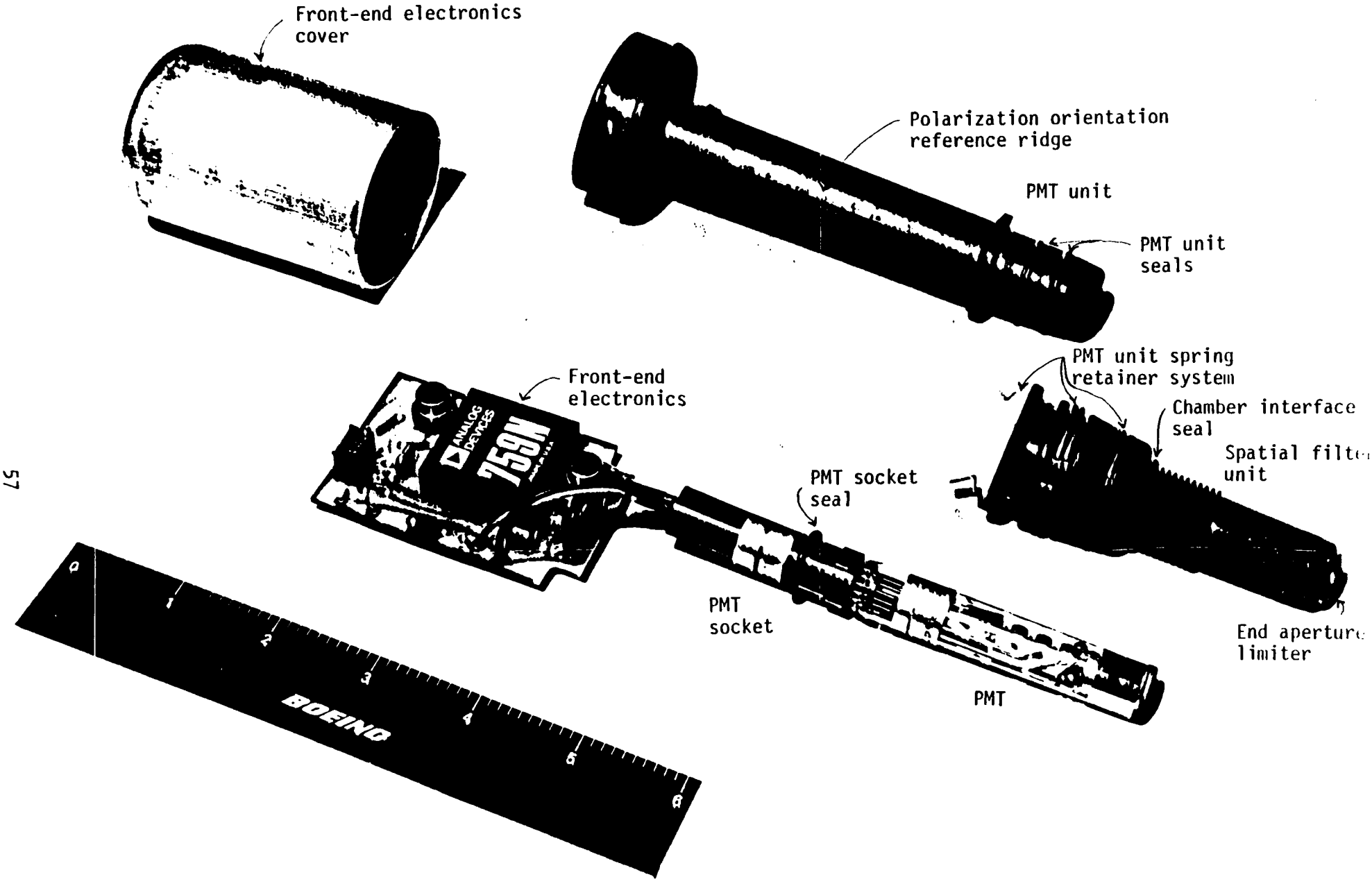

Figure 26. Main Components of Individual Detector Assembly

a polarization analysis capability for each detector was required. Since there are 76 individual detectors and because the nephelometer is a laboratory instrument which could require frequent reconfiguration it was felt that reorientation of the polarizers should be a simple process. By locating the polarizer just in front of the PMT if was possible to avoid chamber disassembly just to rotate or install/remove the polarizers. The initial nephelometer design concept for joining the two detector units was to use a set screw between the units. However, the threads in the sphere would be randomly oriented and it was not possible to establish a consistent orientation without extensive rework of each unit. In addition, analysis showed that access to the set screws would be very difficult for some of the detectors in the fully assembled nephelometer. The final design utilizes a double O-ring seal and a custom snap-ring system to retain the detector in the desired location and still allow easy modification of the detector polarization.

As the design developed it quickly became apparent that even the simplest concepts would be too expensive to machine. Further, using a plastic molded piece would allow full development of the design with little impact on cost. It was decided to use black colored 40% glass-fiber-filled polyphenylene sulfide (PPS). The basic properties of the selected material are given in Table 6. The glass fiber filler gives this material high dimensional stability and very low mold shrinkage. The black color provided excellent opacity and made it optically suitable in the system. Using glass instead of carbon fibers yielded a nonconductive polymer which avoided problems in HV biasing of the enclosed PMTs. PPS has excellent mechanical, chemical and thermal characteristics and was fully suitable for this application. Using a fiber filled polymer did add some dimensional limitations to the design but the resultant stability proved to be very beneficial. The final injection-molded assemblies met all the design goals and proved to be highly functional and operationally flexible. Figure 26 shows the main components of the individual detector assembly. The PMT, its socket, and the front-end electronics are part of the data acquisition system and their function will be discussed later. The important mechanical features of this design are outlined below.

The individual detector adapter set has five main parts that assemble into two basic units. Starting at the sphere, the end aperture limiter, spatial filter, and spring clip are assembled into the spatial filter unit that normally remains attached to the sphere. This assembly has three primary functions: (1) sealing of the sphere port, (2) spatially filtering the light reaching the detector, and (3) providing mechanical support for the photomultiplier tube (PMT) assembly. The lens, which is part of the spatial filter, is located in the small end of the spatial filter unit against a molded in ridge. The lens is sealed by an Oring and these are held in place by a snap ring. The end aperture limiter is pressed into the spatial filter unit after the snap-ring retainer and helps to retain and seal the lens as well as limit the input aperture. This seals the inside of the spatial filter assembly against air infiltration. The aperture is dropped in from the other side and held in place by a small circular snap-ring. An Oring is located between the aperture and its spring clip to allow removal of the aperture. The outer surface of the spatial filter unit is threaded and has an O-ring that seals the outer periphery of the assembly when it is screwed into one of the SAE/MS internal straight-thread boss individual detector ports machined into the chamber sphere. A counterbored surface surrounding each SAE/MS boss port on the chamber sphere provides a reference surface that fixes the distance of the installed spatial filter assembly from the center of the sphere. Once the spatial filter unit has been installed in the sphere, it will not normally need to be removed and should be considered a fixed installation. However, it has been designed to allow removal, should the need arise, without major disassembly of the scattering chamber. A spring clip assembly, consisting of two shaped flat springs and three circular clips, is installed on the outside of the large end of the spatial filter unit to provide snap-in retention of the PMT unit.

Table 6. Properties of RTP 1307

Characteristic	Property
Color	Black
Glass fiber	40%
Specific gravity	1.62
Mold shrinkage, 1/8-in section	0.001 in/in
Water absorption, 24 hours at 23°C	0.02%
Impact strength	
IZOD, notched 1/4 in	1.4 ft-lb/in
Unnotched 1/4 in	7.0 ft-lb/in
Tensile strength	20,000 psi
Tensile modulus	2×10^6 psi
Flexural strength	30,000 psi
Flexural modulus	1.6×10^6 psi
Compressive strength	25,000 psi
Rockwell hardness	123
Volume resistivity	10^{16} ohm CM
Deflection temperature	
at 264 psi	500°F
at 66 psi	500+°F
Coefficient of linear thermal expansion	1.2×10^{-5} in/in/°F

The PMT assembly is composed of a moulded PMT unit, the PMT and its socket, the front-end electronics and their cover. The PMT is installed in its socket and then inserted into the PMT unit until it rests against a stop ridge near the inboard end. An O-ring is slipped over the PMT socket prior to installation. It is provided to block stray light which might enter through the cable hole in the front-end electronics cover. The front-end electronics are installed on a printed circuit board attached to the outboard end of the PMT socket. This electronics board is equipped with long multiwire cables that connect it to an interface box mounted on the laser shelf. The front-end electronics cover is a cylindrical, deep-drawn aluminum box which fits on a special molded flange on the outboard end of the PMT unit and is retained by two screws. Two O-rings are located in grooves on the outside of the PMT unit near the inboard end to seal out light at the interface and provide a friction fit with the spatial filter assembly to hold the desired polarizer orientation with respect to the sphere. The polarizer is installed against the ledge just inside the inboard end of the PMT unit and retained by a circular snap ring. The mold parting lines in the PMT unit provide reference points for proper orientation of the polarizer in the PMT unit. The PMT unit has been designed to be readily removed and rotated for both maintenance and operational convenience. A large ridge running circumferentially around the outside of the PMT unit, just outboard from the PMT unit seals, provides the surface against which the special spring clip assembly on the spatial filter unit acts to hold the PMT unit in place. The inboard side of this same ridge interfaces with the upper end of the spatial filter unit to fix the distance of the PMT unit from the center of the sphere. Two polarization orientation reference ridges are provided on the outside of the PMT unit to serve as a ready visual and tactile index for polarizer orientation. The retaining screws on the front-end electronics cover are also aligned with these ridges to provide an additional indicator of the polarizer orientation in the assembled unit.

Insertion of the PMT unit into a spatial filter assembly mounted on the sphere is designed to be accomplished by simply pressing the PMT unit in until the spring clip snaps it up into place against the spatial filter assembly. the polarizer is then oriented by rotating the PMT unit until the index ridges indicate that the polarizer is properly oriented. Removal is accomplished by pulling the PMT assembly straight out. The multichannel nephelometer has been designed with a minimum 15 inch clearance from the center of the sphere in all directions to ensure easy removal of any of the assemblies.

3.4 Array Detector Assemblies

There are four array detector assemblies in the multichannel nephelometer, each of which contains 8 narrow rectangular PMTs. Because of their size they are supported at both ends. One end attaches to the light scattering chamber and the other is supported by an auxiliary plate mounted to the table. Since reflected light was not considered to be a significant problem for the array units in the near-forward direction, no spatial filter was needed and a much simpler optical design was used. Basically, it consists of an anti-reflection-coated window to seal the system, followed by a rotatable polarizer. The polarizer was placed outside the sealing element so that it could be rotated or removed without breaking the air seal of the system. The polarizer is followed by an aperture plate that is immediately in front of the array of eight rectangular PMTs, mounted contiguously. Thin black plastic separators are inserted between the PMTs to prevent cross talk as a result of light reflecting off the curved surface of one tube directly into an adjacent one. The aperture plate together with the rectangular shape of the PMTs gives each tube a 1.64^{o} square acceptance region when measured from the nominal particle location. Since the array is not circularly symmetric it must remain fixed. It

was therefore necessary to achieve polarizer rotation independent from the fixed orientation of the detectors and scattering chamber.

Figure 27 shows the array detector assembly concept design. The array detector assembly consists of three main components, the adapter cone, the polarizer mount assembly and the PMT/electronics assembly. The adapter cone attaches directly to the scattering chamber and is sealed on the outside by an O-ring. Like the spatial filter units in the individual detector assemblies, these units help establish the integrity of the chamber and normally remain attached to the chamber. The array detector window is mounted inside the adapter cone and is sealed with an O-ring and grease. A snap-ring holds them in place.

The heart of the array detector assembly is the PMT/electronics assembly. This unit includes the aperture plate, PMTs, array front end electronics, PMT/electronics housing, and an end plate. The PMT/electronics housing is a PVC tube which houses the assembly. The housing was made of nonconductive plastic to avoid HV biasing problems with the PMTs. The aperture plate is mounted to the inboard end of the housing, just in front of the PMTs. The PMTs are plugged into sockets which are attached to the electronics mounting plates. The majority of this unit consists of the electronics area which holds three printed wiring circuits for the front-end electronics. The orientation of the PMTs and the PMT/electronics assembly is fixed by the end plate which ties the housing firmly to the auxiliary plate.

The polarizer mount assembly which is indicated by the shaded area in Figure 27 is not firmly fixed but floats between the adapter cone and the PMT/electronics assembly. The polarizer is mounted in a ring at the inboard end with a set screw. The main body of the polarizer mount assembly is another large plastic tube which is coaxial around the PMT/electronics unit. When assembled, the outside of the array assembly can be rotated to reorient the polarizer.

Photographs of the array assembly prior to finishing and installation are shown in Figure 28. In views a and b the adapter cone is shown separated from the rest of the unit. View c shows the array detector separated into its three main units. View d shows how the aperture plate limits the FOV of the PMTs which are visible through the aperture slot. Views e, f, and g show the sockets mounted to the electronics mounting plate and the PMTs plugged into the sockets.

3.5 Nozzle Vignetting

Following final determination of the detector locations and viewing geometry, a detailed evaluation and design of the aerosol system interface with the scattering chamber was undertaken. The viewing area of the individual detectors is a 5-mm (0.2-inch) diameter circle at the center of the sphere. When this is considered together with the 45° angle of the detectors in the "B" detector planes and the geometry of the nozzle tips, the minimum distance between the nozzles that will prevent vignetting of any detectors in the "B" planes or horizontal "A" plane is approximately 0.53 inch. At this distance the nozzles are still within the FOV of 11 of the detectors in the vertical "A" plane and completely block the view of the center of the sphere for 4 of those detectors. The mechanically limited minimum spacing for the aerosol nozzles was therefore set to 0.60 inch (each nozzle 0.30 inch from the center) to allow minor variation for detector pointing tolerances and still ensure there is no vignetting of any detectors in three of the planes. At this setting, vignetting in the fourth, vertical, "A" plane is reduced to eight detectors with at least one of the nozzles in their FOV and only two or, marginally, three detectors whose view of the sphere center is totally blocked.

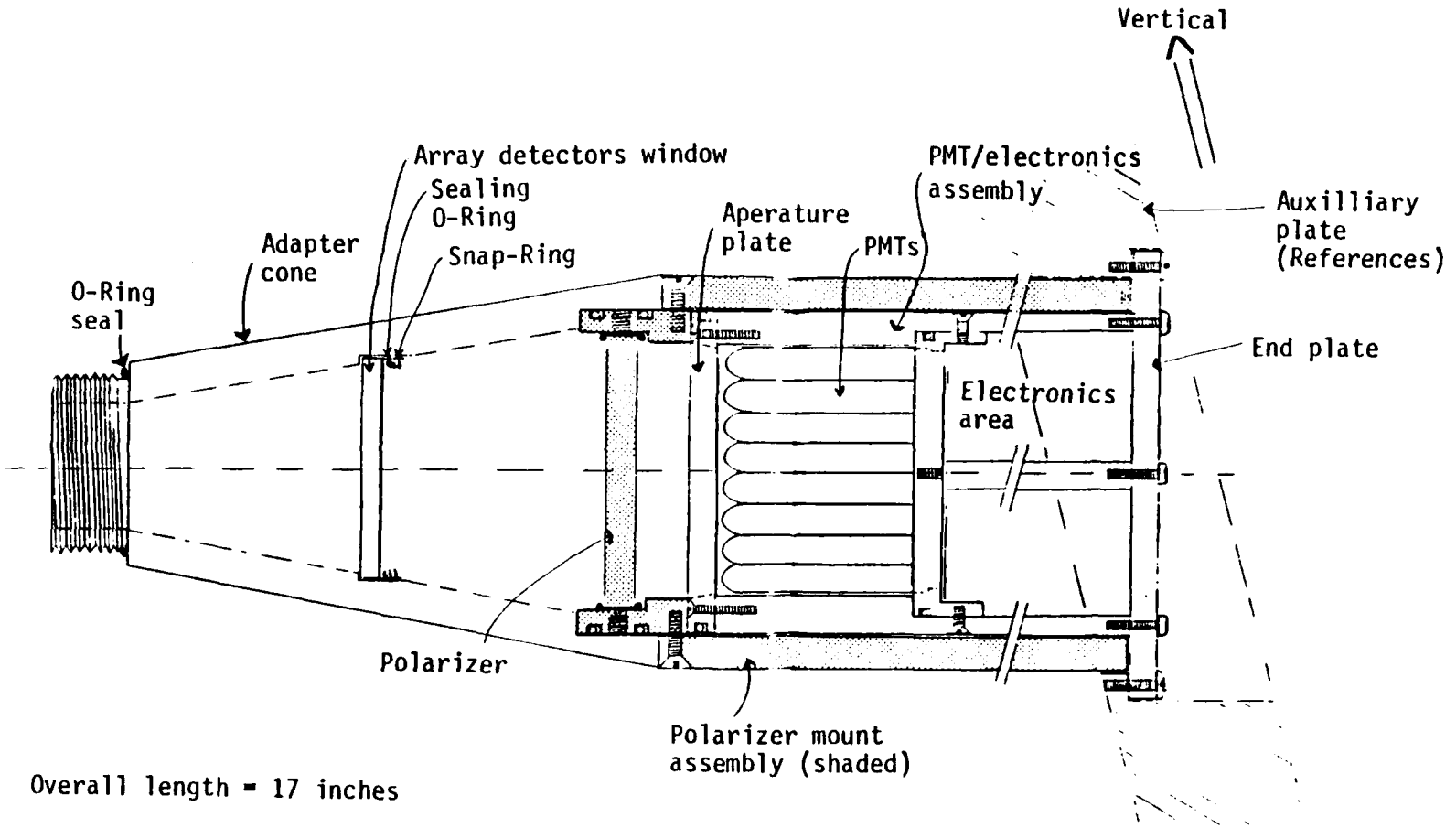

Figure 27. Layout Drawing of Array Detector Assembly

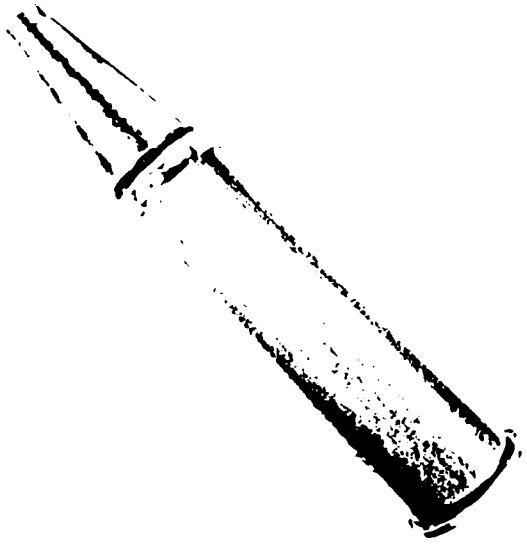

a) Array Detector Housing (scale ≅ 1/5 X)

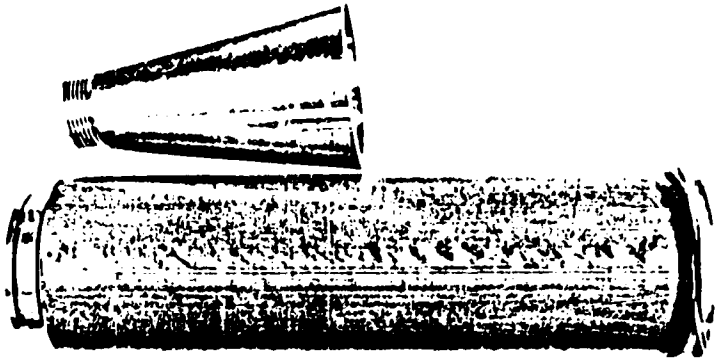

b) Adaptor Cone, Polarizer Mount, & End Plate (scale ≅ 1/3 X)

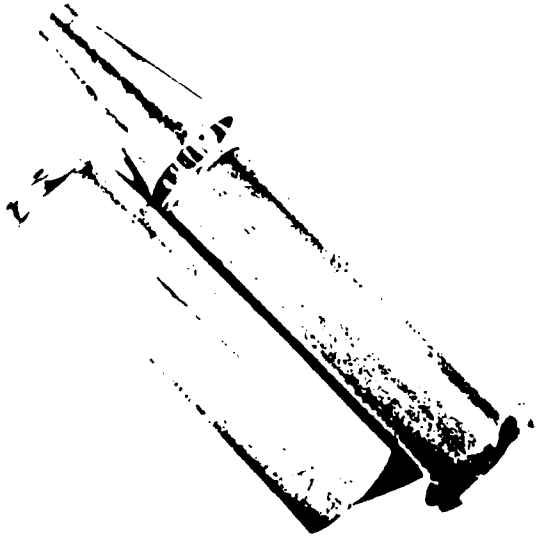

c) Polarizer Mount removed from PMT/electronics housing (scale ≅ 1/5 X)

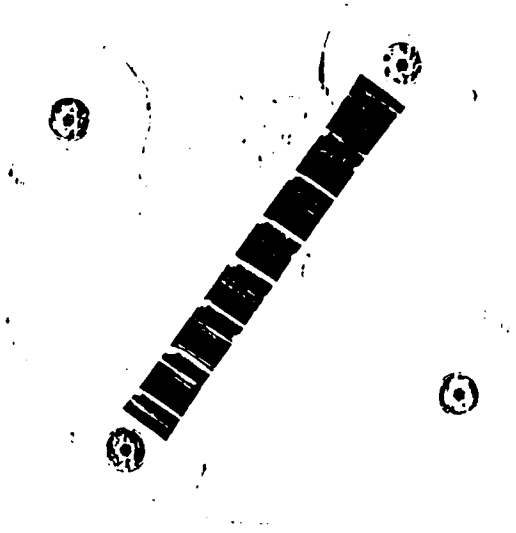

d) View of PMT's through aperture (full scale)

Figure 28. Array Detector Assembly Photos

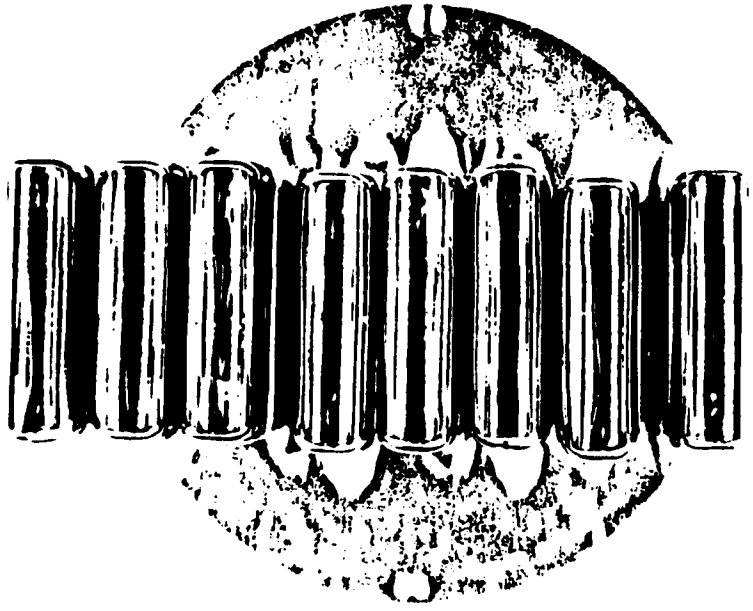

e) Top view of exposed PMT's

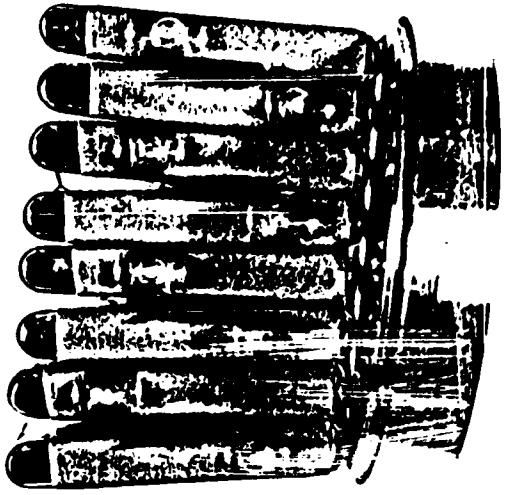

f) Side view of PMT's on electronics mounting plate

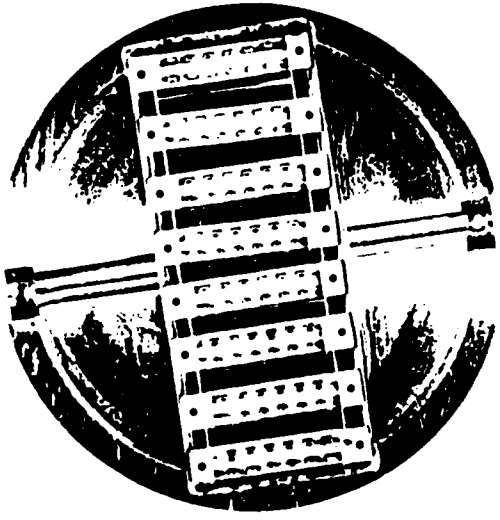

g) PMT sockets underneath electronics mounting plate

Figure 28. (continued)

The nozzles are designed to mechanically allow a 1.5 inch adjustment from their minimum position, yielding a nozzle separation of up to 3.6 in. As noted in Section 2 of this report, with the proper aerosol system settings, this entire range of adjustment can be used to establish a stable aerosol jet. How much vignetting actually occurs will depend on what nozzle spacings are used. For example, at a balanced nozzle spacing of 0.80 inch, only four detectors have a nozzle in their field of view and none have their view of the sphere center totally blocked. At 1.2 inch balanced spacing, vignetting affects only three detectors, at 1.4 inch it decreases to two detectors, and at 1.6 inch only one detector is partially vignetted, A full 2.0-in spacing is required to guarantee that neither of the nozzles will be within the FOV of any detector.

It should be noted that this analysis addressed only the presence of, and possible obscuration by, the nozzle in the FOV of the detectors. No attempt was made to assess the resulting impact on the detector readings. In many cases it is expected that vignetting will result in only a partial, software-correctable modification of the readings from the affected detectors.

3.6 Integrated Light Scattering System

Prior to integration into a total system all of the aluminum parts were black anodized to provide a durable surface to reduce reflections within the system. As a further deterrent to unwanted light scatter within the light scattering chamber, the interior surfaces of the chamber hemisphere were also painted flat black just prior to final assembly. Figure 29 shows the partially assembled backscatter hemisphere prior to installation on the scattering chamber. The lenses are visible in some of the assembled and installed individual detector assemblies. The open auxiliary and input window ports are also visible. Figure 30 shows the partially assembled forward scatter hemisphere mounted on the open light scattering chamber. The four large holes in the center are the input apertures of the array detector adapter cones. The open beam dump port is in the very center. Also visible are the two aerosol nozzles and the two alignment pins which establish the proper location of the hemispheres during chamber assembly. Figure 31 is a similar view of the open chamber with the light scattering chamber/aerosol system interfaces visible.

Figure 32 shows an exterior view of the assembled light scattering chamber and other components of the light scattering system. The beam cover has been removed in this view to allow visibility of the laser port and upper beam steering mirror. Figure 33 shows another view of the chamber system from the beam dump end. Finally, Figure 34 shows a close up view of the backscatter side of the light scattering chamber. In this view the individual detector assemblies and the chamber end of the input window assembly are plainly visible. The large auxiliary port is also visible with a one inch diameter viewing window installed. Adjacent to the auxiliary port are two additional port inserts which can be used to install an individual detector assembly or to plug the port completely. A rubber stopper can be used to block the light from the open window port during measurement.

4.0 DATA ACQUISITION SYSTEM

4.1 Photodetector Selection.

Photomultiplier tubes were chosen as photodetectors instead of the GaAsP photodiodes originally proposed. Although the photocells are sensitive to the smallest signals, approximately 40 photons for the worst case in our system, the amplifier input noise is much greater for the bandwidth necessary to track the scattered light pulse.

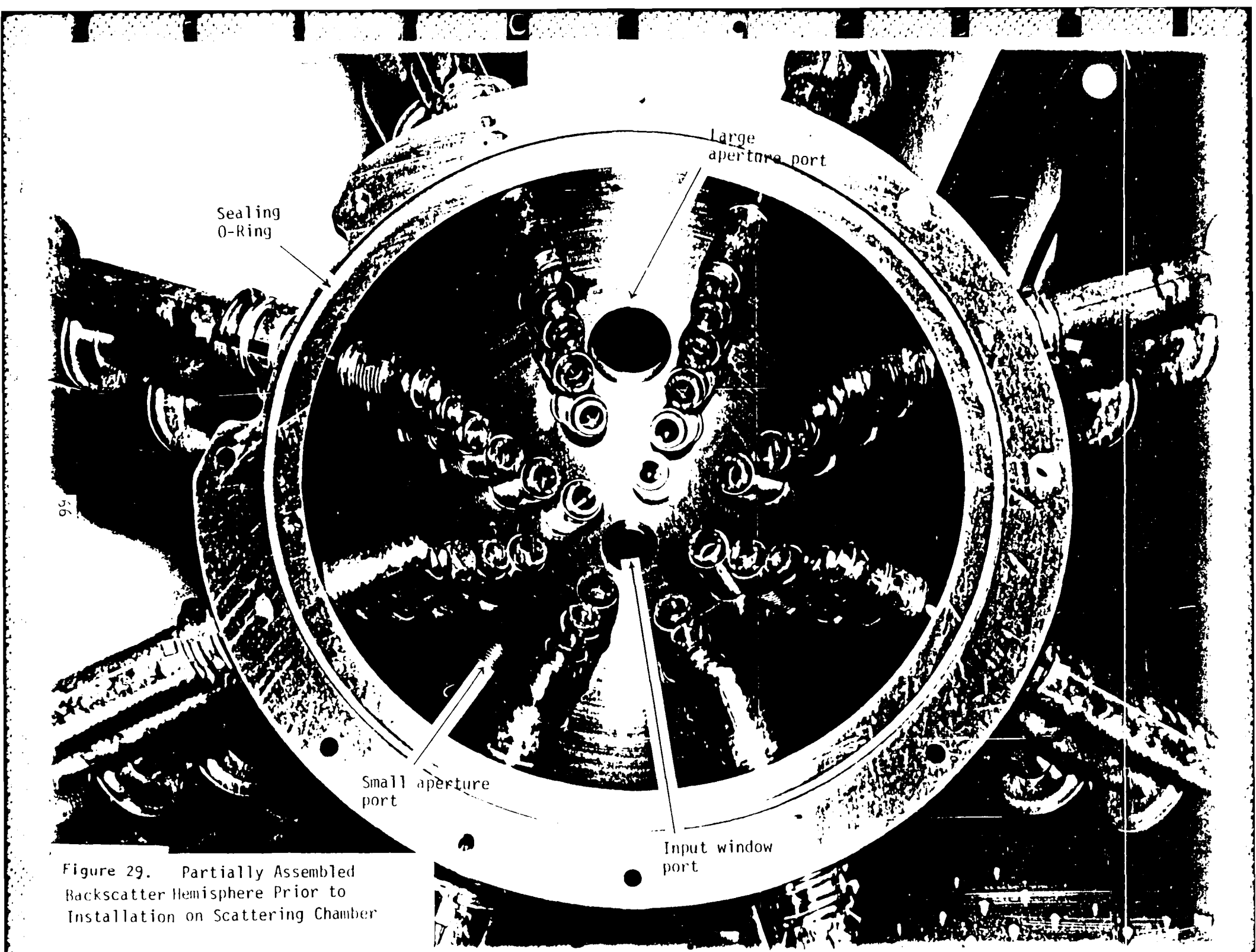

Figure 29. Partially Assembled Backscatter Hemisphere Prior to Installation on Scattering Chamber

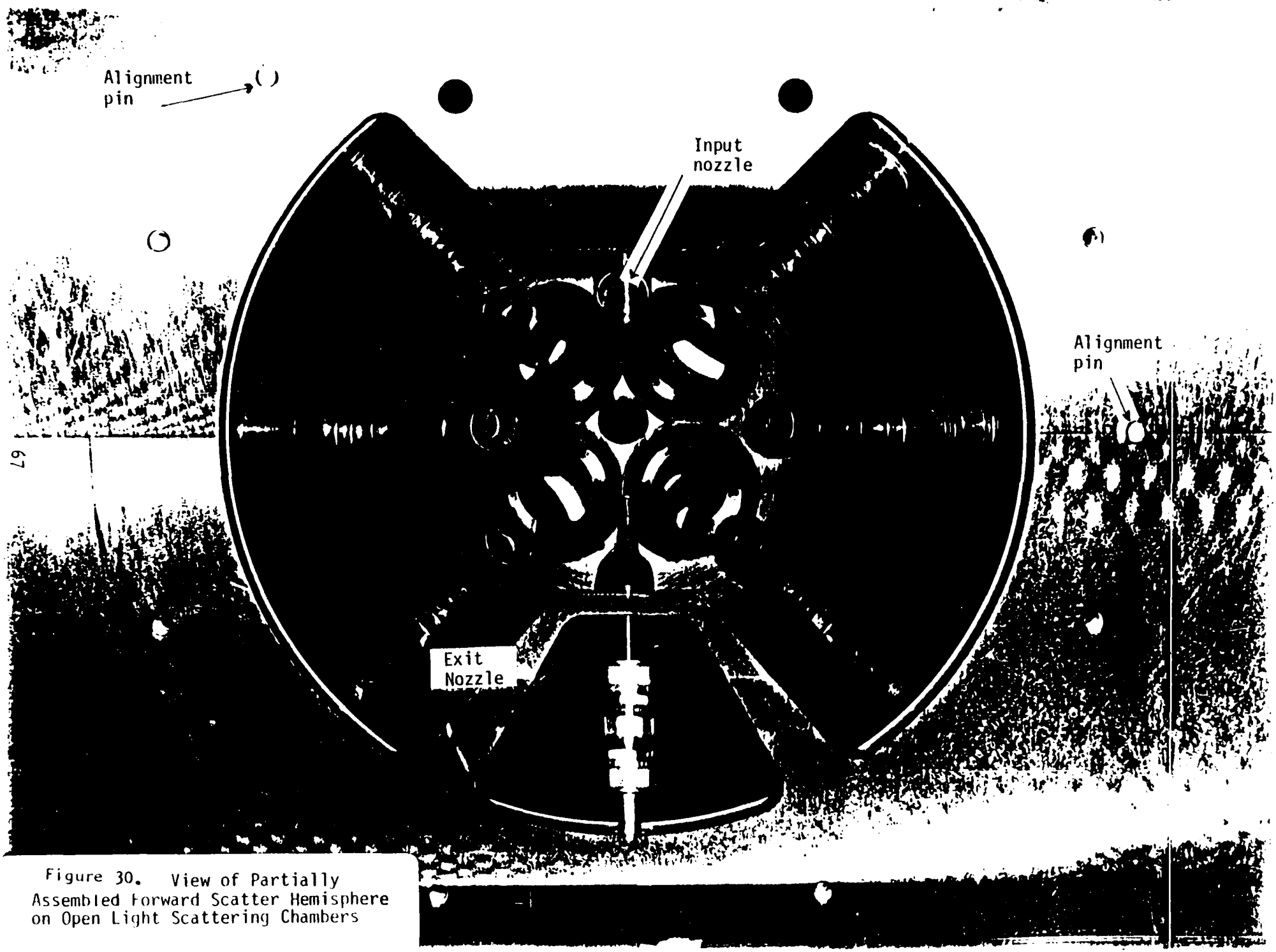

Figure 30. View of Partially Assembled Forward Scatter Hemisphere on Open Light Scattering Chambers

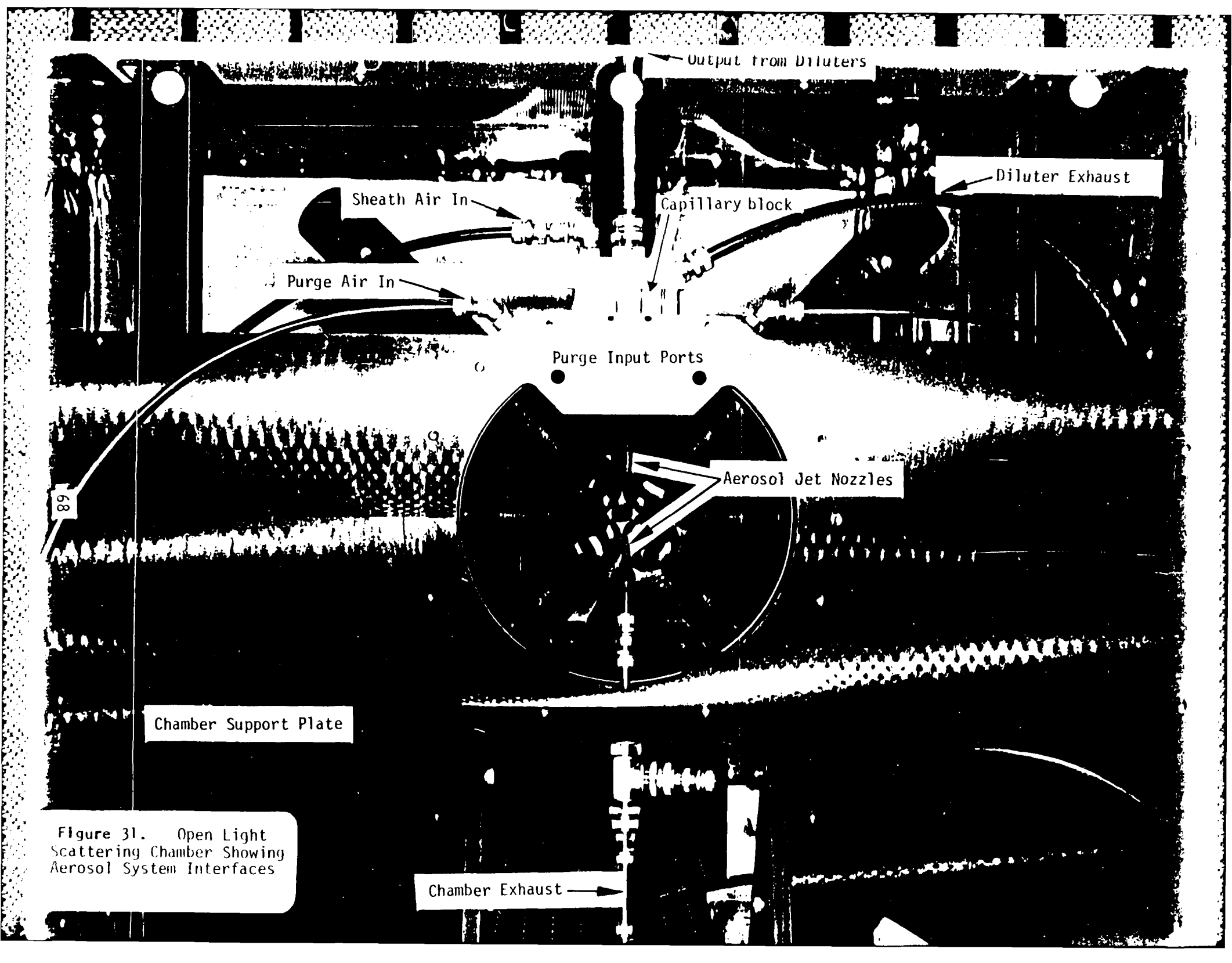

Figure 31. Open Light Scattering Chamber Showing Aerosol System Interfaces

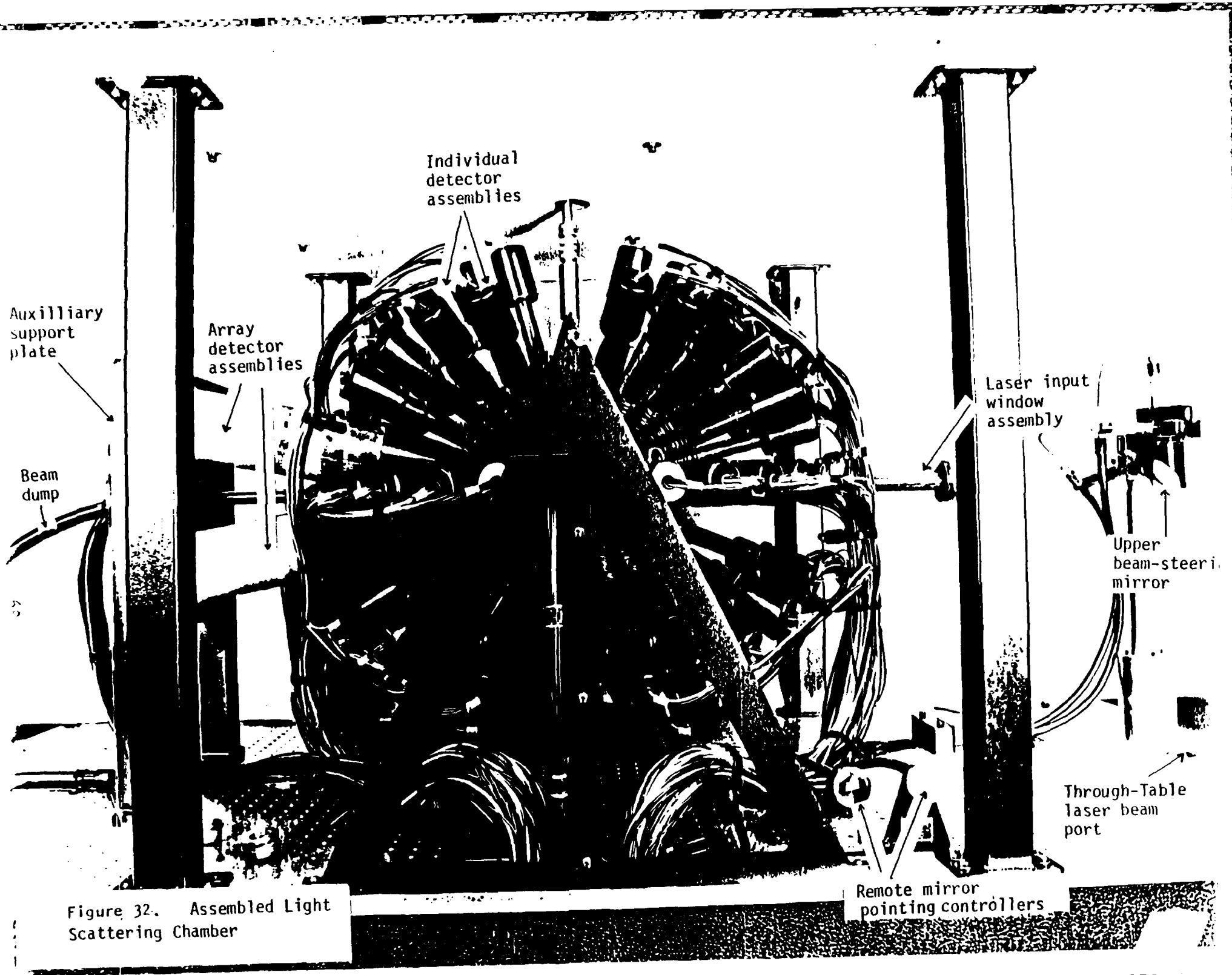

Figure 32. Assembled Light Scattering Chamber

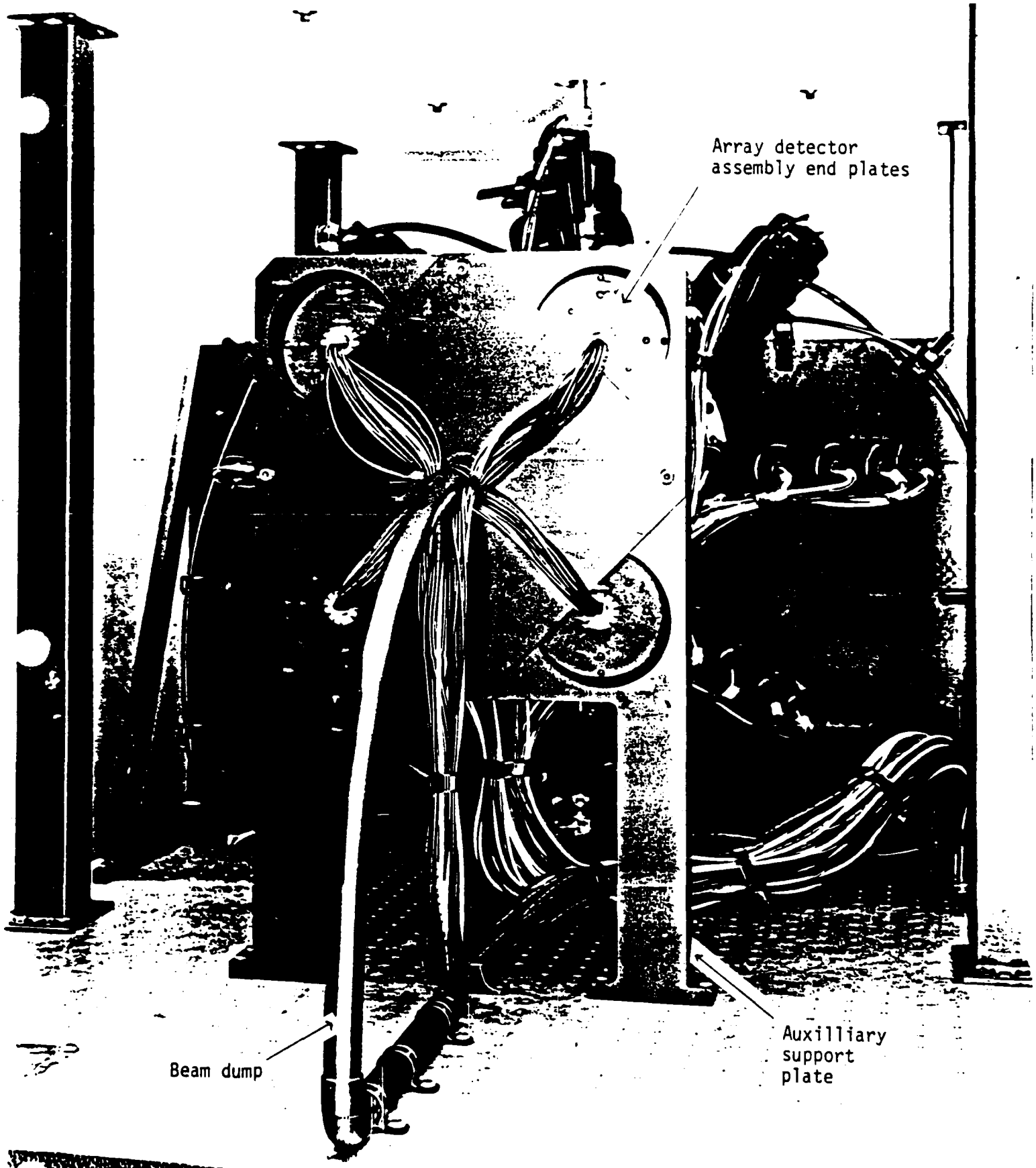

Figure 33. View of Assembled Light Scattering Chamber from Beam Dump End

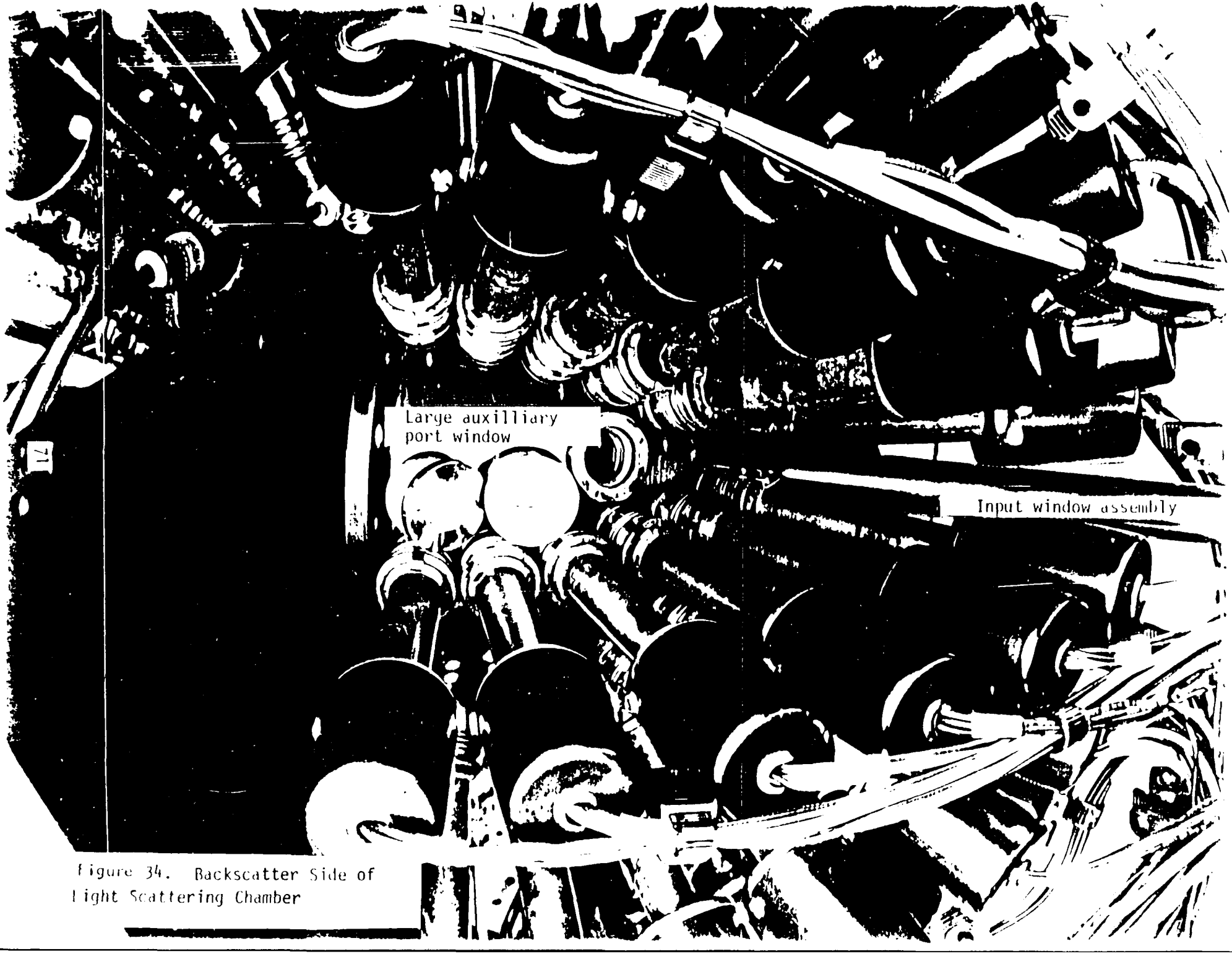

Figure 34. Backscatter Side of Light Scattering Chamber

The amplifier tested, considering both current and voltage noise sources, has the lowest noise commercially available for that bandwidth: 20 kHz. To utilize the photodiodes the amplifier must have more than two orders of magnitude less noise with the same amplifier gain. A third option, the use of avalanche photodiodes (APD), was also rejected. These devices exhibit almost noiseless gain when reverse biased the appropriate amount. The nominal 100 gain that is achievable is well below that for PMTs and would have fallen short of satisfying our requirements. Additionally, a fundamental concern with APDs is a large gain variation due to ambient temperature changes. This would have to be compensated very carefully to maintain the accuracy of the system. Our rejection was thus based upon insufficient APD gain and the uncertainty of maintaining an acceptable temperature compensation.

4.2 Front-end Electronics Design.

A block diagram of the data acquisition system is given in Figure 35. A low-pass filter (LPF) with an upwardly adjustable bandwidth and a high-pass filter (HPF) combine to form a bandpass filter (BPF), which acts as the load for the photomultiplier tube anode. A gain stage then feeds the input of a logarithmic amplifier which compresses the signal's dynamic range. A track-and-hold (T/H) amplifier is then fed this compressed signal. A timing signal generated in a discrimination circuit initiates the computer's acquisition of scattering data by placing the T/H amplifiers in their HOLD mode. The computer later resets the system and sets the T/H amplifiers to track the signal from the photomultiplier tubes.

Signals detected by the PMT are from two basic sources. These are represented in Figure 36 by a particle scatter term (I_p) and a molecular scatter term (I_m). Particle scatter is gaussian shaped in time due to the gaussian TEM_{00} intensity profile of the laser beam and thus dominated by AC components. The always present molecular term consists of both DC and AC (noise) components. The DC component is due to the high power laser beam intersecting air molecules in the detector field of view. The AC component derives from the laser beam noise fluctuations (0.2% rms of the DC component). Both molecular components are unwanted. The DC component was easily removed by employing a high-pass filter (HPF) in each channel's preamplifier section. Prior to final testing and delivery to the customer, the AC noise component had been improperly assessed as a signal contribution based only upon a percentage of the particle scatter (i.e., 0.2% rms of the AC particle scatter) which, being well below the design accuracies, was discounted. The more important molecular contribution was overlooked. This was not realized until the nephelometer system had been delivered and its final integration and testing begun. Had there been no oversight in assessing this noise, the preamp design would have been identical to that which was delivered anyway. This is because only one method could have been used to eliminate the noise component and still allow the use of a real time, non-integrating light scatter measurement system. Basically, the noise has to be eliminated at the source to do any good (see Section 5).

The LPF, Figure 36, presents a load for signal currents from the PMT anode and optimally band limits the signal noise; the bandwidth is switch selectable. Resistor R is the main current-to-voltage conversion element. SW selects the highest RC product to limit both the developed signal and noise bandwidths to 2 Khz. When greater bandwidth is desired, SW can be toggled to a lower RC product to yield a 20-kHz bandwidth. Dynamic range is approximately five decades. Four predetermined gain settings were required for the PMTs corresponding to the scattering angle regions of (1) 9°-21°, (2) 28°-76°, (3) 102°-150°, and (4) 154°-166° from the forward direction. These settings are obtained by varying the high-voltage supplied to the individual PMTs.

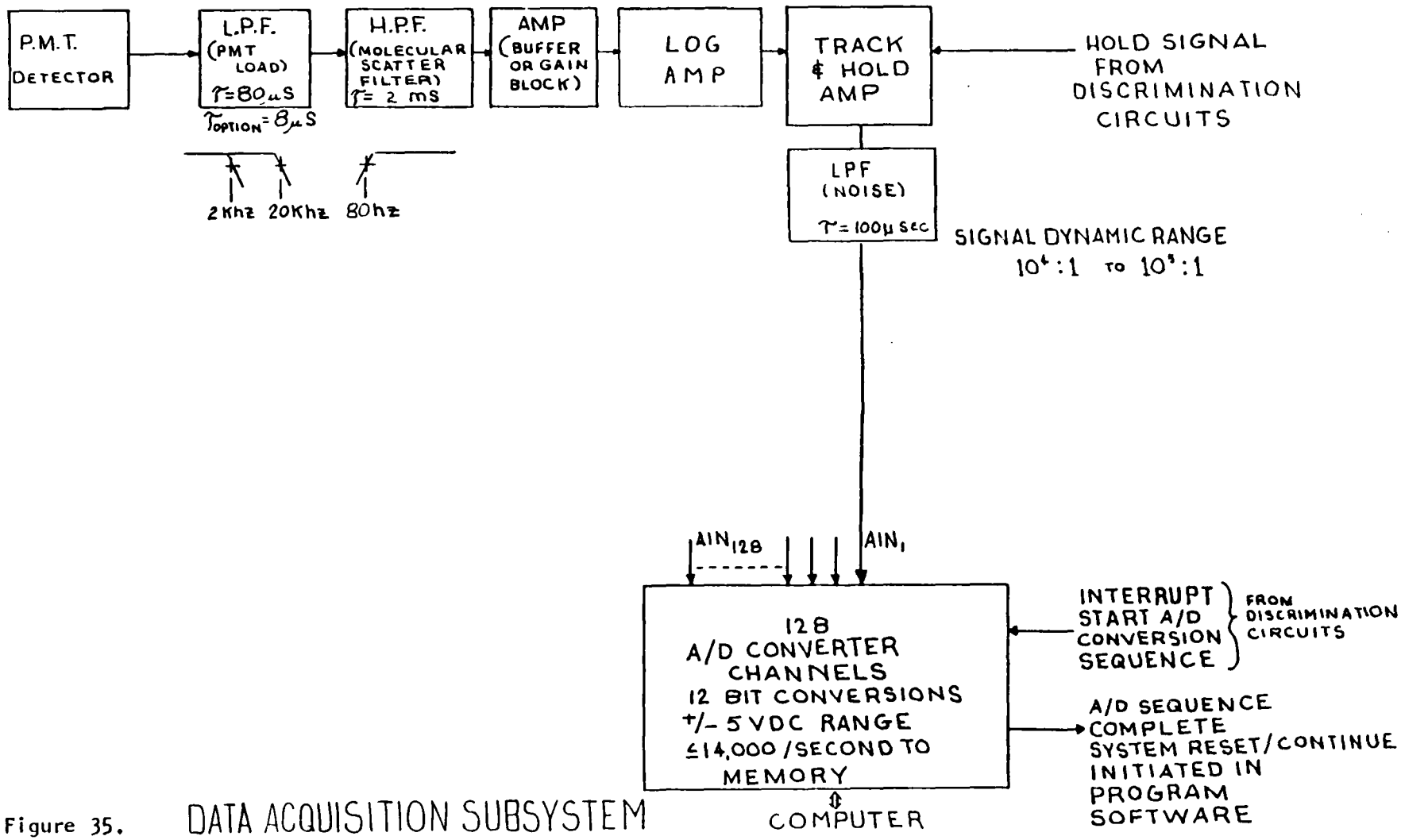

Figure 35. DATA ACQUISITION SUBSYSTEM

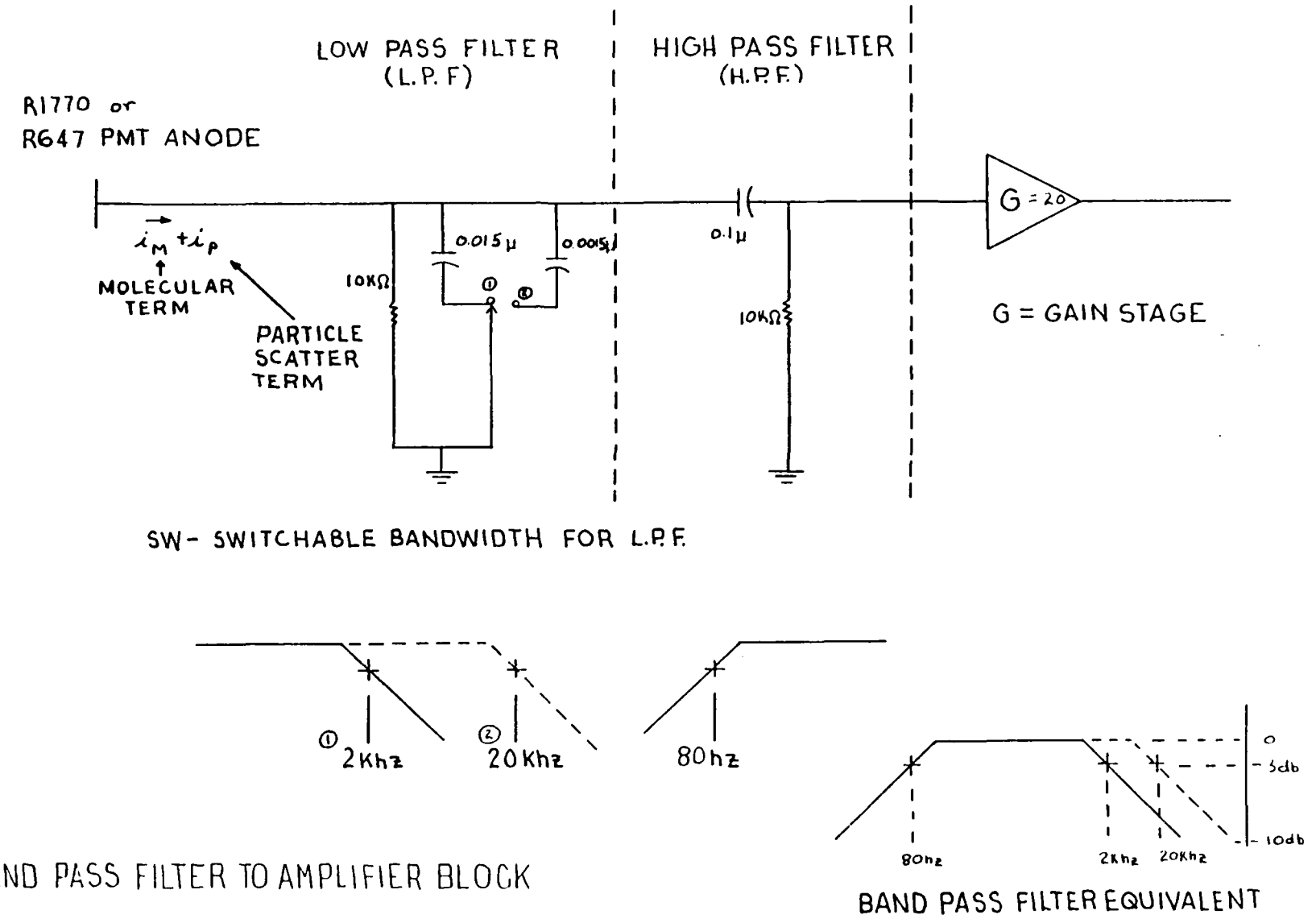

Figure 36. BAND PASS FILTER TO AMPLIFIER BLOCK

The HPF isolates any significant DC voltage level induced by molecular scatter. A nodal circuit analysis was made based on the illustrated components using the two selectable bandwidths obtainable with SW. The bandwidths computed were 80 Hz to 2 kHz and 80 Hz to 20 kHz, +0/-3 dB from the in-band maximum responses. Very little signal energy exists below 200 Hz for the gaussian-like scatter signals from the expected particle velocities. A full electronic circuit from PMT to T/H input was assembled on a plug-in breadboard and tested for bandwidth and dynamic range using a wideband, rectangular light pulse to excite the PMT. No special shielding techniques were used and the circuits performed as predicted.

In Figure 37, the log amplifier compresses the four or five decade dynamic range of the signal in a nonlinear fashion effectively yielding a one to two decade dynamic range signal. Resolution is reduced at high signal input levels and increased at low levels. The bandwidth of the selected log amplifier is approximately 20 kHz over a five-decade input signal range, allowing it to follow a signal from the preamplifier in either of the two design bandwidths (2 and 20 kHz). In order to ensure full 20 kHz response for the smallest signals of interest, an offset was introduced in the log-amp to bias it on (E_{OFF}). A secondary effect of this offset was a modification to the log-amp transfer function away from a fixed three volt per decade. This is broken down in the table of Figure 37 for an idealized two volt output with zero volt input. The result is a sliding response starting at three volts per decade for large input signals (1-10 volts) decreasing to one volt per decade for smaller signals (1-10 millivolts) and to very little response, though still measurable, at 10 to 100 millivolts per decade for the smallest input signals of interest (100 microvolts - 1 millivolt). Special calibrations are performed prior to aerosol measurements with the system, that determine the exact value of E_{off} for each channel so that a subsequent software routine can properly correct for this electronic adjustment. The T/H amplifier output reproduces the log amplifier output signal until it is placed in the hold mode with a signal from the discrimination circuits. Some time after the hold signal is applied (under 1.5 microseconds), switching transients die down, and the output level is valid (sample to hold delay time). Scattering data is coupled via single-ended coaxial cables, to remote RC noise filters which are located in the computer cart. These filtered signals are then fed directly to the microcomputer mounted A/D converters with reduced degradation from externally induced noise (EMI, vibration, etc.). The signal is then digitized and timing signal sets the T/H amp to follow the log-amp output. It takes only 10-15 microseconds for the T/H amp to attain its specified 0.01% tracking accuracy after receipt of the timing signal. A hardware delay is provided to guarantee that valid tracking occurs prior to the next scattering signal that is considered for measurement.

The cylindrical housings for the single channel and multi-element front-end electronics meet the space constraints and facilitate mechanical rotation of the polarizers. Wiring from each of the detector electronic assemblies is via special multiwire connector/cable assemblies to a large distribution box mounted on the same level as the laser head. Cables from the computer analog input distribution panel terminate within the distribution box at companion connector receptacles. Within the box, 108 separate PMT high-voltage levels are derived from the main high-voltage power supply with voltage divider networks. They are routed to their appropriate detector cable connector assemblies. All other special cables, including bipolar +15 volt power and T/H inputs to the electronics, and T/H outputs from the electronics, are distributed within this box, also.

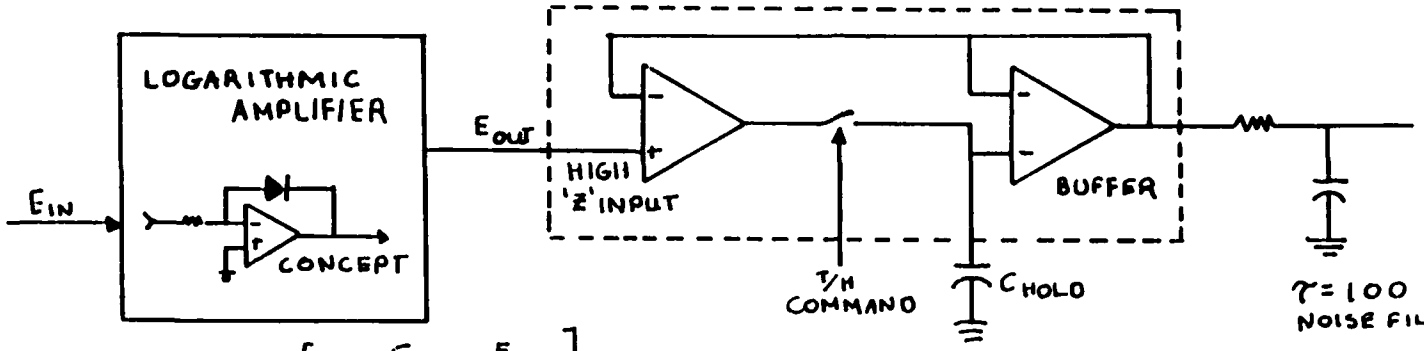

$$E_{OUT} = K\left[\log_{10}\frac{E_{IN} - E_{OFF}}{E_{REF}}\right]$$

EXAMPLE: $K = -3$ For $E_{IN} \geq 0$

5 DECADE RANGE

E_{IN}	E_{OUT}
10^{V}	-7.50^{V}
1^{V}	-4.51^{V}
100^{mV}	-1.69^{V}
E_{REF}	-0.254^{V}
10^{mV}	0.823^{V}
1^{mV}	1.822^{V}
$100^{\mu V}$	1.981^{V}
0^{V}	2.000^{V}

$E_{REF} = 31.6^{mV}$

$E_{OFF} = -6.81^{mV}$

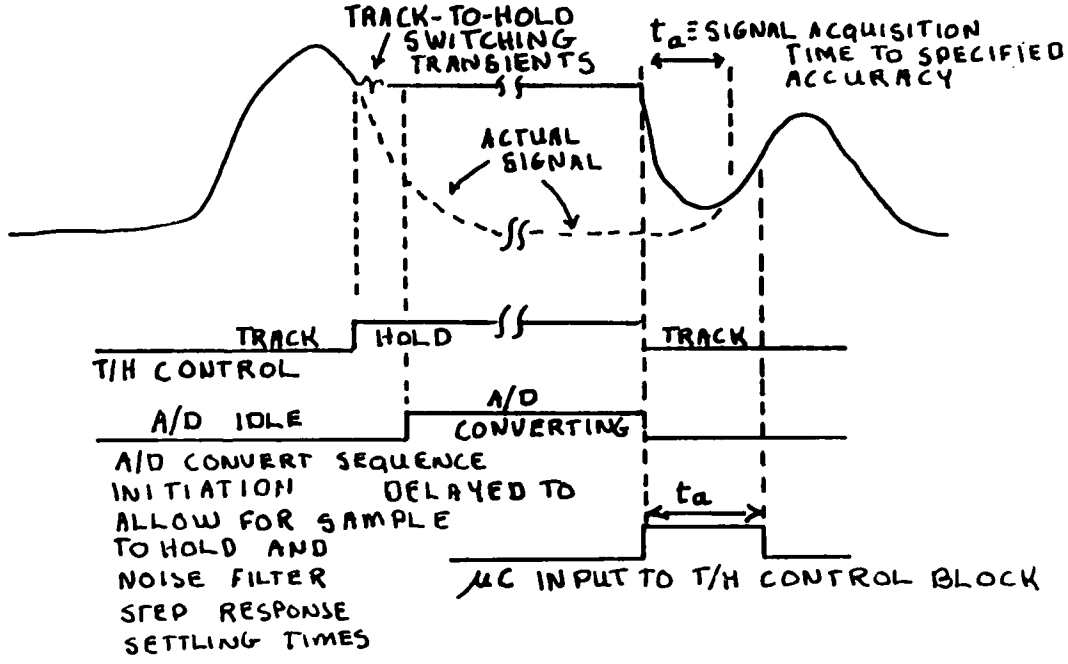

Figure 37. Log Amp to Track and Hold Block

4.3 Analog-to-Digital (A/D) Interface to Computer.

Data conversion from analog to digital is performed with Data Translation DT2762/2772 computer plug-in cards over ±10 volt with 12 bits of resolution. Each bit of conversion error (+5 millivolt), converted to an equivalent log amplifier input, is a constant 0.4% signal error assuming that we didn't introduce the offset previously discussed. RMS digitizing errors due to nonlinearities and a +10°C temperature variation are about 1.5 bits or a 0.6% signal error. Errors from other sources, for example the PMT calibration and the laser power reference measurement, which are described in [1] the instruction manual, are much greater than A/D errors. Upon transit of a valid particle, the discriminator circuits set the T/H amplifiers to HOLD and subsequently initiate a sequence of computer-controlled A/D conversions of the detector signals. After digitizations are completed and data has been stored in a RAM memory buffer, the computer releases the system to continue TRACKing particle scatter. The t_a time, Figure 37, is set by a multivibrator in the discrimination circuit to allow the T/H amplifier time to acquire the signal to within its 0.01% accuracy specification.

4.4 Timing and Discrimination Concepts.

The block diagram of Figure 38 presents the signal processing involved to (1) select the proper time to digitize the scatter information and (2) discriminate against unwanted scatter information. This method, in conjunction with the particle entrainment system, ensures that light-scattering data is obtained which corresponds to the particle near the laser beam center. In addition, scattering data is not obtained for "slow" or "fast" moving particles. Two signal processing sections are needed; they utilize signals generated by two of the near forward detectors in positions of expected high light scatter.

After the Nephelometer Final Design document was submitted, further analysis was conducted relating to the expected signal shapes that would have resulted from using the discrimination circuits described in that report. Those circuits would not have performed exactly as described for all the signals and therefore were redesigned.

The discrimination circuit that was used employs wave-shaping to obtain signals related to a particle's velocity and its position in the laser beam. Since the laser beam has a gaussian (TEM_{00}) amplitude variation, a non-band limited PMT preamplifier signal will have a gaussian envelope based on the particle position in the beam, which in turn is a beam transit time variable:

$$VPRE \propto e^{(-2t^2/T^2)}$$

where

- t = the time required for the particle to reach the beam center from its current position (at the design velocity)
- T = the time of transit from the edge of the beam to the beam center (at the design velocity)

[1] Ibid.

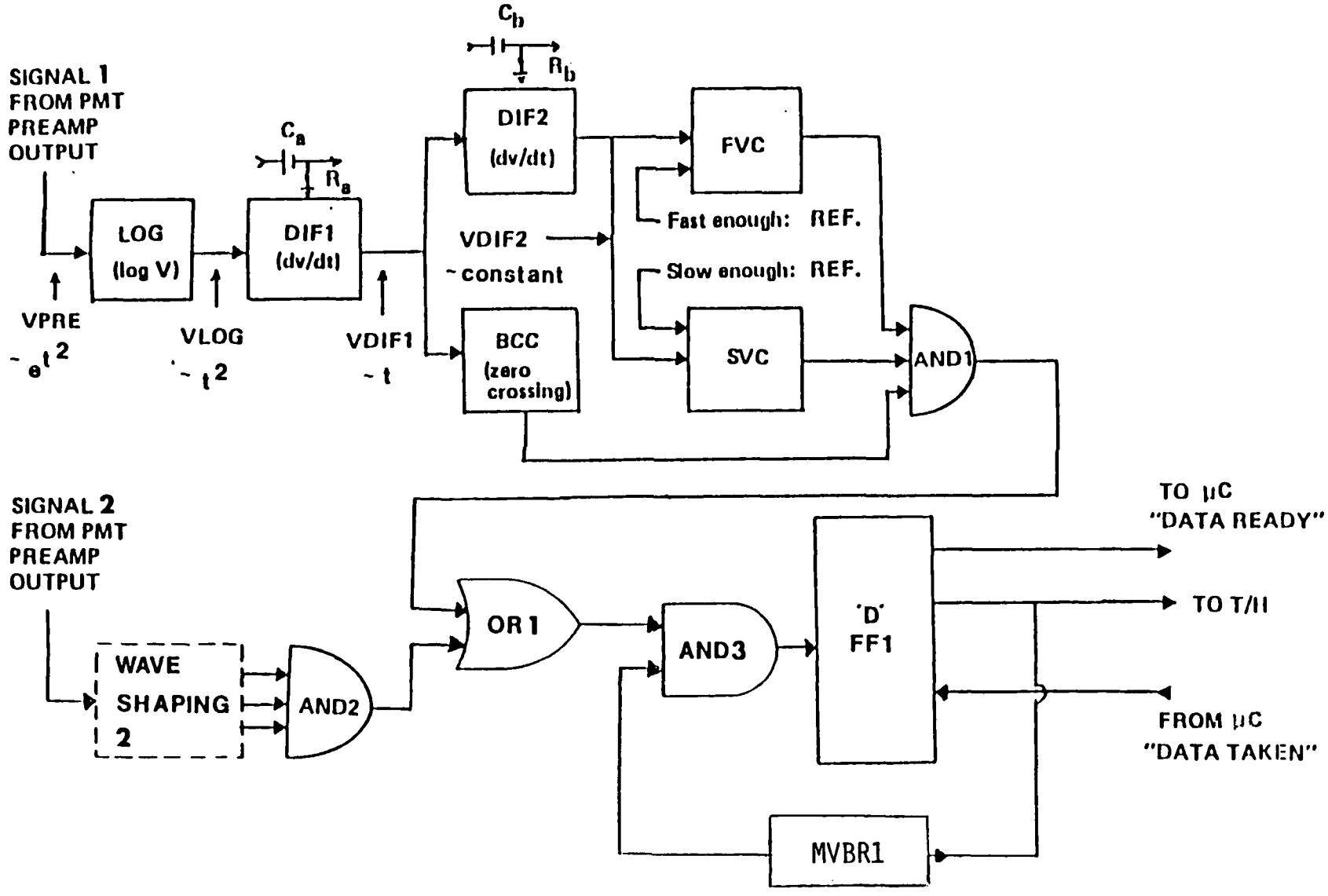

Figure 38. Signal Discrmination and Timing

The output from the logarithmic amplifier employed in each detector front-end electronics package is a signal with a quadratic time dependence:

$$VLOG \propto t^2$$

The output from DIF1, the first differentiator circuit, is a linear, time-dependent signal, assuming constant particle velocity:

$$VDIF1 \propto t$$

The output from DIF2, the second differentiator, is a constant proportional to a particle's velocity during its transit through the laser beam. This again assumes a relatively constant particle velocity:

$$VDIF2 = \text{constant}$$

Two signals, each from a different high scatter position photodetector, undergo wave shaping in the discrimination and timing block, Figure 38. The only difference is that one signal has been amplified two orders of magnitude more than the other. This is to cover signals corresponding to all particles in the designed size range of 0.3 to 10 microns. Identical processing occurs for each signal so only the 'signal one' process is described. The DIF1 output is fed to a "zero crossing" comparator whose output is a pulse having a HI- to-LO transition at the time the particle is passing through the beam center. This signal is fed directly to AND1 and is gated to AND2 if AND1 is enabled by its remaining two inputs. The DIF2 output feeds two voltage comparators. SVC, the slow-velocity comparator, has a HI output enabling AND1, as long as the particle is not traveling too fast. FVC, the fast-velocity comparator, has a HI output enabling AND1, as long as the particle velocity is not too slow. Therefore, as long as the particle transits the beam within a "correct velocity window" and has not reached the halfway point, AND1's output will reflect the output from BCC. Either signal one or signal two can satisfy the discrimination constraints or they both can. In any case the first signal arriving at OR1 is applied to AND3. When a particle of interest transits the beam center and an A/D sequence is not presently in progress, AND3 passes the HI-to-LO output from OR1 to the input of FF1. FF1 then sets the T/H amplifiers in a HOLD configuration, triggers the computer to initiate a data acquisition routine, and disables AND3. The computer A/D routine will always finish before the output of FF1 reenables AND3. When a routine is completed, MVB1 is triggered from FF1 and its output introduces an additional disabling condition on AND3. This input prevents any signals from reinitiating an A/D sequence for 700 microseconds while the T/H amplifiers return to a TRACK condition. This appears larger than is actually needed, but system tests show that data transfer between storage devices in the computer are the limiting factor to system speed. This delay would have to be twice as large to make a measurable reduction in system throughput.

4.5 Computer.

A laboratory grade computer system supports data acquisition and analysis. It contains a PDP-11/23+ Digital Equipment Corporation minicomputer with floating point hardware. Memory consists of 256K bytes of RAM, 800K bytes on 5-1/4 inch floppy disk drives, and 10M bytes on a Winchester-based hard disk drive. The system hardware is enclosed in a short rack-mounted cabinet on casters. A graphics supported VT-240 terminal and an LA-50 printer are supplied as operator I/O devices. Figure 39 gives additional computer specifications.

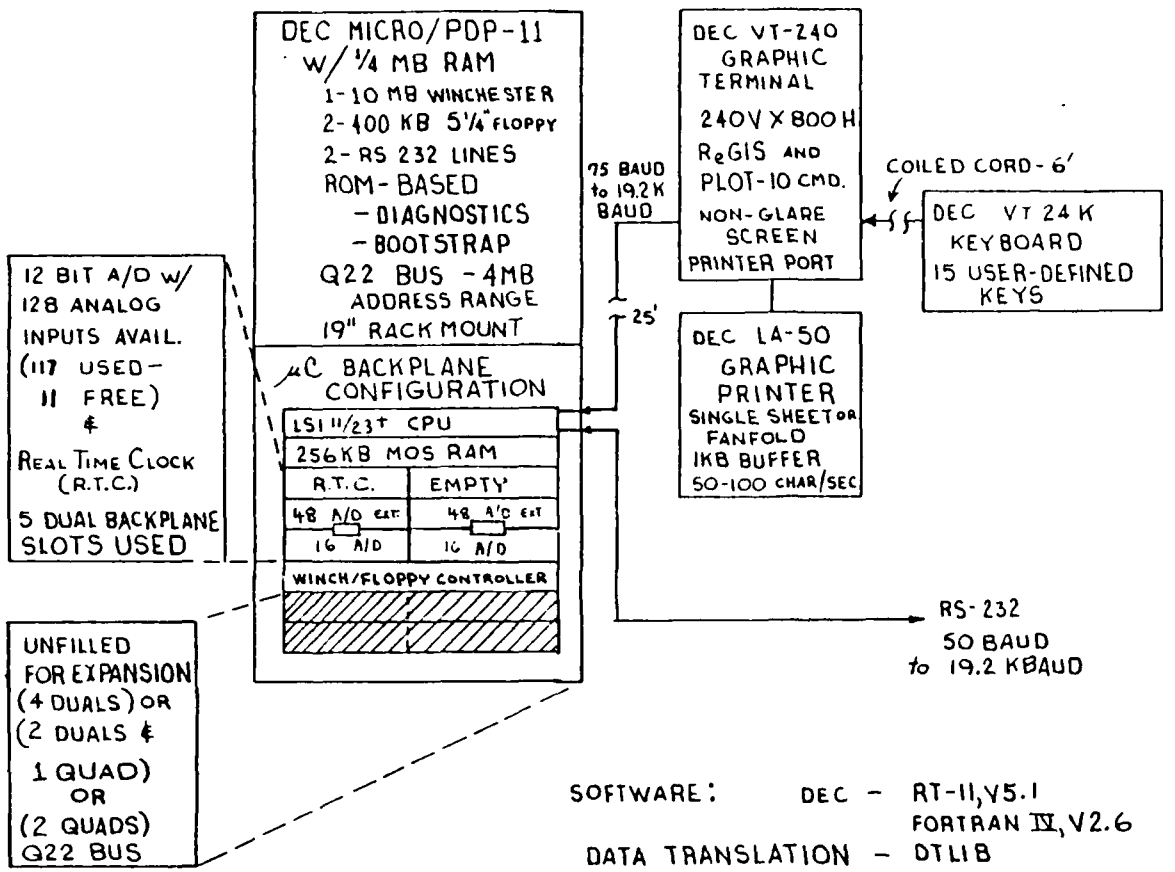

SOFTWARE: DEC - RT-11, V5.1
FORTRAN IV, V2.6
DATA TRANSLATION - DTLIB

CUSTOMER'S FUTURE
HARDWARE OPTIONS:

- MORE ANALOG AND DIGITAL I/O
- ARRAY PROCESSING BOARD
- CP/M COPROCESSOR
- LSI 11/73 (PDP 11/10 EQUIV.) PROCESSOR
- MORE RAM
- MS/DOS COPROCESSOR
- TSX+ MULTIUSER SHELL FOR RT-11

Figure 39. Computer Specifications

The computer system was selected and optimized for a single user requiring real-time (i.e., immediate/asynchronous) interaction with other system elements. Up to two tasks, high and low priorities, may be resident in memory and run, via time sharing, under the RT-11 software. The low-priority task, possibly program development or data analysis, would be interrupted with an external signal from the hardware supporting and high-priority task. When finished, the high-priority program would relinquish control to the low-priority task. Programs were written in (compiled) Fortran IV and assembly language, for increased execution speed.

The computer storage capability, broken down in Table 7, was determined by (1) system generation and program compilation requirements, (2) long-term storage file sizes, and (3) available supplier system configurations. Two of the 5-1/4 inch floppy disks should be sufficient to store four statistical samples. The Winchester hard disk is used to hold the operating system and program software and to store data during program execution. A medium resolution graphics terminal supports both ReGIS and PLOT-10 command protocols and a graphics-compatible printer allows hard copy output. The computer is expandable and upgradeable through the use of more powerful computer boards or array processors, digital and analog I/O, or remote terminals. It also contains two quad (or four dual) wide unused Q-bus backplane slots. Eleven A/D input channels are as yet unassigned and are available for operator use. Finally, running under RT-11, it is compatible with a vast amount of software available through both DEC and second source vendors.

4.6 Microcomputer Software.

The operating system of the microcomputer consists of RT-11 (version 5.1) with the Fortran IV/RT-11 (version 2.6) programming language from Digital Equipment Corporation (DEC), coupled with the DTLIB (version 2.2) data collection software from Data Translation. Additional software written by Boeing is used to operate the A/D converter boards and presently supports only the single task of data collection. The RT-11 software, on the other hand, has the capacity to support two tasks, such as data collection and program development.

The Boeing software includes two macro-level subroutines that interface the track-and-hold circuitry with the program controlling the data collection process. One of these subroutines monitors an event flag, generated by the discrimination circuits, to determine whether the nephelometer has gathered valid scattering data, while the other resets the discrimination circuits.

The controlling program transfers data values from the 128 A/D converter channels into a buffer in core memory. These data include voltages from the optical detector preamplifiers, laser power monitor, flow meters, power supplies for the front-end electronics and eleven channels which are unused at this time. It remains only for the operator to connect to these channels at the distribution box within the computer cart to record other analog data of interest. The decision to store all 128 channels derived from the simplicity of its software implementation, the desire to reduce further software revision to "add" these channels if needed in the future and the fact that system throughput was not noticeably reduced by doing so.

When the core buffer has received values from approximately 10 particles, the data is written to a larger buffer located on the hard disk and under control of that disk using DMA. Once the hard disk is in control of DMA data transfer, the data collection program begins taking data for the next 10 particles using a second core memory buffer for storage. The first core buffer to disk transfer is usually accomplished before the

Table 7. Computer Storage Capability

- 128 DATA VALUES PER PARTICLE (2 BYTES PER DATA VALUE)
  - 108 DETECTOR SIGNALS
  - 4 FLOW VALUES
  - 4 POWER SUPPLY MONITORING SIGNALS
  - 1 LASER POWER MONITOR SIGNAL
  - 11 CHANNELS FOR UNSPECIFIED DATA
- 1000 PARTICLE SAMPLE FOR STATISTICAL ANALYSIS
- 240K BYTES PER STATISTICAL SAMPLE
- FOUR STATISTICAL SAMPLES FOR MUELLER MATRIX
- 1M BYTE MAXIMUM STORAGE FOR MUELLER MATRIX CLASSIFICATION
- MICRO PDP-11/23+ MINICOMPUTER
  - FLOATING POINT HARDWARE CHIP
  - TWO 400K BYTE 5-1/4" FLOPPY DISKETTE DRIVES
  - ONE 10M BYTE 5-1/4" WINCHESTER DISK DRIVE FOR OPERATING SYSTEM AND FAST STORAGE
  - 128 CHANNELS OF A/D INPUTS
  - REAL TIME CLOCK
- VT-240 GRAPHICS TERMINAL (240V x 800H)
  - ReGIS COMMAND PROTOCOL (GRAPHICS, VT125)
  - PLOT-10 COMMAND PROTOCOL (GRAPHICS, TEK-4010)
- LA-50 GRAPHICS PRINTER
- RT-11, V5.1 REAL-TIME OPERATING SYSTEM SOFTWARE
- FORTRAN IV, V2.6 PROGRAMMING LANGUAGE SOFTWARE
- DTLIB A/D SOFTWARE (DATA TRANSLATION)

second buffer is filled. Thus, when the second buffer is full, the program can direct the hard disk drive controller to transfer data from it using DMA and in turn start filling up the first core buffer, writing over the previous data. This asynchronous interleaving of core memory data transfer utilizing hard disk DMA allows system throughout to be increased a great deal. Using the STEP subsystem described below the speed at which data is recorded with the nephelometer has been tested successfully at over 90 particles/sec. The same tests using earlier software without DMA hard disk control allowed an effective particle throughput of about 14 particles/sec.

Data transfer speeds to a floppy diskette only allow a particle throughput of about 40 to 50 particles/second. In addition, due to its limited storage capacity, the operator must ensure the floppy has enough space remaining to store the scatter data. If there isn't, then the data file will not close out properly and data for that run might be lost. The floppy diskettes are best used to provide long-term storage for data when an experiment is completed. The multi-diskette backup utility available in the RT-11 operating system transfers the data values from the buffer on the hard disk to floppy diskettes, thus releasing the buffer for use in subsequent experiments.

4.7 Software Test Electronics Package (STEP).

Because of the unpredictable delivery schedules for mechanical and electrical hardware, the early receipt of ordered software, and the difficulty in writing and debugging software for real-time control without the luxury of testing it on the target hardware, a special electronics package was constructed. This package is shown in Figures 40 and 41, a block diagram and circuit diagram, respectively.

Functionally, the STEP package consists of (1) a two-frequency selectable triangle-wave generator, (2) a T/H amplifier, (3) a continuously adjustable clock, (4) a pushbutton, single-pulse generator, (5) a nine-position selectable voltage reference, (6) two LED indicators, (7) a controlling node to steer clock pulses to the T/H amplifier and computer, and (8) A/D converter to distribution box connectors. The triangle-wave generator ramps between $\pm$10V DC at a 1- or 100-Hz selectable rate and feeds the T/H input. The adjustable clock can be set between 7 and 100 pulses/second, thus mimicking particle flow in the final system. Since there is no connection between these two rates, they are uncorrelated. The T/H output feeds 24 A/D input channels. The switchable reference feeds an additional 20 inputs. The STEP +5V DC supply feeds 42 inputs and the remaining 42 inputs are fed from ground.

Operation consists of first sending a RESET command to the STEP, just as a nephelometer data collection software program would be required to do. This command will cause a green LED to flash once and the controlling node to be cleared, which in turn will place the T/H amplifier in its TRACK mode. The output of the T/H amplifier will then be a triangle wave at the selected frequency. Depending on the "particle clock" switch position, the controlling node will be set by either the next free-running clock pulse or the operator (by initiating a single pushbutton-induced clock pulse). In either case, the T/H amplifier will switch to its HOLD mode, and the computer will be triggered to start a data acquisition sequence. Simultaneously, a red LED will flash once. The computer program will then initiate a collection sequence, consisting of performing A/D conversions on the 128 channels available. After conversions are completed, the computer sends a RESET command to the STEP, returning it to its TRACK mode. The LEDs were supplied to give the operator a better feel for the subsystem operation. The STEP chassis is rack mounted beneath the distribution box in

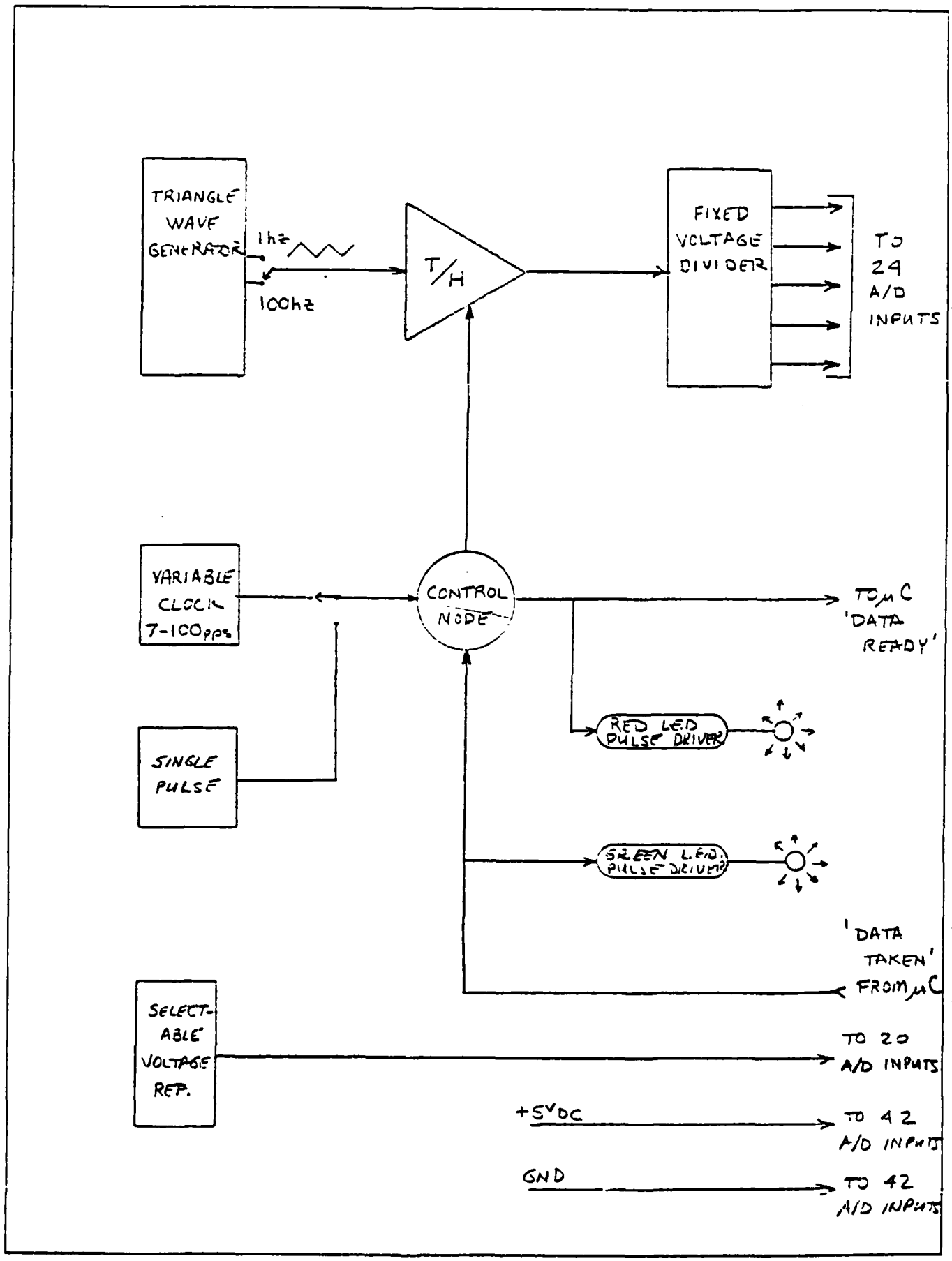

Figure 40. Software Test Electronics Package: Block Diagram

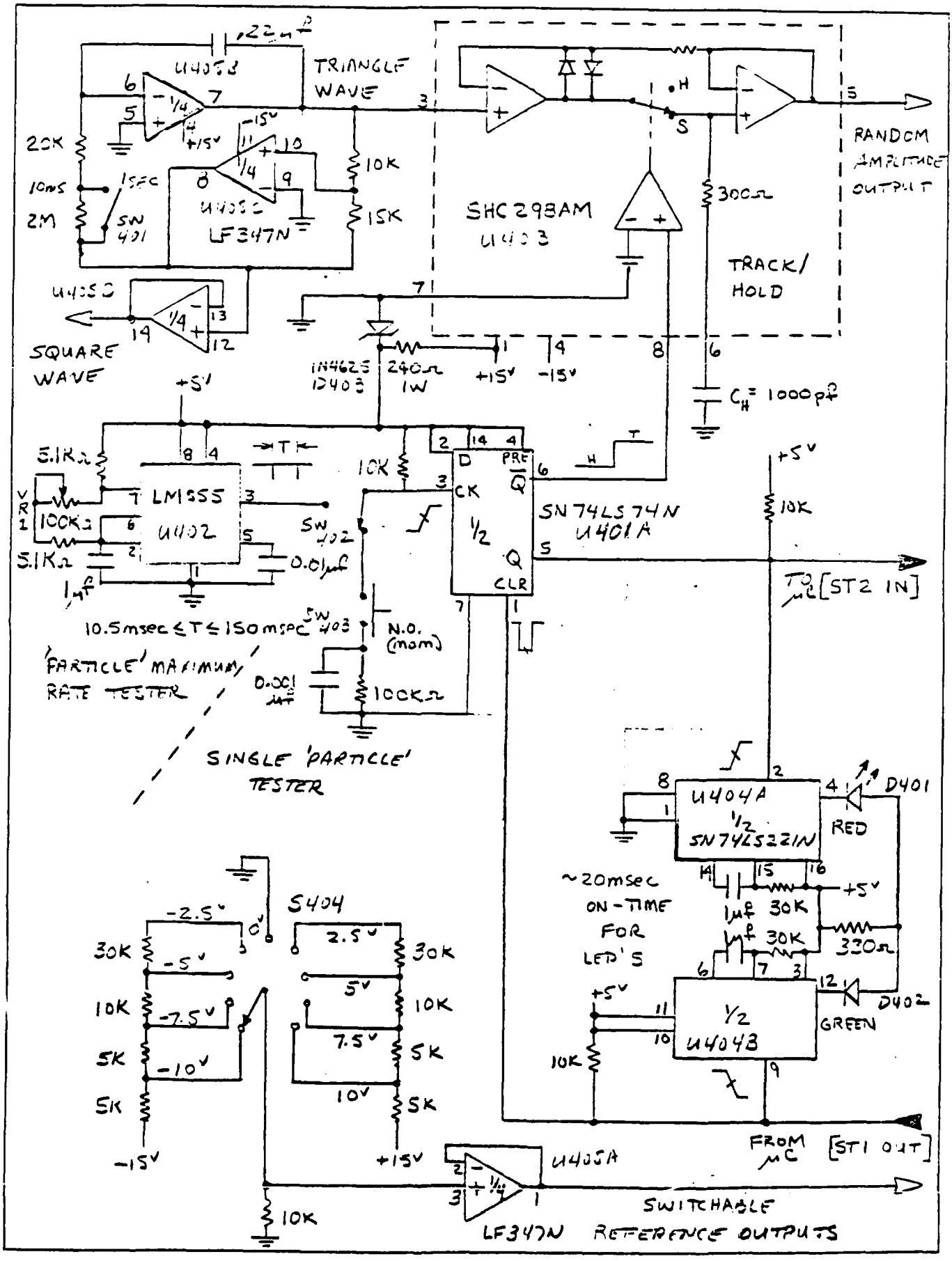

Figure 41. STEP circuit.

Table 8. Data Acquisition System Characterizations

CONDITIONING ELECTRONICS

- BANDWIDTHS
- NOISE LEVELS
- DYNAMIC RANGE
- TEMPERATURE VARIATION EFFECTS
- POWER SUPPLY VARIATION EFFECTS
- PROPAGATED ERRORS
- DISCRIMINATOR, LIMITS OF OPERATION

COMPUTER

- SOFTWARE INSTALLATION AND VALIDATION
- STORAGE CAPACITY
  - CONSIDER OPERATING SYSTEM
  - PROGRAM MEMORY
  - DATA FILE OVERHEAD
- CONTROL AND COMPATIBILITY WITHIN SYSTEM

A/D CONVERTERS

- SOFTWARE OPERATION
- REAL-TIME INTERRUPTS

the rear of the computer cart. The STEP package was used successfully to interact with and debug Boeing-written software for the multichannel nephelometer and is installed in the computer at this time.

4.8 Data Acquisition System Enclosure.

The system is housed in a desk-high, rollaround, RETMA standard rack illustrated in Figure 2. The system terminal and keyboard sit atop the rack, and the companion printer is placed at the rear of the terminal. This configuration provides a comfortable workstation for a seated operator, with the terminal at the height of a standard 30 inch high desk. Cabling is shown conceptually as a main signal input bundle, 10 to 20 ft long. The bundle actually contains cables for 108 analog detector signal cables; four power supply, one laser output power, and four flowmeter monitoring cables; power supply output cables; and two digital control cables. Detector signal coaxial cables enter the terminal block and connect to it via spade lugs. R-C low-pass filters are installed for all signal lines to reduce noise. A 3M-type connector routes these signals into the A/D conversion boards mounted in the computer backplane. The terminal block employs a plexiglass cover for safety.

4.9 System Tests and Characterizations.

Table 8 lists three categories of system characterizations that were performed on the data acquisition system prior to delivery of the multichannel nephelometer. The conditioning electronics include the filters, T/H amplifiers, and log amplifiers of Figure 35, and the discrimination electronics of Figure 38. The computer is described in Figure 40. The A/D converters are shown in Figure 35. Table 9 gives the materiel list for major components of the data acquisition system.

5.0 SYSTEM INTEGRATION AND TEST

The three systems described in Sections 2 through 4—the aerosol sampling system, the light-scattering system, and the data acquisition system--have been integrated into a single instrument. As the system development progressed, the main emphasis of system integration and test was to get the system up and operating. The multichannel nephelometer is a complex system and as problems arose it was frequently difficult to isolate their causes. As a result, the basic effort to get the system operating consumed the available resources and a more ambitious plan to fully characterize the operation of the system could not be pursued. Unfortunately, the system as delivered was not fully operational.

The signal from an aerosol particle is basically a gaussian pulse which must be identified as a valid pulse and then measured. The air molecules in the chamber also scatter light from the laser beam into the system detectors. While the incoming laser beam and the resulting molecular scatter is basically a DC signal and easily filtered, there is an AC component of the laser beam (less than 0.2% RMS of the laser beam intensity) which is in the system passband. The nepholemeter has a dynamic range of four to five orders or magnitude to cover the expected signals from particles in the range of 0.3 to 10 microns. The residual ac signal from the molecular scatter, which was overlooked during early design and development, is higher than the signals from all of the smaller particles. This currently limits the usable range to particles from about 3 or 5 microns to 10 microns in size, putting severe constraints on system utility.

Table 9. Materiel List for Data Acquisition System

P/N	Item	Manufacturer	Quantity
759N	logarithmic amplifier	Analog Devices	120
SHC298AM	track/hold amplifier	Burr-Brown	120
OPA111	operational amplifier	Burr-Brown	120
DT2762-SE	A/D conversion board	Data Translation	2
DT2772-64SE	A/D expansion board	Data Translation	2
DT2769	real-time clock board	Data Translation	1
DTL1B	A/D converter software	Data Translation	1
DT701-MA-20	terminal panel w/19" rack	Data Translation	1
DT701-50	terminal panel	Data Translation	2
MLSI-H984	19" rollaround rack	MDB	1
11C23-RA	Micro/PDP-11 computer	Digital Equip.	1
KEF11-AA	floating point coprocessor	Digital Equip.	1
VT-240	graphics terminal	Digital Equip.	1
VT24K-AA	keyboard	Digital Equip.	1
LA50-RA	graphic printer	Digital Equip.	1
QJ013-A3	RT-11, V5.1 (software)	Digital Equip.	1
QJ813-A3	Fortran IV/RT-11, V2.6 (software)	Digital Equip.	1

The customer, the Army Chemical Research and Development Command, is currently in the process of obtaining a laser beam modulator system ("noise eater") to reduce the laser noise approximately 2 orders of magnitude. This effort is expected to render the nephelometer fully operational.

5.1 Aerosol Sampling System.

The development of the aerosol system was accomplished independently of the rest of the systems and was covered in Section 2. As indicated, the aerosol system has been found to be fully usable. There are, however, several characteristics which have not been fully resolved. Using the aerosol generator sources which were available, including a dense sugar aerosol which was used for stream visualization, the dilution system was found to be more than adequate. Generally, only one of the diluters was needed. As noted in Section 2, there are questions as to how effective the diluters are in tandem because of the capillary system. No quantitative measurements have been made on the system to characterize the actual dilution ratio nor to determine sample bias. Knowing exact dilution ratios is not critical for studying the scattering patterns since the flexibility of the system allows empirical determination of a suitable dilution ratio. Determination of the exact dilution system characteristics and system biases could potentially increase the usability of the system since it could allow full characterization of an unknown source aerosol. However, this is not required to fulfill the basic purpose of the multichannel nephelometer, which is to allow the characterization of the light scattering of a large number of non-spherical particles.

Particle rotation is the one question of significant concern which remains unresolved regarding the aerosol system. The original specifications called for rotation of less than 1% (i.e., less than 3.6^{o}) during particle scatter pattern measurement. The aerosol jet flow is too complex for analysis within the current state of the art so attempts to calculate what particle rotation rates to expect proved fruitless. The rotation criteria, if significant rotation is present, could be fairly complex depending on jet parameters, location in the jet, and particle characteristics. The design and setup for a measurement test, including appropriate sources and instrumentation, and the subsequent data reduction and analysis is not a trivial operation. As a result of the effort that was required for the basic system development, experimental measurement of particle rotation was not performed. Rotation, however, is not expected to be a problem. As noted in Section 4, the measurement concept of the data acquisition system is the simultaneous "freezing" of all detector scattering signals at their peak values within a 1.5 microsecond time period. A particle would have to rotate at a rate exceeding 6000 revolutions per second to exceed the 1% rotation specification.

5.2 Light Scattering System.

The integration and test of the light scattering system involved the characterization of the FOVs and responsivity calibrations of the PMTs to yield a usable system. As originally designed and built, the aperture in the individual detector spatial filter units was a precision 1 mm pinhole. After the system was assembled this was found to be too small. As discussed in the individual detector assembly portion of Section 3, the problem basically reduced to a conflict between reducing the detector FOV, achieving the desired pointing accuracy of the spatial filter units, and attaining perfect placement of the scattering point with the aerosol particle in the center of the laser beam at the exact sphere center at the moment of data acquisition. The full impact of these interactions was not recognized and the sensitivity of the spatial filter to tolerance variations had been overlooked. Several approaches to resolving the problem within the constraints of the then existing equipment were investigated and tested. These included the use of a

different focal length lens, reconfiguration variations which modified the lens/aperture distance, and modification of the aperture size. Even if a total redesign were considered, the basic conflict did not change substantially. It was finally decided that the optimal solution was to change the aperture size. The system was therefore delivered with a 0.157" (4.0 mm) aperture installed.

The detectors were calibrated individually in a special setup to allow an absolute calibration to a known input signal. Using MIE theory, a Fortran program was developed, and run on a VAX 11/750, to predict the light scatter received at each detector location. Inputs to this program included the detector size (solid angle of subtense), laser power available in the beam, particle size, particle refractive index and the detector angular scatter position with reference to the direction of particle illumination. The gaussian nature of the laser beam was used to determine the laser intensity at the center of the beam.

The result of this analysis is synopsized in the accompanying graphs in Figure 42. These show the received power expected for particles of DOP in the size range 0.3 microns to 10 microns when they pass through the center of a 0.7 watt TEM_{00} laser beam. With this data the volt per watt responsivity of the PMT/amplifier combinations for each of four angular ranges was determined. A setup was developed and a jig made to allow placement of an expanded laser beam spot of approximately 5 mm diameter at the detector center, to allow easy illumination of each assembled detector module. Additionally, a rotating slot was placed in the laser beam path to generate pulses of light so that the AC coupled amplifiers would function properly. A set of calibrated neutral density filters was available. Next, using a calibrated silicon photodiode with a 1 cm^2 active area for a reference and no neutral density filters, the desired power for each detector angular position was adjusted from the laser. Compensation was made for any neutral density filters which would be used to obtain the flux used in the next step, that of substituting an actual nephelometer detector assembly for the photodiode. The PMT high voltage supply was then adjusted to obtain a one volt pulse height (as seen on a CRT screen) at the output of the detector assemblies gain stage. The value of the high voltage was noted (to the nearest 5 volts) and when this task had been performed for all detectors, the high voltage distribution board was loaded with appropriate dropping resistors to obtain the specified voltage. A slight variation of this method was used to calibrate the array detection assemblies. Since only one high voltage could be used for each array of eight detectors, one detector was calibrated to meet the above described process and the remaining seven detectors' responsivities were measured with respect to the calibrated detector. A computer file held the detector responsivities (PMTCAL.DAT), as supplied at the time of delivery. Another file (VDIVDR.DAT) gave the high voltage needed for each PMT and the 1% resistors used to obtain it.

Another important consideration in the light scattering system is alignment. The detectors are aligned mechanically with the sphere center. As noted before, the pointing errors of the detectors was addressed by increasing the FOV of the individual detectors so that a large fraction of each detector FOV intersected in the center of the sphere. Although the aerosol nozzles are mechanically centered there are still possibilities of variation in the aerosol jet location as a result of nozzle spacing, operating parameters and such. However, if the aerosol system is functioning properly these variations are slight. Further, the light intensity drops off rapidly as one moves away from the center of the beam. The finite laser beam also introduces an intensity variation factor which must be considered in system alignment. During the light scattering system integration a special alignment plate was fabricated which allows placement of a small hole at the mechanical center of the sphere. The hole is taped over with Scotch Magic^{TM} tape and by shining the laser through this hole and evaluating the tape scatter images transmitted

through each of the spatial filter assemblies, it was possible to confirm the pointing accuracy of the individual detectors. Subsequent evaluation with the aerosol jet confirmed that the aerosol jet also intersects the center of the chamber. Exact alignment of the laser beam with the chamber was also possible by adjusting the laser beam controls for maximum intensity through the alignment plate hole. Detailed instructions for realigning the system are given in [1]the instruction manual. Since the laser is mounted on the same table, realignment of the laser is only required when the controls have been changed or the laser has been moved.

The last major consideration for the light scattering system prior to delivery concerned laser safety. The laser incorporated into the multichannel nephelometer is a Class IV laser which is potentially hazardous for both eye or skin exposure. The nephelometer has been designed to provide beam enclosures and other safeguards so as to make the nephelometer a Class I system which presents no accessible hazards to the operator. A detailed report of the laser safety considerations was submitted to the Food and Drug Administration for certification.[2] Laser safety concerns for operation, maintenance, and service of the multichannel nephelometer are given in the instruction manual.[1]

The data acquisition system integration and testing phase was in large part an R&D effort in itself. As electronic samples and computer hardware/software arrived, bench testing led to changes in all areas of the proposed circuitry and Boeing supplied software support, that had been defined in the proposal and final design documents.

The original front-end electronics called for using the log-amp as the output stage -- after the T/H amplifier. This had to be changed to increase the normal dynamic range of the logamp from 4 decades of voltage input up to about five decades. This was done by increasing the voltage-induced input current a factor of five beyond the recommended design log conformance specification. Although the input current would still be maintained below the devices maximum safe value, the manufacturers engineering staff indicated that log conformance at high currents could not be assured for DC values (due to temperature increases, etc.). Thus the logamp had to be operated in a pulse-mode, and the nearest to this was to drive it off the preamp section which output would yield a current pulse for each particle transmitting the laser beam. The T/H amp and logamp positions were reversed in the delivered nephelometer. Subsequent testing of PC board constructed front-end electronics packages verified that an ideal 150 microsecond (or slower) gaussian shaped current waveform was amplified properly by the preamp and that the five decade dynamic range requirement was satisfied with the logamp in this configuration.

The discrimination circuit initially was specified as utilizing pulse width windowing to determine whether a signal was derived from a valid particle's scatter. This circuit would not have functioned properly. Its operation was based upon a faulty assessment of the waveforms obtained from the waveshaping stages of the circuit. After a more

[1]Ibid.
[2]Model Change Report on Laser Products (Non-Medical): For the Multichannel Nephelometer, Model No. 1, FDA Accession No. 8521754, Boeing Aerospace Company, Seattle, WA. October 1985.

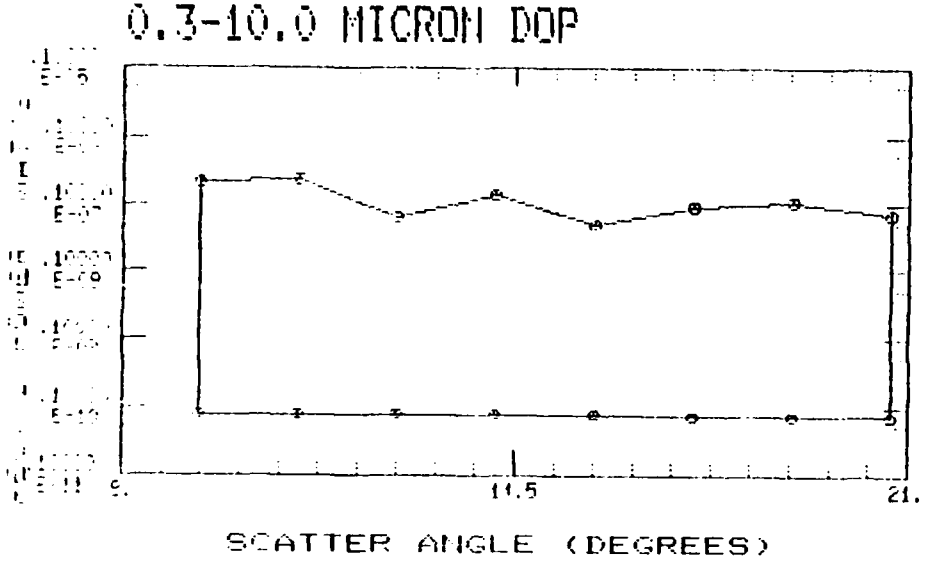

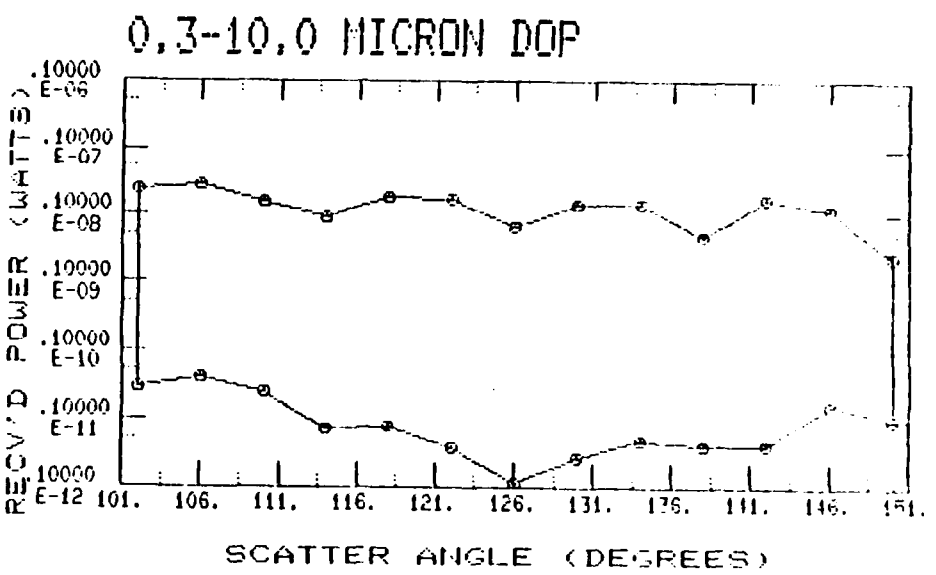

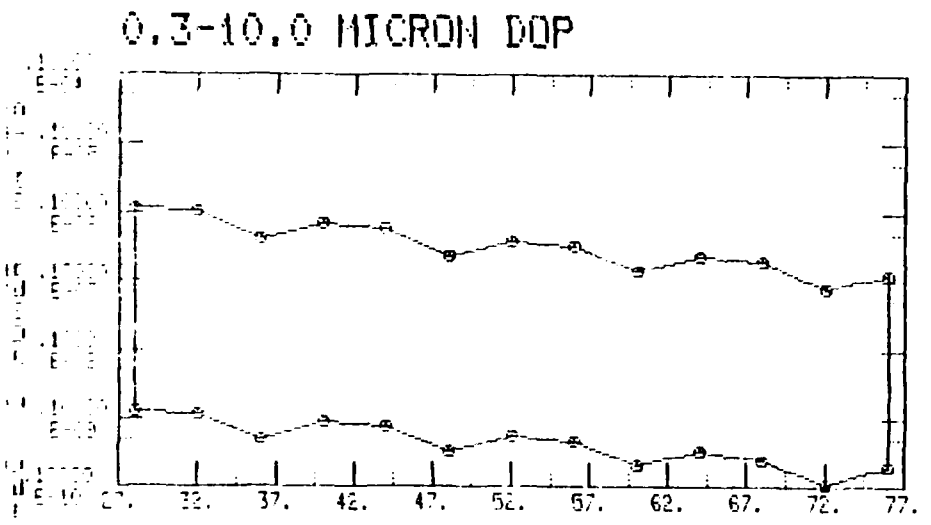

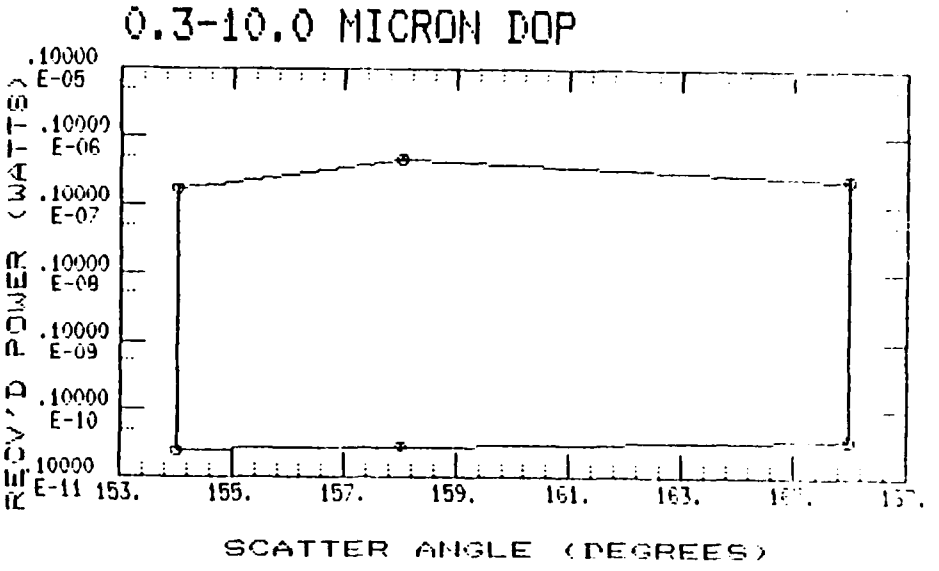

Figure 42. Predicted MIE Scatter for Dioctyl Phthalate (DOP)

detailed analysis of these stages was made, discrimination based upon level comparisons with voltages corresponding to particle position and velocity was implemented. Subsequent breadboarding and testing with a gaussian waveform confirmed the functioning of this circuit. The waveform was generated with a Wavetek model 275 arbitrary waveform generator under control of a Hewlett Packard HP9825 computer. The discrimination circuit was constructed on a vector board due to its uniqueness and the expectation that further fine tuning would be required when integrating it with the other nephelometer system components. Additionally, two forward detector channels, with different gains and duplicate waveshaping circuits, were used to allow discrimination over the expected five decade signal range, rather than the single circuit initially specified.

After receiving a majority of the PMT's, it was realized that the inherent gain variation between tubes was such as to preclude using a single high voltage setting to supply all channels. The relative gain range from least to most sensitive was over 50:1 for the 1/2" round PMT's. The only cost effective way to address this problem was to tailor the HV to each tube. This was accomplished using precision dropping resistors placed on a centralized distribution board for each PMT. Actual selection of each resistor value was performed during the responsivity calibration of the PMT/preamp combination explained previously in this Section. PMT and preamp component variations were addressed simultaneously to minimize the use of precision components.

Initially an electronic interlock to guarantee Class I operation was proposed, and the components needed for its implementation exist in the discrimination board. Worst case exposure limits were subsequently found to be below Class I specifications at all times. Therefore, this interlock was bypassed to reduce system complication.

Since software takes a large percentage of product development, when the A/D hardware was ordered, a package of software (DTLIB) to support it was also obtained. After hardware installation, a Fortran program calling DTLIB routines was written and debugged using the STEP module. The fastest operation obtained was a 14 particle per second equivalent. Since this satisfied the data collection requirement of 10 particles per second, further efforts to increase system throughput were curtailed. Further software development went into operator interfacing for ease of use. When the nephelometer program was complete, and encouraged by the ease of earlier assembly language development, further work went into developing additional assembly language routines to control the A/D converters directly and into Fortran routines to use double buffering and hard disc controlled DMA. The result of this work was a wholly Boeing written program (no DTLIB support) that was able to operate at a rate in excess of 90 particles per second using the STEP module. This is the program that was subsequently delivered to CRDC.

After assembly of the detector assemblies and their power distribution box, a high level of 180 Hz noise was initially present on the preamp outputs. This was minimized by ground-strapping the box to the metal optical table. It appeared as though the laser lead or supply was radiating (RFI) up through the table top and into the detector electronics. By connecting the optics table to the distribution box (which itself was grounded) the RFI was blocked.

Tests were performed to determine the required warmup time for stable data acquisition. Three of the array channels and six of the individual channels were monitored for two hours each for drift at the output of the log amp, Figure 43. This

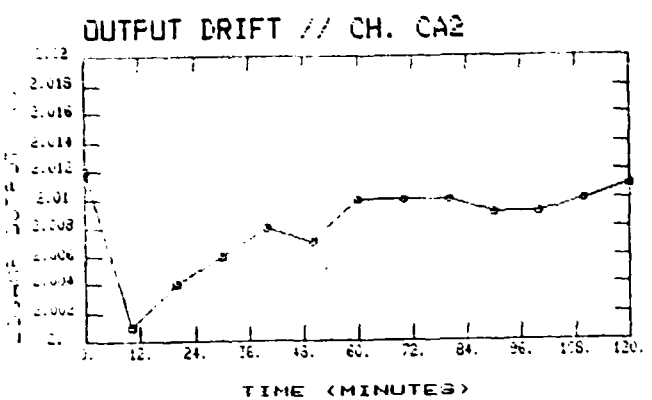

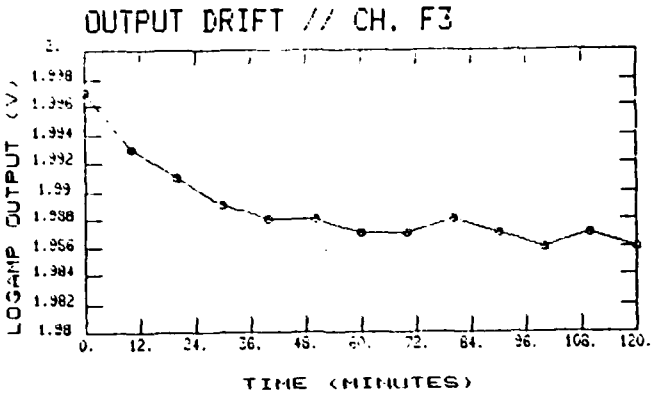

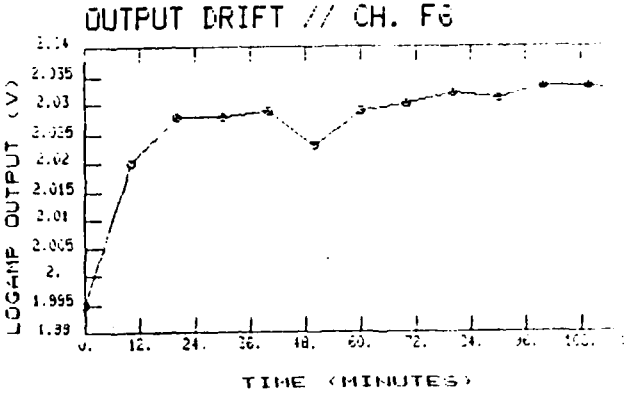

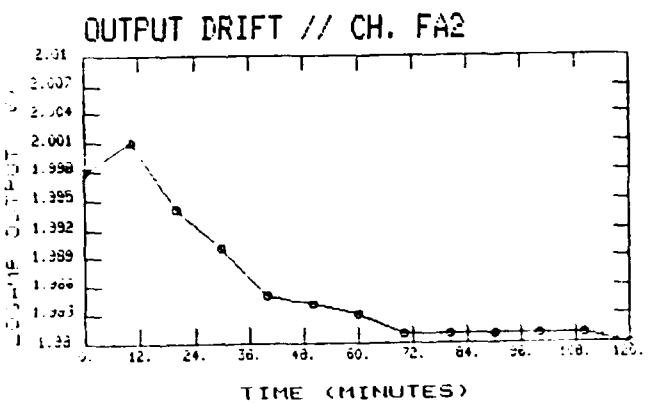

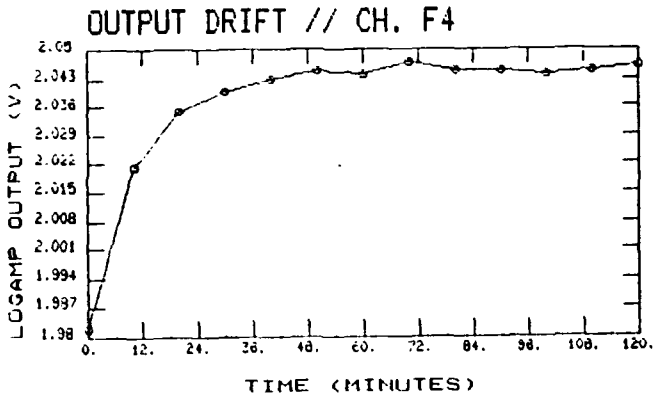

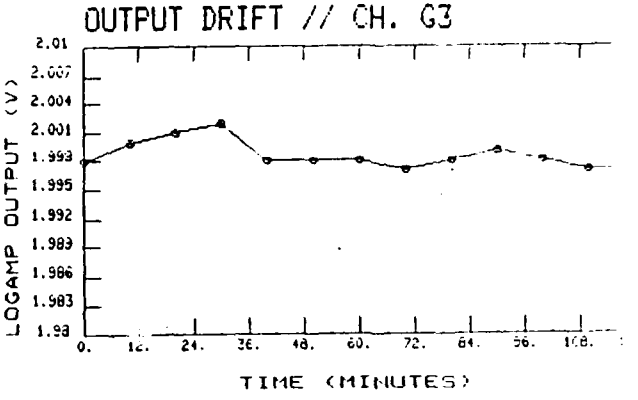

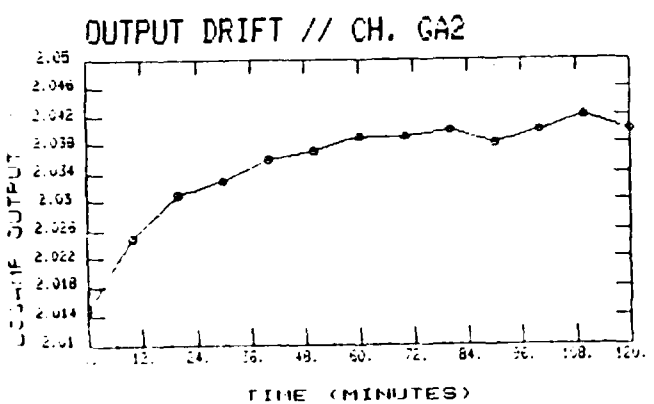

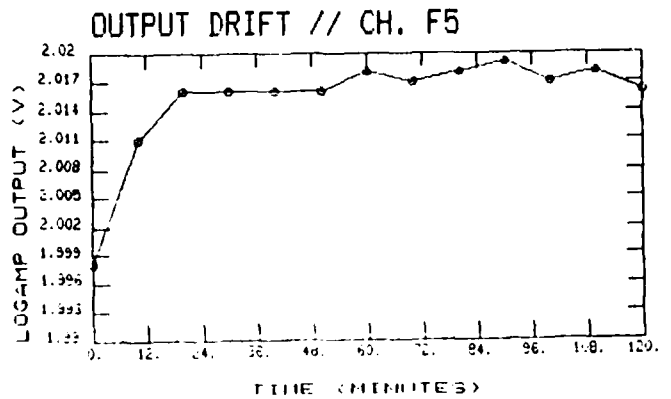

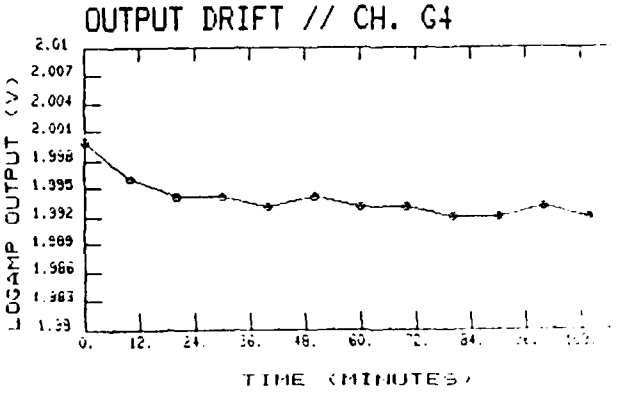

Figure 43. Logamp Output Drift Versus Time

tested not only the preamp electronics but the bipolar power supply. A warmup time prior to operation or alignment was determined to be one half hour for the electronics, as pointed out in [1]the instruction manual.

At one point in system integration a catastrophic failure was induced on the electronics by accidentally crossing a 110 VAC line and the -15 volt power supply line, both located on the rear of the bipolar supply. The result was loss of 30 log amps, 30 T/H amps, 70 opamps in the front end electronics and one multiplexer ICX in one of the A/D boards. It was subsequently determined that the OPA100 opamps from Burr-Brown were no longer available. This was unexpected since the devices had only been on the market for about two years at the time. A decision was made to replace all OPA100's with OPA111's, a lower noise, faster and less expensive device which was introduced after our purchase of the original OPA100's. All needed IC's were repurchased and repairs made to all equipment including the A/D board and the bipolar power supply which had also been damaged. Further, the power supply 110 VAC power connections were changed to preclude this failure mode in the future. After repairs all channels performed as they had prior to the incident.

An intermittent electronic oscillation hampered our initial efforts to test the functioning of the discrimination circuits. This signal was finally isolated to an unstable drive condition of the buffer amplifiers for the two signals to the discrimination circuit. While trying to drive the coax cables connecting them to the discrimination board, the buffers pulled enough current from the bipolar supply lines to be 'felt' by the discrimination circuit logamps. Since the nature of the logamp is to amplify very small signals disproportionately to large ones, the effective logamp gain caused a much larger current draw to drive its load from the same power lines. By decoupling power to the logamps, this oscillation 'noise' was eliminated.

To date, system operation has been tested with large particles, but due to laser beam 'noise' (previously mentioned) the system particle dynamic range, and thus final integration and testing, does not meet the system requirements. As far as can be determined only two methods could be used to reduce this noise, and only one of these, beam modulation, is easily implemented. Since the problem is source noise, and a real time wideband signal is needed, the laser has to be quieted down. Currently a 'noise eater' has been ordered for the laser to reduce the noise an expected factor of about 50:1 or better. The 'noise eater' is a laser beam modulator that also monitors the laser beam optically. The optical signal is used to control the modulator such that as laser beam power (optical signal) rises above a preset level the modulator is made to transmit less light so that the preset laser power output for the modulator is stable. Conversely, power drops below the preset level are compensated in the modulator by transmitting more light. Commercially available devices use either A-O (acousto-optic) or E-O (electro-optic) modulation. The E-O device (which was ordered) reduces noise the most.

A second method for reducing the effects of laser noise might be considered which does not require an isolated modulation scheme, but which could provide comparable results if care is taken. This method would utilize a separate, laser beam power monitor with a bandwidth equal to the front-end electronics and a high-current-drive/buffer combination to directly drive the other, now grounded, inputs to the detector preamps with a signal equal in amplitude and phase (polarity) to the noise signal. The concept is simple, but the implementation is not since very close matching of the noise signal is needed for this to work. Additionally, the problem of different gains for different

[1]Ibid.

channels is a major complication. In any case, noise cancellation of a factor of 10 to 100 should be attainable with only moderate care in matching noise levels, with the above scheme. As mentioned earlier, it is expected that with the proper installation of the 'noise eater', system operation will finally attain its design goals. If noise is still a problem, the concept of out-of-phase noise cancellation may be implemented to increase noise rejection, though additional wiring would be required.

END 1-87
DTIC